

Aus der Medizinischen Klinik mit Schwerpunkt
Rheumatologie und Klinische Immunologie
der Medizinischen Fakultät Charité – Universitätsmedizin Berlin

DISSERTATION

Oberflächenexpression der AMP-Desaminase 2 auf humanen
Immunzellen und ihre Rolle im extrazellulären
Purinmetabolismus

zur Erlangung des akademischen Grades
Doctor medicinae (Dr. med.)

vorgelegt der Medizinischen Fakultät
Charité – Universitätsmedizin Berlin

von

Lisa Ehlers
aus Peine

Datum der Promotion: 25.11.2022

Inhaltsverzeichnis

Abkürzungsverzeichnis	4
Zusammenfassung	6
1. Abstract.....	6
1.1 Abstract (Deutsch)	6
1.2 Abstract (Englisch).....	7
2. Einleitung	8
2.1 Extrazellulärer Adeninnukleotid-Stoffwechsel	8
2.2 Imbalance extrazellulärer Adeninnukleotide im Rahmen von Entzündung.....	8
2.3 AMP-Desaminase 2	9
2.4 Zielsetzung der Arbeit	10
3. Material und Methodik.....	11
3.1 Zellgewinnung und Zellkultur	12
3.1.1 Gewinnung humaner Immunzellen	12
3.1.2 Zellkultur.....	12
3.2 Isolation und Verifizierung des Zielproteins aus der Membranfraktion	12
3.2.1 Proteinanreicherung mittels Immunpräzipitation	12
3.2.2 Western Blot.....	13
3.2.3 Massenspektrometrie	14
3.3 Isolation des Oberflächenproteins mittels Oberflächenbiotinylierung	14
3.4 Proteinnachweis mittels Oberflächenfärbung	15
3.4.1 Durchflusszytometrie und Immunfluoreszenzmikroskopie	15
3.4.2 Reduktion der Genexpression von AMPD2 mittels RNA-Interferenz	18
3.5 Differenzielle Analyse der Proteinexpression im Kontext von Entzündung	18
3.5.1 Patientenkollektiv	19
3.5.2 Bestimmung der Nukleosid- und Zytokinkonzentrationen.....	20
3.6 Statistische Analysen	20
4. Ergebnisse	20
4.1 Nachweis von AMPD2 an der Zelloberfläche	20
4.2 Oberflächenexpression von AMPD2 auf humanen Immunzellen unter inflammatorischen Bedingungen.....	22
4.3 Regulation und anti-inflammatorisches Potential extrazellulärer Adeninmetabolite	25
5. Diskussion.....	25
5.1 Pathophysiologische Bedeutung von AMPD2	26

5.2 eAMPD2 im Kontext des extrazellulären Purinmetabolismus.....	27
5.3 Limitationen und Ausblick	29
6. Literaturverzeichnis	32
Eidesstattliche Versicherung.....	41
Anteilerklärung an der erfolgten Publikation	42
Auszug aus der Journal Summary List	45
Druckexemplar der ausgewählten Publikation.....	46
Lebenslauf	82
Publikationsliste	85
Danksagung.....	87

Abkürzungsverzeichnis

A1R	Adenosin A1-Rezeptor
A2AR	Adenosin A2A-Rezeptor
A2BR	Adenosin A2B-Rezeptor
A3R	Adenosin A3-Rezeptor
ADA	Adenosin-Desaminase
ADP	Adenosindiphosphat
AICAR	5-Aminoimidazol-4-carboxamid-Ribonukleotid
AMP	Adenosinmonophosphat
AMPD	AMP-Desaminase
AMPK	AMP-aktivierte Proteinkinase
APC	Allophycocyanin
ATIC	AICAR-Formyltransferase
ATP	Adenosintriphosphat
BFA	Brefeldin A
BSG	Blutsenkungsgeschwindigkeit
CD39	Ektonukleosidtriphosphatdiphosphohydrolase 1
CD73	Ekto-5'-Nukleotidase
CIA	Kollagen-induzierte Arthritis
CNT	konzentrierender Nukleosidtransporter
CRP	C-reaktives Protein
Dex	Dexamethason
DMEM	Dulbecco's Modified Eagle Medium
DRFZ	Deutsches Rheumaforschungszentrum
eADO	extrazelluläres Adenosin
eAMPD2	oberflächliche AMPD2
eATP	extrazelluläres ATP
EGF	Epidermaler Wachstumsfaktor
ENT	äquilibrierender Nukleosidtransporter
FCS	fetales Kälberserum
FDR	Falscherkennungsrate
FITC	Fluoresceinisothiocyanat
GAPDH	Glycerinaldehyd-3-phosphat-Dehydrogenase
GTP	Guanosintriphosphat
HEK293	Human embryonic kidney 293-Zellen
HRP	Meerrettichperoxidase

iBAQ	Intensity Based Absolute Quantification
IMP	Inosinmonophosphat
IP	Immunpräzipitation
LFQ	Label-Free Quantification
LPS	Lipopolysaccharid
MACS	magnetische Zellsortierung
MN	Monensin
MTX	Methotrexat
NAD ⁺	Nicotinamidadenindinukleotid
PBMC	mononukleäre Zelle aus dem peripheren Blut
PE	Phycoerythrin
PerCP	Peridinin-Chlorophyll-Protein-Komplex
PHA-L	Phytohämagglutinin-L
PMA	Phorbol-12-myristat-13-acetat
RA	rheumatoide Arthritis
RRID	Research Resource Identifier
SDS-PAGE	Natriumdodecylsulfat-Polyacrylamidgelelektrophorese
scr	scrambled
T _H 1-Zellen	Typ 1 T-Helferzellen
T _H 2-Zellen	Typ 2 T-Helferzellen
T _H 17-Zellen	Interleukin-17-produzierende T-Helferzellen
TNF- α	Tumornekrosefaktor-alpha
TLR	Toll-like-Rezeptor
Tregs	regulatorische T-Zellen

Zusammenfassung

1. Abstract

1.1 Abstract (Deutsch)

Extrazelluläre Purine tragen maßgeblich zur Regulation des inflammatorischen Milieus bei: Während ATP als proinflammatorisches Alarmin wirkt, vermittelt Adenosin entzündungshemmende Effekte. Das Gleichgewicht dieser Adeninmetabolite wird im Wesentlichen durch die Ektonukleotidasen Ektonukleosidtriphosphatdiphosphohydrolase 1 (CD39) und Ekto-5'-Nukleotidase (CD73) vermittelt, die ATP über AMP zu Adenosin verstoffwechseln. AMP-Desaminasen (AMPD) sind Enzyme des intrazellulären Purinstoffwechsels, die die Desaminierung von AMP zu IMP katalysieren. Damit erleichtern sie einerseits den Abbau von ATP und verringern andererseits den AMP-Bestand für die Adenosin-Produktion durch CD73. An der Zelloberfläche humaner Immunzellen ist dieser Mechanismus bisher nicht beschrieben. Ziel dieser Arbeit war die Analyse der Expression von AMPD2 an der Oberfläche humaner Leukozyten sowie deren Regulation unter inflammatorischen Bedingungen.

Mittels Immunpräzipitation (IP) aus Membranfraktionen sowie durch Anreicherung des Oberflächenproteins mittels Oberflächenbiotinylierung wiesen wir AMPD2 in der Plasmamembran von HEK293 Zellen, HMEC-1 Zellen, U-937 Zellen und CD14+ Monozyten nach. Der Proteinnachweis erfolgte mittels Western Blot und Massenspektrometrie. Zusätzlich visualisierten wir die Oberflächenexpression immunfluoreszenzmikroskopisch auf U-937 Zellen sowie auf humanen mononukleären Zellen aus dem peripheren Blut (PBMCs). Durchflusszytometrisch zeigten wir eine signifikante Steigerung der Expression der oberflächlichen AMPD2 (eAMPD2) auf humanen Monozyten nach Toll-like-Rezeptor (TLR)-Stimulation ($p=0,0078$) sowie eine Reduktion dieser durch Inhibition des sekretorischen Wegs ($p=0,0078$). Durch die zusätzliche Behandlung mit Dexamethason (Dex) ließ sich der Effekt der Immunstimulation teilweise reduzieren. Im Vergleich zu bezüglich Geschlecht und Alter vergleichbaren Kontrollen zeigten PBMCs von Patient*innen mit rheumatoider Arthritis (RA) eine erhöhte Grundexpression von eAMPD2. Eine erhöhte eAMPD2-Expression auf CD14+ Monozyten war nicht mit einer Reduktion der extrazellulären Adenosinkonzentration (eADO) verbunden. Hingegen konnten wir das anti-inflammatorische Potential von extrazellulärem IMP im Sinne einer Reduktion der Sekretion von Tumornekrosefaktor-alpha (TNF- α) durch PBMCs nachweisen.

Zusammenfassend identifiziert diese Arbeit erstmals eAMPD2 als Ektoenzym auf humanen Immunzellen als neuen Regulator des extrazellulären Purinstoffwechsels. Durch AMP-Verbrauch könnte die Desaminase den Abbau von proinflammatorischem ATP erleichtern und

das bestehende System der Ectonucleotidasen CD39 und CD73 um die Produktion des langlebigen anti-inflammatorischen Moleküls IMP ergänzen.

1.2 Abstract (Englisch)

Extracellular purine metabolites are powerful mediators of the inflammatory milieu: ATP acts as a pro-inflammatory alarmin, while adenosine represents a potent anti-inflammatory molecule. The ectonucleotidasen ectonucleoside triphosphate diphosphohydrolase-1 (CD39) and ecto-5'-nucleotidase (CD73) regulate the balance of these metabolites by catalysing the sequential degradation of ATP to adenosine via AMP. Intracellular AMP deaminases (AMPD) mediate AMP deamination to IMP. Thereby, they facilitate degradation of ATP on the one hand and impair adenosine production by reducing AMP supply for CD73 on the other hand. The mechanism of AMP deamination has not yet been recognised on the surface of immune cells. This study examined the surface expression of AMPD2 in human leukocytes and its modification under inflammatory conditions.

We performed immunoprecipitation (IP) from membrane fractions as well as enrichment of surface protein by surface biotinylation to detect AMPD2 in the plasma membrane of HEK293 cells, HMEC-1 cells, U-937 cells and CD14+ monocytes. The enzyme was identified by western blot and mass spectrometry. Additionally, surface expression was visualised with the help of immunofluorescence microscopy of U-937 cells and human peripheral blood mononuclear cells (PBMCs). Flow cytometry revealed a significant increase in surface AMPD2 (eAMPD2) expression on human monocytes after toll-like receptor (TLR) stimulation ($p=0.0078$), while a reduction was observed after Golgi transport inhibition ($p=0.0078$). Concomitant incubation with dexamethasone (Dex) partly prevented the increase caused by immunostimulation. PBMCs from patients with rheumatoid arthritis (RA) showed an elevated expression of eAMPD2 compared to sex- and age-matched healthy controls. An increase in eAMPD2 expression on CD14+ monocytes was not associated with reduced levels of extracellular adenosine (eADO). On the other hand, we verified the anti-inflammatory potential of extracellular IMP by demonstrating a reduction in tumor necrosis factor- α (TNF- α) secretion from PBMCs.

In summary, this study shows AMPD2 surface expression on human immune cells for the first time and thereby identifies a novel ectoenzyme in the extracellular purine metabolism. We hypothesise that the deaminase enhances the degradation of pro-inflammatory ATP by removing AMP from the extracellular space and adds the production of long-lived anti-inflammatory IMP to the existing system of ectonucleotidasen.

2. Einleitung

2.1 Extrazellulärer Adeninnukleotid-Stoffwechsel

Extrazelluläre Purinmetabolite gehören evolutionär zu den ältesten Signalmolekülen.¹ Sie vermitteln ihre Effekte über zwei Rezeptorfamilien: P1- und P2-Rezeptoren. Extrazelluläre Purinnukleotide binden an P2-Rezeptoren, die sich in ionotrope P2X-Rezeptoren und metabotrope P2Y-Rezeptoren unterteilen lassen.^{2 3} Andererseits stellen P1-Rezeptoren G-Protein-gekoppelte Rezeptoren dar, die für die Signaltransduktion von Adenosin verantwortlich sind.⁴ Vier Adenosinrezeptoren (A1R, A2AR, A2BR, A3R) werden unterschieden und vermitteln in verschiedenen Geweben eine Vielzahl von Effekten.⁵

Zwei Stoffwechselwege – der kanonische und der alternative Weg – bestimmen wesentlich das Gleichgewicht extrazellulärer Adeninnukleotide. Der kanonische Weg setzt sich zusammen aus den Ektonukleotidasen Ektonukleosidtriphosphatdiphosphohydrolase 1 (CD39) und Ekto-5'-Nukleotidase (CD73). An den enzymatischen Abbau von ATP und ADP zu AMP durch CD39 schließt sich die von CD73 katalysierte Produktion von Adenosin mittels phosphorolytischer Spaltung des AMPs an.⁶ Im Gegensatz dazu stellen die Enzyme des alternativen Wegs – CD38 und CD203a/PC-1 – AMP aus NAD⁺ bereit.^{7 8} Zwei weitere Mechanismen beeinflussen die extrazelluläre Adenosinkonzentration: Die extrazelluläre Adenosin-Desaminase (ADA) vermittelt den Abbau von Adenosin zu Inosin.⁹ Zusätzlich erfolgt ein Austausch von Adeninnukleotid(s)iden mit dem Intrazellularraum. ATP wird sowohl über die Kanalproteine Pannexin-1 und Connexin-43 als auch mittels vesikulären Transports in den Extrazellularraum abgegeben.¹⁰⁻¹³ Der Transport von Adenosin erfolgt über zwei Familien von Nukleosidtransportern: äquilibrierende Nukleosidtransporter (ENT) und konzentrierende Nukleosidtransporter (CNT).¹⁴⁻¹⁶ Die beschriebenen Stoffwechselwege spielen in vielen Geweben eine wichtige Rolle. Die folgende Arbeit fokussiert sich auf den extrazellulären Adeninnukleotid-Stoffwechsel von Immunzellen.

2.2 Imbalance extrazellulärer Adeninnukleotide im Rahmen von Entzündung

Drury und Szent-Györgyi beschrieben erstmals 1929 die physiologische Bedeutung von eADO im Herzmuskel.¹⁷ In den letzten Jahren rückte die Dysregulation des extrazellulären Adenosinstoffwechsels als pathophysiologischer Faktor sowie therapeutischer Angriffspunkt von immunvermittelten Erkrankungen in den Vordergrund.^{18 19} Extrazelluläres ATP (eATP) und eADO sind im Entzündungsgeschehen Gegenspieler. Während eATP ein pro-inflammatorisches Alarmin darstellt, zeichnet sich eADO durch seine hohe anti-inflammatorische Potenz aus.²⁰⁻²⁹ Studien zeigen eine Imbalance dieser Moleküle im Rahmen von Autoimmunerkrankungen: T-Zellen aus der Synovialflüssigkeit arthritischer Gelenke sowie

regulatorische T-Zellen aus dem peripheren Blut von Psoriasispatient*innen wiesen eine verringerte Expression von CD73 verbunden mit einer verminderten Produktion von Adenosin auf.^{30 31} Patient*innen mit ankylosierender Spondylitis zeigten eine Reduktion von CD39, A1R und A2BR auf von Monozyten abgeleiteten Makrophagen.³² Umgekehrt beobachteten Walscheid et al. bei Uveitispatient*innen eine erhöhte monozytäre Expression von CD39 und CD73.³³

Eine wichtige Rolle spielt der extrazelluläre Adenosin Gehalt auch im Tumormikromilieu, wo der protektive „Adenosin-Halo [Übersetzung der Autorin]“ (S. 842)⁴ eine effektive Anti-Tumor-Immunantwort unterbindet.^{4 34} Aus dieser beachtlichen Relevanz für inflammatorische Prozesse ergibt sich das Interesse, den extrazellulären Purinmetabolismus pharmakologisch zu beeinflussen.¹⁹ Erste klinische Studien zeigten ein verringertes Tumorstadium durch Blockade der Adenosinproduktion und -wirkung.³⁵⁻³⁹ Diese Beobachtungen unterstreichen die klinische Relevanz des extrazellulären Purinstoffwechsels von Immunzellen.

2.3 AMP-Desaminase 2

Während der intrazelluläre Purin Gehalt durch ein komplexes Enzymsystem reguliert wird, sind nur wenige Ektoenzyme am extrazellulären Adeninnukleotid-Stoffwechsel beteiligt.⁴⁰ AMP-Desaminasen katalysieren die Desaminierung von AMP. Drei Gene kodieren für die Isoformen AMPD1, AMPD2 und AMPD3, die sich in ihrer Gewebeexpression unterscheiden.⁴¹ Während AMPD1 die muskuläre und AMPD3 die erythrozytäre Isoform darstellen, wird AMPD2 unter anderem in Leber, Gehirn und Leukozyten exprimiert.⁴²⁻⁴⁴ Die Desaminierung von AMP stellt den geschwindigkeitsbestimmenden Schritt des Purinstoffwechsels dar und ermöglicht die Synthese von Guaninnukleotiden aus dem vorherrschenden Adeninnukleotid-Bestand.^{40 45 46} Durch den Abbau von AMP erhöhen AMPDs die ATP:AMP-Ratio und fördern so die Energiegewinnung mittels ATP-Hydrolyse.^{40 47 48} Im Gegensatz zu ihrer prominenten Rolle im Zytosol wurde die Desaminierung von AMP im Extrazellularraum bisher kaum untersucht. Dunkley und Manery beschrieben in den 1960er Jahren die Desaminierung von AMP an der Muskeloberfläche.^{49 50} In der Folge wiesen Rao und Pipoly AMPD an der Innenseite der Erythrozytenmembran nach.^{51 52} Das Vorkommen von AMPD an der Oberfläche von Leukozyten ist hingegen bisher nicht beschrieben. Mit der Desaminierung von AMP entziehen AMPDs CD73 das Substrat für die Adenosin-Synthese. Umgekehrt hat ein hereditärer oder pharmakologischer Funktionsverlust von AMPD einen Anstieg der Adenosinkonzentration zur Folge.^{46 53 54} Gleichzeitig geht mit der Oberflächenexpression von AMPD2 das Konzept der extrazellulären IMP-Produktion einher (Abbildung 2.1). In Anbetracht der zuvor beschriebenen immunologischen Bedeutung des extrazellulären Puringleichgewichts betrachteten wir die potentielle Existenz eines solchen Mechanismus auf der Zelloberfläche als besonders relevant.

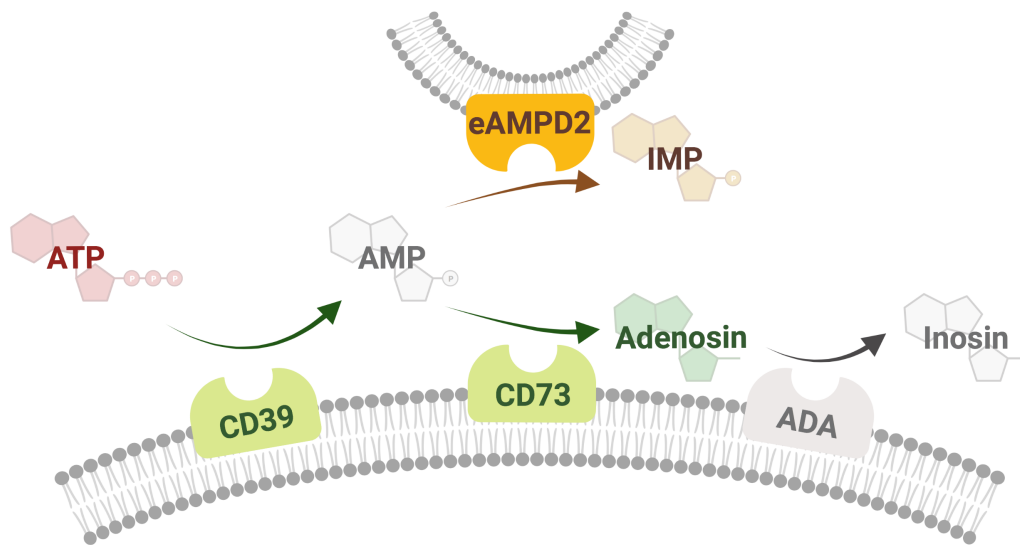


Abbildung 2.1 Modell der Rolle von eAMPD2 im extrazellulären Purinmetabolismus.

Legende: ADA, Adenosin-Desaminase; AMP, Adenosinmonophosphat; ATP, Adenosintriphosphat, eAMPD2, oberflächliche AMP-Desaminase 2; IMP, Inosinmonophosphat. Erstellt mit BioRender.com, modifiziert aus Ehlers et al.⁵⁵

2.4 Zielsetzung der Arbeit

Unter Annahme einer möglichen Beteiligung der AMP-Desaminierung am extrazellulären Purinmetabolismus untersuchten wir die Oberflächenexpression von AMPD2 auf primären humanen Immunzellen sowie deren Veränderung unter inflammatorischen Bedingungen.

Erstes Ziel dieser Arbeit war es, die Oberflächenexpression von AMPD2 nachzuweisen und methodisch vielfältig zu bestätigen. Zu diesem Zweck wurden die Isolation von Membranprotein und eine Oberflächenfärbung an Zelllinien etabliert und nachfolgend an humanen Leukozyten verifiziert.

Aufgrund der oben beschriebenen Bedeutung des extrazellulären Adeninnukleotid-Stoffwechsels im Rahmen entzündlicher Prozesse, befasste sich unsere zweite Fragestellung mit der Veränderung der Oberflächenexpression unter inflammatorischen Bedingungen. Wir untersuchten zunächst *in vitro* den Einfluss verschiedener Immunstimulationen sowie immunmodulierender Medikamente auf die Oberflächenexpression von AMPD2. In der Folge analysierten wir die Expression von eAMPD2 auf PBMCs von Patient*innen mit RA im Vergleich zu nach Geschlecht und Alter vergleichbaren gesunden Spender*innen.

Das dritte Ziel behandelt die funktionelle Relevanz der extrazellulären Desaminierung von AMP. Entsprechend unserer Hypothese könnte der zusätzliche AMP-Verbrauch durch eAMPD2 eine Reduktion der eADO-Produktion bedingen. Folglich untersuchten wir den extrazellulären Adenosin Gehalt in Abhängigkeit von verschiedenen Expressionsniveaus von eAMPD2. Zusätzlich ergänzt die Oberflächenexpression von AMPD2 das System der Ektonukleotidasen

um die Produktion von extrazellulärem IMP, sodass wir schlussendlich den Einfluss dieses Metaboliten auf das inflammatorische Milieu analysierten.

3. Material und Methodik

In der dieser Dissertationsschrift zugrundeliegenden Publikation beschreiben wir erstmals die Oberflächenexpression von AMPD2 auf humanen Leukozyten. Die umfassende Methodik wird im Detail in der Publikationsschrift dargestellt.⁵⁵ Im Folgenden möchte ich im Schwerpunkt auf die Herausforderungen der sicheren Feststellung der Membranlokalisation eines auch zytosolisch vorliegenden Proteins eingehen.

Unser Vorgehen fußte auf drei Verifizierungsschritten (Abbildung 3.1), die im Folgenden im Detail beleuchtet werden: (i) Membranfraktionierung mit anschließender IP des Zielproteins, (ii) Oberflächenbiotinylierung gefolgt von einer massenspektrometrischen Analyse sowie (iii) Durchflusszytometrie und Immunfluoreszenzmikroskopie nach erfolgter Oberflächenfärbung. Vorangestellt wird diesen Methoden eine Darstellung der Zellkulturbedingungen. Zum Abschluss wird das methodische Vorgehen zur Untersuchung des Expressionsverhaltens abhängig von verschiedenen inflammatorischen Stimuli *in vitro* und *in vivo* dargestellt.

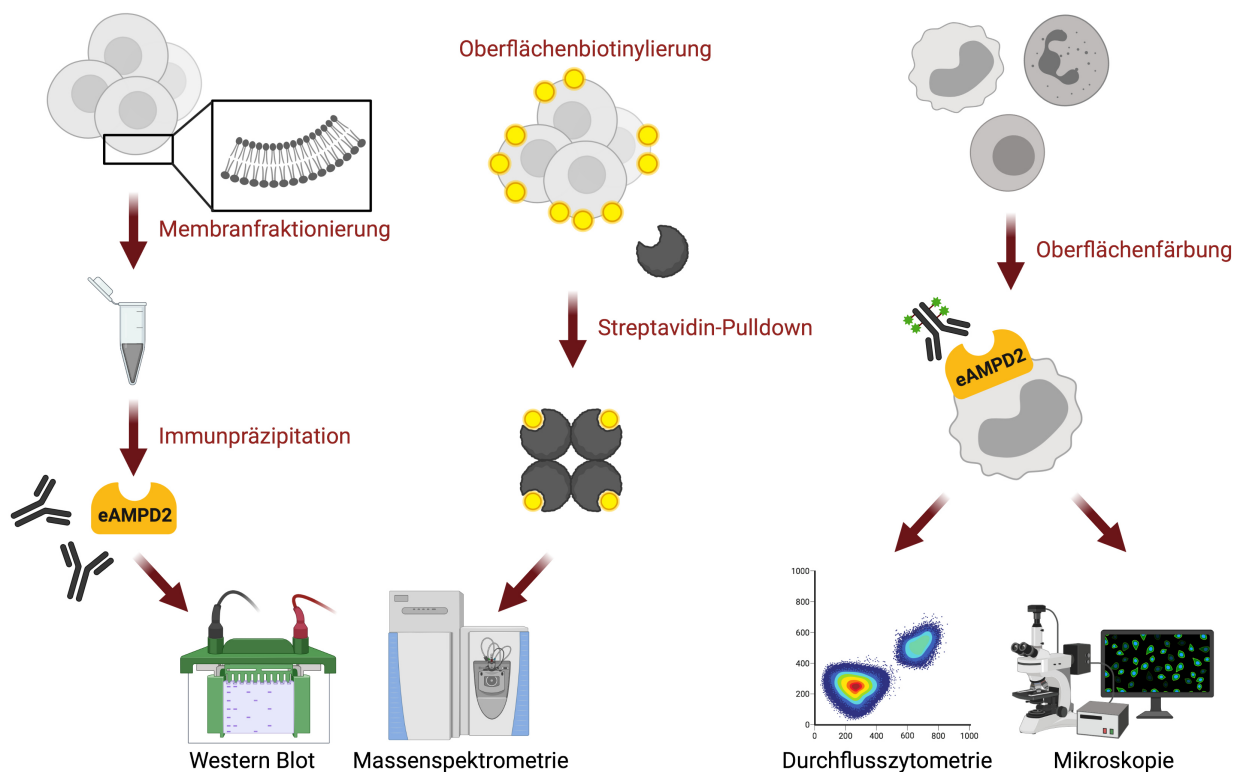


Abbildung 3.1 Verifizierungsschritte zum Nachweis von eAMPD2 an der Zelloberfläche. Erstellt mit BioRender.com.

3.1 Zellgewinnung und Zellkultur

3.1.1 Gewinnung humaner Immunzellen

Die Isolation humaner Leukozyten erfolgte aus heparinisiertem peripheren venösen Blut. PBMCs wurden mittels Dichtegradientenzentrifugation auf Ficoll-Paque™ PLUS (GE Healthcare) gewonnen. Zur Analyse polymorphkerniger Zellen wurden die roten Blutkörperchen mit Erythrozyten-Lysepuffer (0,01 M KHCO₃, 0,155 M NH₄Cl, 0,1 mM EDTA, pH 7,5) lysiert. Die Isolierung CD14⁺ Monozyten bzw. CD15⁺ neutrophiler Granulozyten wurde mittels magnetischer Zellsortierung (MACS) mit Anti-CD14- und Anti-CD15-Microbeads (Miltenyi Biotec) durchgeführt. Eine Kontrolle der Zellreinheit von > 97% erfolgte durchflusszytometrisch (Publikation Supplementary Figure S1B+C⁵⁵).

3.1.2 Zellkultur

Die Zellkulturbedingungen sind in Tabelle 3.1 aufgeführt. Die Kultivierung der Zellen erfolgte unter kontrollierten Bedingungen in einem CO₂-Brutschrank (5% CO₂, 18% O₂) bei 37°C. Die bei der Behandlung der Proben verwendeten Konzentrationen sind Tabelle 3.2 zu entnehmen.

3.2 Isolation und Verifizierung des Zielproteins aus der Membranfraktion

Die wesentlichen Herausforderungen der Erstbeschreibung der Membranständigkeit eines Proteins bestehen in der Reinheit der Membranfraktion sowie der Spezifität des Proteinnachweises. Um diese kritischen Punkte zu adressieren, erfolgte in dieser Arbeit die Verifizierung der Oberflächenlokalisation von AMPD2 in multiplen, sich gegenseitig bestätigenden Schritten. Zur Untersuchung des Membranproteins wurden zunächst Membranfraktionen gewonnen, aus denen im Folgenden AMPD2 mittels IP angereichert wurde. Neben dem Proteinnachweis im angereicherten Membranprotein gewährleistet diese Methode durch massenspektrometrische Analyse des Immunpräzipitats die Verifizierung der Antikörperspezifität.⁵⁶ Im Gegensatz dazu bietet der Western Blot eine größere Sensitivität mit der Einschränkung des indirekten Proteinnachweises.

3.2.1 Proteinanreicherung mittels Immunpräzipitation

Zelllysate wurden mittels IP-Lysepuffer (10 mM Tris HCl pH 7,5, 10 mM NaCl, 2 mM EDTA, 0,1% (v/v) Triton X-100, 1 mM PMSF, 2 µg/mL Aprotinin) gewonnen. Die Separation von zytosolischen und Membranfraktionen erfolgte mit dem Mem-PER™ Plus Membrane Protein Extraction Kit (Thermo Fisher Scientific). Die IP wurde über Nacht bei 4°C mit dem Anti-AMPD2-Antikörper Klon QQ13 (2 µL, SCBT, AB_2258261) durchgeführt. Parallel wurde eine

Isotyp-Kontrollprobe mit murinem IgG1 (1:10, 2 µL, Invitrogen, AB_2532935) hergestellt. Im Anschluss erfolgte der Pulldown durch Protein A/G plus Agarose (SCBT).

Tabelle 3.1 Zellkulturbedingungen

Zelllinie (Ursprung) / Zelltyp	Zellkulturmedium*	Zusatz
HEK293 (ATCC®)	DMEM	10% (v/v) FCS 10% (v/v) humanes AB-Serum
Jurkat (ATCC®)	RPMI 1640 Medium	
THP-1 (ATCC®)		
U-937 (ATCC®)		
primäre humane Leukozyten		
HMEC-1 (ATCC®)	MCDB 131 Medium	25% (v/v) FCS, 2 mM L-Glutamin, 10 ng/mL EGF, 0,3 µg/mL Hydrocortison

*Alle Zellkulturmedien waren zusätzlich mit 100 U/mL Penicillin, 100 µg/mL Streptomycin und 50 µM 2-Mercaptoethanol versetzt.

Tabelle 3.2 Zellbehandlung

	Hersteller	Konzentration	Funktion
Pam3CSK4	Tocris	1 µg/mL	Agonist am TLR1/2
Poly (I:C)	Miltenyi Biotec	10 µg/mL	Agonist am TLR3
Lipopolysaccharid (LPS)	Sigma-Aldrich	1 µg/mL	Agonist am TLR4
Flagellin (FlC)	Sigma-Aldrich	100 ng/mL	Agonist am TLR5
FSL-1	Tocris	1 µg/mL	Agonist am TLR2/6
Resiquimod (R848)	Tocris	1 µg/mL	Agonist am TLR7/8
ODN 2006	Miltenyi Biotec	0,5 µM	Agonist am TLR9
Phytohemagglutinin-L (PHA-L)	Sigma-Aldrich	5 µg/mL	Lektin, T-Zellaktivierung durch Quervernetzung von Oberflächenmolekülen inklusive des T-Zell-Rezeptors
Phorbol-12-myristat-13-acetat (PMA)	Sigma-Aldrich	10 ng/mL	Aktivator der Proteinkinase C
Ionomycin	Sigma-Aldrich	1 µg/mL	Calcium-Ionophor, T-Zellaktivierung durch Calciumeinstrom unter Umgehung des T-Zell-Rezeptors
Brefeldin A (BFA)	Sigma-Aldrich	1 µg/mL	Hemmung des Transports zwischen endoplasmatischem Retikulum und Golgi-Apparat
Monensin (MN)	Sigma-Aldrich	0,5 µg/mL	Hemmung des Transports im Golgi-Apparat
Dexamethason (Dex)	Sigma-Aldrich	10 ⁻⁸ M, 10 ⁻⁵ M	synthetisches Glucocorticoid
Methotrexat (MTX)	medac	0,8 µM	Hemmstoff der Dihydrofolatreduktase
ATP	Sigma-Aldrich	100 µM, 1 mM	
Adenosin	Sigma-Aldrich	1 µM, 50 µM	
IMP	Sigma-Aldrich	100 µM, 1 mM	
Inosin	Sigma-Aldrich	100 µM, 1 mM	

3.2.2 Western Blot

Die Zelllysate wurden nach Zugabe von Laemmli-Probenpuffer bei 95°C für 10 Minuten denaturiert und mittels SDS-Polyacrylamid-Gelelektrophorese nach Molekülmasse aufgetrennt.

Es erfolgte die Übertragung auf PVDF-Trägermembranen (Merck Millipore) und der anschließende Proteinnachweis unter Verwendung der folgenden Antikörper: Anti-Alpha-Tubulin (100 ng/mL, polyklonal, abcam, AB_2288001), Anti-AMPD2 (1:500, QQ13, SCBT, AB_2258261), Anti-Beta-Aktin (1:10.000, BA3R, Invitrogen, AB_10979409), Anti-Calreticulin (1:2000, polyklonal, Thermo Fisher Scientific, AB_2069607), Anti-CD14 (Biotin, 1:50, TM1, DRFZ), Anti-Cytochrom b (1:200, SCBT, AB_2088887), Anti-Glycerinaldehyd-3-phosphat-Dehydrogenase (GAPDH) (1:100, 6C5, Merck Millipore, AB_2107445), Anti-Lamin B1 (1:200, B-10, SCBT, AB_10947408), Anti-Pan-Cadherin (1:500, CH-19, abcam, AB_305544). Die Visualisierung wurde durch enzymatische Chemilumineszenz mithilfe HRP-gekoppelter Anti-Maus-IgG (1:10.000, Promega, AB_430834), Anti-Kaninchen-IgG (1:10.000, Promega, AB_430833) und Anti-Huhn-IgY (1:5.000, Thermo Fisher Scientific, AB_2534727) Antikörper sowie HRP-gekoppeltem Streptavidin (R&D Systems) gewährleistet.

3.2.3 Massenspektrometrie

Die massenspektrometrische Analyse der IP-Proben erfolgte nach Reduktion und Verdau von den Agarose-Kügelchen. Die Peptide wurden mittels Hochleistungsflüssigkeitschromatographie auf einer Mikrosäule (Dr. Maisch GmbH) getrennt. Die Analyse wurde an einem Q Exactive Plus oder HF-X Hybrid Quadrupole-Orbitrap Instrument (Thermo Fisher Scientific) durchgeführt. Das MaxQuant Software Package (v1.6.0.1) diente zur Datenanalyse. Die MS²-Spektren wurden in einer internen Andromeda Suchmaschine gegenüber einer humanen UniProt Datenbank (HUMAN.2017, HUMAN.2019) durchsucht. Zur Peptid- und Proteinidentifizierung wurde eine Falscherkennungsrate (FDR) von 1% festgelegt. Die Berechnung der iBAQ (Intensity Based Absolute Quantification) und LFQ (Label-Free Quantification) Intensitäten erfolgte durch integrierte Algorithmen. Der Datensatz der Proteomanalysen wurde über PRIDE dem ProteomeXchange Konsortium zur Verfügung gestellt (dataset identifier PXD022350).⁵⁷

3.3 Isolation des Oberflächenproteins mittels Oberflächenbiotinylierung

Obwohl die in 3.2.1 geschilderte Methode des Proteinnachweises mittels IP aus Membranfraktionen den Vorteil der Anreicherung des Zielproteins durch spezifische Antikörper bietet, ist diese Methode durch die Charakteristika der Membranfraktion in ihrer Aussagekraft limitiert: Durch Membrananreicherung mithilfe eines Detergens nach Zellpermeabilisierung schließt diese Prozedur auch intrazelluläre Kompartimente wie die nukleäre Membran ein. Auch kann aus einem Vorliegen in der Membranfraktion nicht auf eine Lokalisation an der Zelloberfläche geschlossen werden. Aus diesem Grund führten wir als zweiten Verifizierungsschritt eine Oberflächenbiotinylierung durch. Zur Anreicherung des Oberflächenproteins wurden HMEC-1 und U-937 Zellen sowie CD14+ Monozyten im intakten Zustand

biotinyliert und anschließend lysiert. Die Isolation der Oberflächenfraktion wurde im Anschluss mittels NeutrAvidin™ Agarose ermöglicht. Daraufhin erfolgte wie oben geschildert der Proteinnachweis von AMPD2 mittels Western Blot und Massenspektrometrie in der angereicherten Probe im Vergleich zu einer nicht biotinylierten Kontrolle.

3.4 Proteinnachweis mittels Oberflächenfärbung

Die Oberflächenfärbung mithilfe Fluoreszenzfarbstoff-gekoppelter Antikörper stellte die dritte methodische Säule des Oberflächennachweises dar. Mittels anschließender Durchflusszytometrie sowie Immunfluoreszenzmikroskopie ermöglichte dieser Schritt die Visualisierung der Oberflächenexpression des Zielproteins. Ähnlich der Oberflächenbiotinylierung erfolgte auch hier durch Verwendung intakter Zellen die isolierte Betrachtung des Oberflächenproteins unter Ausschluss intrazellulärer Kompartimente sowie der inneren Plasmamembran. Darüber hinaus erlaubt die Durchflusszytometrie die vergleichende Analyse verschiedener Zelllinien und Zelltypen sowie Kulturbedingungen und Spender mit hohem Durchsatz.

Um auf diese Weise das Expressionsverhalten des Zielproteins zuverlässig zu untersuchen, ist die Spezifität der Färbemethode essentiell. Die entsprechenden Schritte der Antikörpervalidierung werden im Folgenden aufgeführt. Sie umfassten (i) die Gewährleistung suffizienter Zellintegrität, (ii) die Eliminierung der Färbung durch Inkubation mit einem ungekoppelten, für das Zielprotein spezifischen Antikörper im Überschuss und (iii) die Reduktion der Oberflächenfärbung nach Knockdown des Zielproteins.

3.4.1 Durchflusszytometrie und Immunfluoreszenzmikroskopie

Die Färbungen für die Durchflusszytometrie erfolgten auf Eis. Um eine unspezifische Antikörperbindung zu verhindern wurden die Zellen zur Blockade der Fc-Rezeptoren mit 10% (v/v) humanem IgG (Kiovig [50 mg/mL], Baxter AG) inkubiert. Die verwendeten Antikörper sind Tabelle 3.3 zu entnehmen. Zum Ausschluss toter Zellen wurden 7-AAD (BD) und DAPI (Sigma-Aldrich) verwendet. Da insbesondere Monozyten in Zellkultur eine große Empfindlichkeit aufweisen, die eine unspezifische Antikörperbindung an nicht intakte Zellen bedingen kann, führten wir zur zusätzlichen Gewährleistung der Zellintegrität vor Beginn der Färbung eine Entfernung sterbender Zellen mittels magnetischer Sortierung durch (Dead Cell Removal Kit, Miltenyi Biotec). Die Spezifität der Färbung wurde durch Blockade des Zielproteins mit einem unkonjugierten spezifischen Antikörper sichergestellt. Zu diesem Zweck wurde vor Zugabe des Fluoreszenz-markierten Antikörpers parallel zum Färbeansatz eine identische Probe für zehn Minuten mit unkonjugiertem Antikörper im 25-fachen Überschuss inkubiert. Vor der intrazellulären Färbung erfolgte die Fixierung und Permeabilisierung mit -20°C kaltem 90% (v/v)

Methanol. Die durchflusszytometrischen Messungen wurden am MACSQuant Analyzer 10 (Miltenyi Biotec) und LSRFortessa™ Durchflusszytometer (BD) durchgeführt und mit der FlowJo™ Software (Version 7.6.4 und 10.7.1, BD) analysiert. Die Gatingstrategie ist in Abbildung 3.2 dargestellt. Die verschiedenen Leukozytenpopulationen wurden wie folgt

Tabelle 3.3 Antikörper

Zielstruktur	Isotyp	Klon	Fluorochrom	Verdünnung	Hersteller	RRID
AMPD2	Kaninchen, IgG	polyklonal	unkonjugiert	1:50	Thermo Fisher Scientific	AB_2543627
CD3	murin, IgG2a, κ	OKT3	Brilliant Violet 510™	1:20	BioLegend	AB_2561943
CD3	murin, IgG1, κ	UCHT1	Alexa Fluor® 594	1:20	DRFZ	AB_2619695
CD4	murin, IgG1, κ	M-T321	APC-Vio® 770	1:10	Miltenyi Biotec	AB_2657994
CD8	murin, IgG1, κ	GN11/134D7	Alexa Fluor® 647	1:200	DRFZ	n.a.
CD8	murin, IgG1, κ	GN11/134D7	Alexa Fluor® 700	1:1600	DRFZ	n.a.
CD14	murin, IgG	TM1	FITC	1:400	DRFZ	n.a.
CD14	murin, IgG2a, κ	M5E2	Brilliant Violet 650™	1:20	BioLegend	AB_11204241
CD15	murin, IgM, κ	VIMC6	FITC	1:10	Miltenyi Biotec	AB_244217
CD16	murin, IgG1, κ	3G8	APC/Cyanin7	1:50	BioLegend	AB_314218
CD19	murin, IgG1, κ	HIB19	PerCP/Cyanin5.5	1:100	BioLegend	AB_2073119
CD25	murin, IgG1, κ	BC96	Brilliant Violet 785™	1:20	BioLegend	AB_11219197
CD39	rekombinant human, IgG1	REA739	APC	1:100	Miltenyi Biotec	AB_2657891
CD45	murin, IgG1, κ	HI30	FITC	1:20	BioLegend	AB_314394
CD45RA	murin, IgG2a	4G11	Pacific Orange	1:50	DRFZ	n.a.
CD73	murin, IgG1, κ	AD2	Brilliant Violet 421™	1:50	BioLegend	AB_11204424
CD127	rekombinant human, IgG1	REA614	PE	1:25	Miltenyi Biotec	AB_2654831
CD127	murin, IgG2a, κ	MB15-18C9	FITC	1:10	Miltenyi Biotec	AB_2659850
CCR4	murin, IgG1, κ	L291H4	Brilliant Violet 605™	1:20	BioLegend	AB_2562483
CCR6	rekombinant human, IgG1	REA190	APC	1:20	Miltenyi Biotec	AB_2655933
CXCR3	rekombinant human, IgG1	REA232	PE-Vio® 770	1:50	Miltenyi Biotec	AB_2655739
Isotypkontrolle	Kaninchen, IgG	polyklonal	unkonjugiert	1:125	Invitrogen	AB_2532938
Isotypkontrolle	rekombinant human, IgG1	REA control (S)	APC	1:10	Miltenyi Biotec	AB_2733447
Isotypkontrolle	murin, IgG1, κ	MOPC-21	Brilliant Violet 421™	1:50	BioLegend	AB_10897939
Kaninchen-IgG	Ziege, IgG	polyklonal	PE	1:200	Invitrogen	AB_221651
Kaninchen-IgG	Ziege, IgG	polyklonal	Alexa Fluor® Plus 488	1:500	Thermo Fisher Scientific	AB_2633280
Streptavidin			PE	1:200	Life Technologies	n.a.
Streptavidin			APC/Cyanin7	1:300	BioLegend	n.a.

identifiziert: CD4⁺ T-Zellen wurden unterteilt in CXCR3⁺CCR4⁻CCR6⁻ Typ 1 Helferzellen (T_H1), CCR4⁺CXCR3⁻CCR6⁻ Typ 2 Helferzellen (T_H2) und CCR4⁺CCR6⁺CXCR3⁻ T_H17 Zellen.⁵⁸ Zusätzlich wurden CD8⁺ zytotoxische T-Zellen und CD19⁺ B-Zellen charakterisiert. Monozyten wurden anhand der Expression von CD14 und CD16 unterteilt in drei Subpopulationen: klassisch (CD14^{hi}, CD16⁻), intermediär (CD14^{hi}, CD16⁺) und nicht-klassisch (CD14^{low}, CD16^{hi}).⁵⁹ Die Färbung für die Immunfluoreszenzmikroskopie erfolgte über Nacht bei 4°C nach Fixierung mit 4% (v/v) Paraformaldehyd und Inkubation mit 5% (v/v) FCS. Die Darstellung des Zytoskeletts und der Zellkerne erfolgte mit Phalloidin bzw. DAPI. Es wurden ein LSM 880 konfokales Laser-Scanning-Mikroskop (ZEISS) sowie ein Biorevo BZ-9000 Fluoreszenz-Mikroskop (Keyence) für die Mikroskopie und ImageJ für die Bildanalyse verwendet.

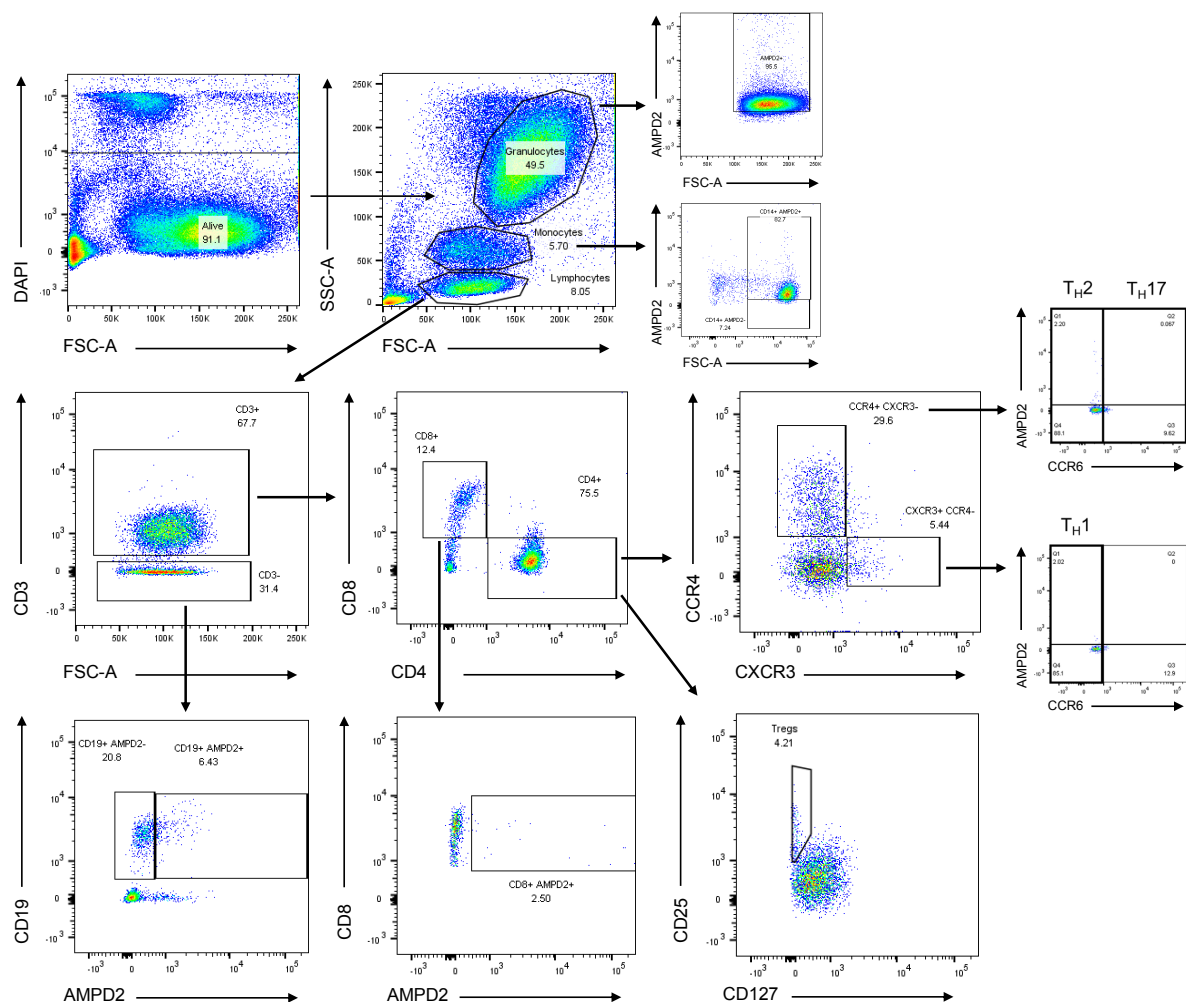


Abbildung 3.2 Gating-Strategie.

Humane Leukozyten am Beispiel einer gesunden Spenderin. Nach Ausschluss toter Zellen mittels DAPI wurden die Leukozytenpopulationen im Forward-Scatter- und Side-Scatter-Plot identifiziert. Die Unterscheidung der Lymphozytenpopulationen erfolgte anhand der Oberflächenexpression von CD3, CD4, CD8, CXCR3, CCR4, CCR6, CD19, CD25 und CD127. Legende: FSC, Forward Scatter; SSC, Side Scatter. Modifiziert aus Ehlers et al.⁵⁵

3.4.2 Reduktion der Genexpression von AMPD2 mittels RNA-Interferenz

Die Reduktion der Genexpression in HEK293 und U-937 Zellen erfolgte mittels Short hairpin RNA (shRNA). Die Sequenzen der Haarnadelstrukturen sind in Tabelle 3.4 angegeben. Zur Kontrolle wurden ein leeres Grundgerüst des lentiviralen Vektors pLKO.1 puro sowie ein Plasmid mit scrambled (scr) shRNA mitgeführt (Addgene #8453, #1864). Nach Isolation der Plasmid-DNA (NucleoBond® Xtra EF, Macherey-Nagel) erfolgte die Transfektion von HEK293 Zellen mit 30 µg. Die Effizienz der Reduktion der Proteinexpression wurde anschließend mittels Western Blot des Gesamtzelllysats ermittelt. Die effektivsten shRNA-Sequenzen sh3 und sh8 wurden daraufhin zur Herstellung lentiviraler Partikel genutzt. Es erfolgte die Cotransfektion von HEK293 Zellen mit dem jeweiligen Expressionsplasmid, dem Verpackungsplasmid pPAX2 sowie dem Envelope-Plasmid pVSVG in einer Gesamtmenge von 30 µg im Verhältnis 3:2:1 mittels Calcium-Phosphat-Präzipitation. Die nach 48 Stunden gewonnenen Virenüberstände wurden mit 10 µg/mL Polybren (Sigma-Aldrich) versetzt. Zur Etablierung eines stabilen Knockdowns von AMPD2 wurden HEK293 und U-937 Zellen in einer 24-Loch-Platte nach Zugabe von 1 mL Virenüberstand durch zweistündige Zentrifugation bei 700xg und 32°C transduziert. Die Selektion der erfolgreich transduzierten Zellen erfolgte im Anschluss durch Zugabe von 1 µg/mL Puromycin (InvivoGen) zum Zellkulturmedium. Die Reduktion der Expression von AMPD2 auf Proteinebene wurde anschließend mittels Western Blot von Gesamtzelllysat und Membranfraktion der selektierten Zellen untersucht. Nach erfolgreicher Etablierung eines effizienten Knockdowns dienten die entsprechenden Zellen als Kontrollansatz zur Überprüfung der Spezifität der Oberflächenfärbung mittels Durchflusszytometrie.

Tabelle 3.4 shRNA-Sequenzen

sh1	CCGGCCAAGGCCAAATATCCCTTTACTCGAGTAAAGGGATATTTGGCCTTGGTTTTTG
sh2	CCGGGCGCTTCATCAAGCGGGCAATCTCGAGATTGCCGCTTGATGAAGCGCTTTTTG
sh3	CCGGGGGTATCTGGGAAGTACTTTGCTCGAGCAAAGTACTTCCAGATACCCTTTTTTG
sh4	CCGGCATCGCTTTGACAAGTTTAATCTCGAGATTAACCTTGCAAAGCGATGTTTTTG
sh5	CCGGGCACGTCTATGGATGGCAAATCTCGAGATTGCCATCCATAGACGTGCTTTTTG
sh6	CCGGATGTGCTGGAACGGGAGTTTCTCGAGGAACTCCCGTTCCAGCACATTTTTTTG
sh7	CCGGGCCTCTTTGATGTGTACCGTACTCGAGTACGGTACACATCAAAGAGGCTTTTTG
sh8	CCGGTCATGCTGGCTGAGAACATTTCTCGAGAAATGTTCTCAGCCAGCATGTTTTTTG

Übernommen aus Ehlers et al.⁵⁵

3.5 Differenzielle Analyse der Proteinexpression im Kontext von Entzündung

Das oben geschilderte Vorgehen stellt den Kern dieser Arbeit dar. Der einwandfreie Nachweis der Oberflächenexpression von AMPD2 ist Basis aller weiteren Untersuchungen. Zudem diente der beschriebene Spezifitätsnachweis der Oberflächenfärbung als Grundlage für die folgende

Analyse des Expressionsverhaltens von eAMPD2 in Abhängigkeit von verschiedenen Kulturbedingungen. Hier bietet die Durchflusszytometrie die Möglichkeit, durch Kopplung von Antikörpern mit verschiedenen Fluoreszenzfarbstoffen multiple Immunzellpopulationen parallel zu untersuchen. Auf diese Weise war auch die vergleichende Betrachtung der Expression der Ektonukleotidasen CD39 und CD73 möglich.

Das einleitend erörterte pro- und anti-inflammatorische Potential von Purinmetaboliten im extrazellulären Raum sowie die vorbeschriebenen Expressionsunterschiede der Ektonukleotidasen CD39 und CD73 im Rahmen von immunvermittelten Erkrankungen veranlassten uns zur Untersuchung der Oberflächenexpression von AMPD2 in diesem Kontext. Zu diesem Zweck wurden humane Immunzellen *in vitro* verschiedenen Immunstimuli ausgesetzt. Zum besseren Verständnis der Regulation wurde zusätzlich beispielhaft der Einfluss von Immunsuppressiva anhand von Dex und MTX sowie der Inhibition des sekretorischen Wegs mittels BFA und MN untersucht. Die Inkubationsbedingungen sind Tabelle 3.2 zu entnehmen.

Um auch den Einfluss inflammatorischer Zustände *in vivo* zu beleuchten, schlossen wir diesen Analysen die Untersuchung der Oberflächenexpression der Ektoenzyme auf PBMCs von Patient*innen mit RA im Vergleich zu einer gesunden Kontrollkohorte an. Die durchflusszytometrischen Messungen erfolgten entsprechend dem in Abschnitt 3.4.1 geschilderten Vorgehen.

Komplettiert wird dieser Abschnitt durch orientierende Experimente zur funktionellen Bedeutung von eAMPD2.

3.5.1 Patientenkollektiv

Es wurden 15 Patient*innen mit der klinischen Diagnose einer RA in unsere Untersuchungen eingeschlossen. Die Vorstellung erfolgte im Rahmen der Rh-GIOP-Studie der medizinischen Klinik mit Schwerpunkt Rheumatologie und Klinische Immunologie der Charité – Universitätsmedizin Berlin. Der Einschluss geschah unabhängig von der klinischen Krankheitsaktivität sowie der aktuellen immunsuppressiven Therapie. Die Krankheitsaktivität wurde anhand der schmerzhaften und geschwollenen Gelenke sowie der Entzündungsparaklinik (BSG, CRP) erfasst. Zusätzlich gewannen wir Proben gesunder Spender*innen, die hinsichtlich Geschlecht und Alter den Patient*innen angepasst ausgewählt wurden. Die Studie wurde in Einklang mit der Deklaration von Helsinki durchgeführt und die Blutentnahme erfolgte nach Aufklärung und mit schriftlichem Einverständnis auf Grundlage des Ethikvotums EA1/207/17 der Charité – Universitätsmedizin Berlin.

3.5.2 Bestimmung der Nukleosid- und Zytokinkonzentrationen

Zur Messung der extrazellulären Adenosinkonzentration wurden CD14+ Monozyten für 24 Stunden mit LPS und mit und ohne Zugabe von BFA stimuliert. Die Bestimmung der Adenosinkonzentration im Überstand erfolgte anschließend enzymatisch in einem fluorometrischen Assay (abcam).

Die TNF- α -Sekretion von PBMCs wurde mittels ELISA (R&D Systems) aus dem Überstand bestimmt. Dazu wurden je 10^6 PBMCs zunächst für 30 Minuten mit ATP, Adenosin, IMP oder Inosin präinkubiert und anschließend für zwei Stunden mit LPS stimuliert.

3.6 Statistische Analysen

Die statistischen Analysen wurden mit dem Programm GraphPad Prism durchgeführt. Bei der Untersuchung der Proben der gleichen Spenderin unter variablen Inkubationsbedingungen wurde der nicht-parametrische Wilcoxon-Vorzeichen-Rang-Test für gepaarte Proben angewendet. Zum Vergleich verschiedener Spendergruppen wurde der nicht-parametrische Mann-Whitney Test genutzt.

Zur Analyse der massenspektrometrischen Messungen wurde die Perseus Software (v1.6.2.1) verwendet. Der Vergleich der Proteinhäufigkeiten erfolgte mittels Zweistichproben-t-Test mit einem Grenzwert der Falscherkennungsrate von 5%.

4. Ergebnisse

Die im Folgenden aufgeführten Ergebnisse fanden Eingang in die Publikation:

Ehlers L, Kuppe A, Damerau A, Wilantri S, Kirchner M, Mertins P, Strehl C, Buttgerit F, Gaber T. Surface AMP deaminase 2 as a novel regulator modifying extracellular adenine nucleotide metabolism. *The FASEB Journal* 2021;35(7):e21684. doi: <https://doi.org/10.1096/fj.202002658RR>

4.1 Nachweis von AMPD2 an der Zelloberfläche

Der Nachweis von AMPD2 an der Zelloberfläche erfolgte wie oben beschrieben in drei sich ergänzenden Schritten. Zuvor identifizierten wir mithilfe von Daten des Human Protein Atlas AMPD2 als häufigste Isoform der AMP-Desaminasen in humanen Leukozyten (Publikation Figure 2A⁵⁵), sodass sich die im Folgenden dargestellten Ergebnisse auf dieses Isoenzym beschränken.⁶⁰

Der erste Nachweisschritt der Membranlokalisierung bestand in der Herstellung einer geeigneten Membranfraktion gefolgt von der IP von AMPD2 mithilfe eines spezifischen Antikörpers. Als einleitendes Experiment zur Etablierung eines geeigneten Modellsystems untersuchten wir

zunächst orientierend die intrazelluläre und extrazelluläre Expression von AMPD2 in verschiedenen Zelllinien. Durchflusszytometrisch konnten wir AMPD2 an der Zelloberfläche nachweisen (Publikation Supplementary Figure 2A⁵⁵). HEK293 und U-937 Zellen zeichneten sich durch die deutlichste Oberflächenexpression aus. Anhand dieser Zellen wurde die Membranständigkeit des Enzyms weiter untersucht. Zunächst bestätigten wir massenspektrometrisch die Identität des Zielproteins: Im Vergleich zur Isotypkontrolle wurde AMPD2 in der IP mittels Anti-AMPD2-Antikörper Klon QQ13 ($\log_2(\text{Anreicherungsfaktor})=16,30$; $-\log_{10}(\text{p-Wert})=5,52$ (LFQ)) signifikant angereichert und stellte das häufigste Protein dar. Die Spezifität ließ sich auch für den polyklonalen Anti-AMPD2-Antikörper ($\log_2(\text{Anreicherungsfaktor})=11,24$; $-\log_{10}(\text{p-Wert})=6,22$ (LFQ)) bestätigen (Publikation Supplementary Table S1, Supplementary Figure S2C⁵⁵). Zweiter Baustein dieses Experiments war die Gewinnung einer Membranfraktion. Aufgrund des reichlichen Bestands an zytosolischem AMPD2 musste sich diese insbesondere durch eine große Reinheit auszeichnen. Durch Anpassung der Inkubationsbedingungen gelang die Isolation von Membranprotein mit minimaler zytosolischer Kontamination (Publikation Supplementary Figure 2D⁵⁵). Diesen Etablierungsschritten folgte der Nachweis von membranständigem AMPD2 mittels Western Blot nach IP aus Membranfraktionen von HEK293 und U-937 Zellen (Abbildung 4.1a). Dieses Ergebnis ließ sich massenspektrometrisch bestätigen ($\log_2(\text{Anreicherungsfaktor})=5,82$; $-\log_{10}(\text{p-Wert})=3,85$ (LFQ)). Nach Etablierung im Modellsystem gelang gleichermaßen der Nachweis in humanen Monozyten ($\log_2(\text{Anreicherungsfaktor})=4,2$; $-\log_{10}(\text{p-Wert})=2,87$ (LFQ)) (Abbildung 4.1a, Publikation Supplementary Table S4⁵⁵).

Supplementary Figure S2D der Publikation⁵⁵ zeigt, dass die in diesem Schritt verwendete Membranfraktion auch Anteile subzellulärer Membranen enthält. Aus diesem Grund folgte in einem nächsten Experiment der Oberflächennachweis von AMPD2 mittels Oberflächenbiotinylierung von HMEC-1 und U-937 Zellen sowie CD14+ Monozyten (Abbildung 4.1b). Massenspektrometrisch bestätigte sich die signifikante Anreicherung von AMPD2 in der biotinylierten Fraktion im Vergleich zur nicht biotinylierten Kontrolle ($\log_2(\text{Anreicherungsfaktor})=3,70$; $-\log_{10}(\text{p-Wert})=2,00$ (LFQ)) (Publikation Figure 2D, Supplementary Table S2⁵⁵).

Als dritte Säule etablierten wir den Nachweis von AMPD2 mittels Oberflächenfärbung. Der eingangs gezeigte durchflusszytometrische Nachweis von eAMPD2 auf verschiedenen Zelllinien wurde in diesem Schritt auch auf humanen Leukozyten erfolgreich durchgeführt. Einen Einfluss mangelnder Zellintegrität auf die Färbeintensität konnten wir mittels Annexin V und Dead Cell Removal ausschließen (Publikation Supplementary Figure S3F⁵⁵). Die Färbung ließ sich erfolgreich mittels überschüssigen unkonjugierten Antikörpers blockieren (Publikation Supplementary Figure S1E⁵⁵). Als weiteren Spezifitätsnachweis der Oberflächenfärbung etablierten wir eine stabile Reduktion der Genexpression von AMPD2 mittels RNA-Interferenz in

HEK293 und U-937 Zellen. Nach Bestätigung der Reduktion der intrazellulären und membranständigen AMPD2-Expression mittels Western Blot (Abbildung 4.1c) reproduzierten wir diesen Effekt durchflusszytometrisch in der Oberflächenfärbung (Abbildung 4.1c). In der Immunfluoreszenzmikroskopie konnten wir zudem die Lokalisation von eAMPD2 an der Zelloberfläche visualisieren (Abbildung 4.1d).

Zusammenfassend konnten wir die Oberflächenexpression von AMPD2 auf humanen Leukozyten mit drei unabhängigen Methoden verifizieren.

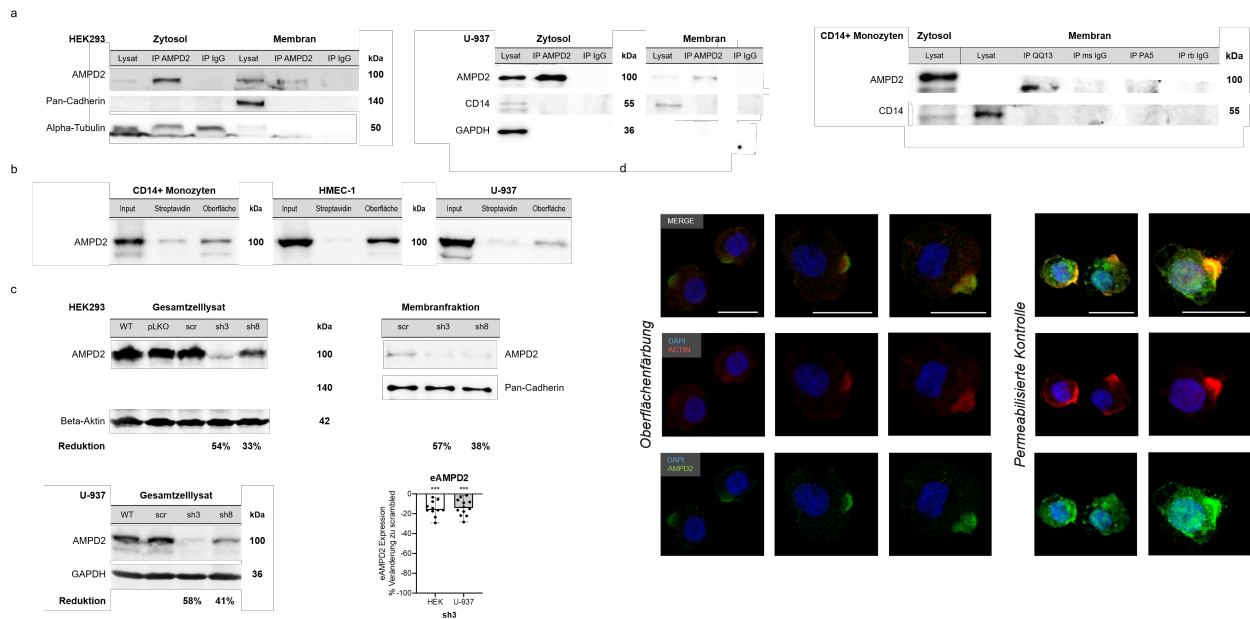


Abbildung 4.1 Oberflächenexpression von AMPD2.

(a) Western Blot der IP von AMPD2 aus zytosolischen und Membranfraktionen von HEK293 Zellen, U-937 Zellen und CD14+ Monozyten gegenüber einer Isotypkontrolle (IP IgG). (b) Nachweis von AMPD2 im Western Blot nach Isolation des Oberflächenproteins mittels Oberflächenbiotinylierung (Oberfläche) im Vergleich zur nicht biotinylierten Kontrolle (Streptavidin). (c) Western Blot Analyse nach Knockdown von AMPD2 mittels RNA-Interferenz in HEK293 und U-937 Zellen. Das nebenstehende Balkendiagramm zeigt die prozentuale Reduktion der Oberflächenfärbung in der Durchflusszytometrie nach Transduktion mit sh3 als Ratio der gMFI (Färbung/Kontrolle) im Vergleich zur Kontrolle mit scrambled shRNA. (d) Immunfluoreszenzmikroskopie von AMPD2 (grün), Aktin (rot) und DAPI (blau) am Beispiel von U-937 Zellen. Die Balkendiagramme zeigen Median und Maximum. ***p<0,001, Wilcoxon-Vorzeichen-Rang-Test. Legende: gMFI, geometrisches Mittel der Fluoreszenzintensität; scr, scrambled. Modifiziert aus Ehlers et al.⁵⁵

4.2 Oberflächenexpression von AMPD2 auf humanen Immunzellen unter inflammatorischen Bedingungen

Das zweite Ziel dieser Arbeit umfasste den Einfluss entzündlicher Verhältnisse auf die leukozytäre Expression von eAMPD2. In einem initialen Experiment an HEK293 und U-937 Zellen zeigten wir zunächst grundsätzlich die Veränderlichkeit der eAMPD2-Expression. Die Inkubation mit BFA und MN – zwei Inhibitoren des sekretorischen Wegs – führte zu einer signifikanten Reduktion der Oberflächenexpression von AMPD2 (HEK293: BFA, p=0,0078 und MN, p= 0,0039; U-937: BFA, p=0,0039 und MN, p= 0,0039) (Publikation Supplementary Figure

S2I⁵⁵). Nach erfolgreicher Etablierung der Oberflächenfärbung von eAMPD2 auf humanen Leukozyten untersuchten wir durchflusszytometrisch die differenzielle Expression auf verschiedenen Immunzellpopulationen. Es zeigte sich eine ausgeprägte Expression auf B-Zellen, Monozyten und Granulozyten, während die untersuchten T-Zell-Populationen (T_H1-, T_H2-, und T_H17-Zellen, Tregs sowie CD8+ T-Zellen) eAMPD2 nur schwach oder gar nicht exprimierten (Abbildung 4.2a). Bezüglich der monozytären Subpopulationen stellten wir keine Unterschiede in der Expressionsintensität fest (Publikation Supplementary Figure S1E⁵⁵).

In einem nächsten Schritt interessierte uns der Einfluss inflammatorischer Stimuli auf die leukozytäre Oberflächenexpression von AMPD2. Zu diesem Zweck ermittelten wir zunächst die Kinetik der eAMPD2-Expression auf PBMCs unter Immunstimulation *in vitro*. Monozyten zeigten eine maximale Steigerung der Oberflächenexpression von AMPD2 nach 20-24-stündiger Inkubation mit LPS, während auf Lymphozyten keine Zunahme zu beobachten war (Publikation Supplementary Figure S3E⁵⁵). Im Folgenden werden aus diesem Grund ausschließlich die monozytären Ergebnisse ausgeführt. Zunächst bestätigten wir den Anstieg der eAMPD2-Expression auf Monozyten durch TLR-Stimulation über 24 Stunden im Vergleich zu unbehandelten Kontrollzellen. Agonisten an den TLR1-8 mit Ausnahme von TLR3 bewirkten eine signifikante Steigerung der Oberflächenexpression von AMPD2 ($p=0,0156$) (Abbildung 4.2b). Der ausgeprägteste Effekt wurde durch den TLR4-Agonisten LPS erzielt und konnte auf magnetisch sortierten CD14+ Monozyten in Monokultur reproduziert werden (Abbildung 4.2c). Die Steigerung der eAMPD2-Expression in stimulierten Monozyten konnten wir zudem mittels Western Blot von monozytären Membranfraktionen bestätigen (Publikation Figure 4F⁵⁵). Darüber hinaus verifizierten wir die zuvor in Zelllinien demonstrierte Reduktion der eAMPD2-Expression durch Inhibition des Golgi-Transports ($p=0,0078$) (Abbildung 4.2c).

Der Einfluss dieser Immunstimuli in Zellkultur legte zugleich die Frage nah, ob umgekehrt auch durch immunsuppressive Medikamente Einfluss auf die Oberflächenexpression von AMPD2 genommen werden könnte. Beispielhaft untersuchten wir diesbezüglich den Effekt von Dex und MTX *in vitro*. Durch simultane Inkubation mit 10^{-5} M Dex – einer Konzentration, die einer Hochdosis-Glucocorticoidtherapie entspricht^{61 62} – wurde die monozytäre Expressionssteigerung von eAMPD2 durch LPS reduziert. Dieses Ergebnis erreichte jedoch nicht ganz die statistische Signifikanz ($p= 0,0547$) (Abbildung 4.2d). Die Inkubation mit Dex allein bewirkte hingegen einen signifikanten Anstieg der eAMPD2-Expression ($p= 0,0078$) (Publikation Supplementary Figure 5B⁵⁵). Im Gegensatz dazu hatte die Inkubation mit MTX keinen Einfluss auf die Oberflächenexpression von AMPD2 (Abbildung 4.2e).

Nachdem wir die Veränderung der monozytären eAMPD2-Expression durch Immunstimulation *in vitro* nachweisen konnten, interessierte uns der Einfluss entzündlicher Zustände *in vivo*. Aus diesem Grund analysierten wir in der Folge PBMCs von Patient*innen mit RA im Vergleich zu geschlechts- und altersgematchten gesunden Kontrollen. Die Charakteristika der untersuchten

Individuen sind Table 3 der Publikation⁵⁵ zu entnehmen. Die eAMPD2-Expression wurde unmittelbar nach Isolation sowie nach 24-stündiger Inkubation mit und ohne LPS ermittelt. Im Vergleich zur Kontrollgruppe zeigten Lymphozyten ($p=0,0127$) und Monozyten ($p=0,0332$) von RA-Patient*innen eine signifikant höhere Grundexpression von eAMPD2 (Abbildung 4.2f). Im Gegensatz dazu zeigten Monozyten nach LPS-Stimulation tendenziell eine geringere Zunahme des Expressionsniveaus im Vergleich zu den gesunden Spender*innen ($p=0,1431$) (Publikation Figure 6B⁵⁵).

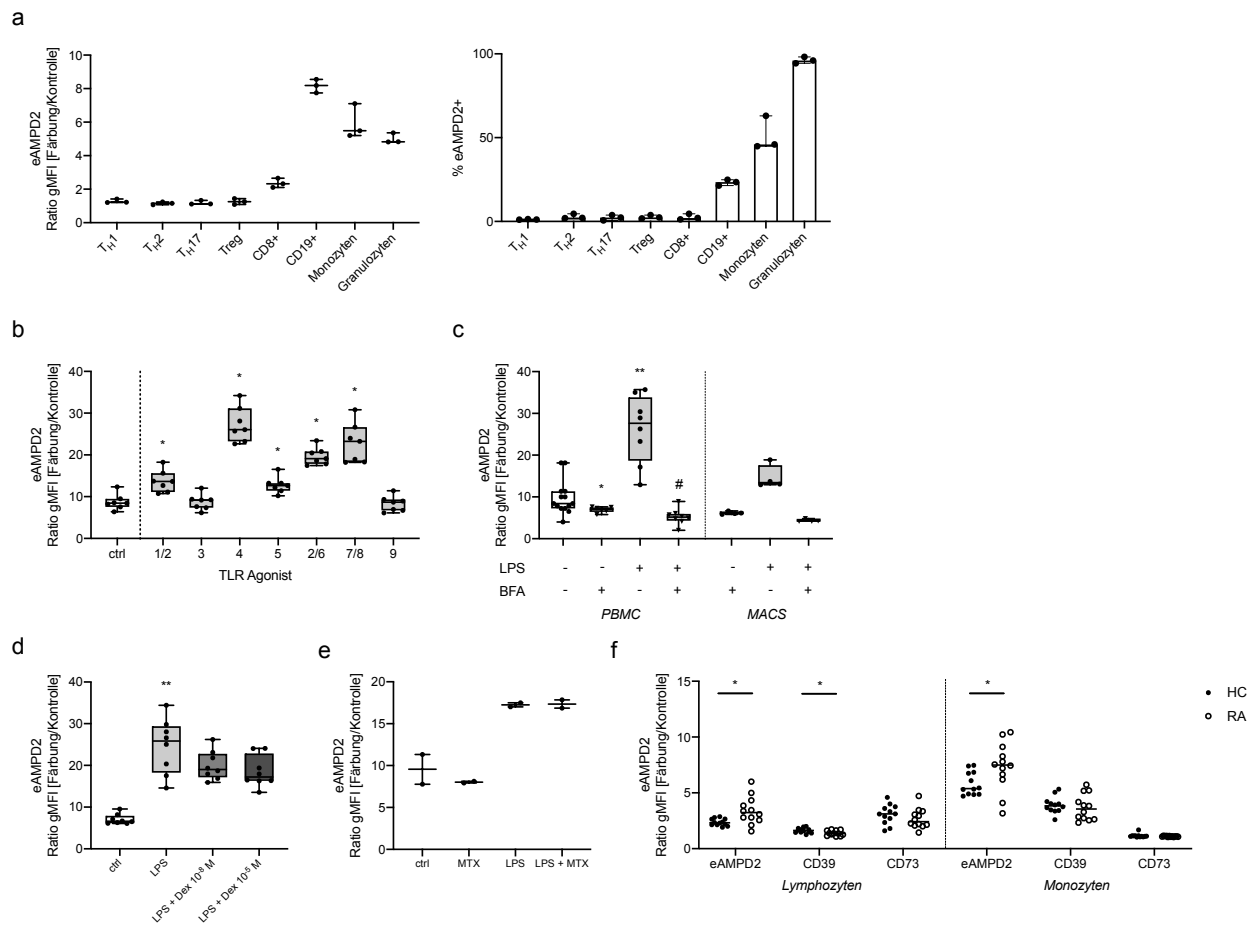


Abbildung 4.2 eAMPD2-Expression unter inflammatorischen Bedingungen mittels Durchflusszytometrie.

(a) eAMPD2 auf humanen Leukozytenpopulationen nach Gating entsprechend Abbildung 3.2. (b) eAMPD2 auf humanen Monozyten nach Immunstimulation durch Agonisten an TLR1/2 (Pam3SCK4), TLR3 (Poly (I:C)), TLR4 (LPS), TLR5 (Flagellin), TLR2/6 (FSL-1), TLR7/8 (Resiquimod) und TLR9 (ODN 2006). (c) eAMPD2 auf humanen Monozyten nach Immunstimulation mit LPS und/oder Inhibition des sekretorischen Wegs mit BFA inkubiert in Co-Kultur mit Lymphozyten (PBMC) oder als Monokultur nach magnetischer Zellsortierung mit Anti-CD14-MicroBeads (MACS). (d) eAMPD2 auf humanen Monozyten nach Immunstimulation mit LPS ± Dex. (e) eAMPD2 auf humanen Monozyten nach Inkubation mit LPS und/oder MTX. (f) Expression von eAMPD2, CD39 und CD73 auf PBMCs von gesunden Spender*innen (HC) im Vergleich zu RA-Patient*innen (RA). Boxplots zeigen Median, oberes und unteres Quartil sowie Minimum und Maximum; Balkendiagramme zeigen Median und Maximum; Linien im Streudiagramm entsprechen dem Median. (b-e) $*p<0,05$, $**p<0,01$ im Vergleich zur unbehandelten Kontrolle, $\#p<0,01$ im Vergleich zu LPS, Wilcoxon-Vorzeichen-Rang-Test. (f) $*p<0,05$, Mann-Whitney Test. Legende: BFA, Brefeldin A; ctrl, unbehandelte Kontrolle; Dex, Dexamethason; gMFI, geometrisches Mittel der Fluoreszenzintensität; HC, gesunde Kontrollen; LPS, Lipopolysaccharid; MTX, Methotrexat; TLR, Toll-like-Rezeptor. Modifiziert aus Ehlers et al.⁵⁵

Insgesamt zeigen diese Ergebnisse eine Steigerung der eAMPD2-Expression durch inflammatorische Einflüsse sowohl *in vitro* als auch *in vivo*.

4.3 Regulation und anti-inflammatorisches Potential extrazellulärer Adeninmetabolite

Nachdem wir Veränderungen der eAMPD2-Expression unter inflammatorischen Bedingungen zeigen konnten, untersuchten wir als drittes Ziel dieser Arbeit näherungsweise die funktionelle Bedeutung der Desaminase auf der Zelloberfläche. Entsprechend unserer in Abbildung 2.1 dargestellten Hypothese vermuteten wir eine Reduktion der extrazellulären Adenosinproduktion als Folge des vermehrten AMP-Verbrauchs durch eAMPD2. Folglich untersuchten wir den Adenosingehalt im Überstand von Immunzellen unter Bedingungen hoher und niedriger eAMPD2-Expression. Entgegen unserer ursprünglichen Annahme sahen wir im Überstand von CD14+ Monozyten nach Stimulation mit LPS – dem Zustand maximaler eAMPD2-Expression – die höchste extrazelluläre Adenosinkonzentration. In der unbehandelten Kontrolle sowie nach zusätzlicher Inhibition des Golgi-Transports – Bedingungen mit moderater eAMPD2-Expression – zeigten sich niedrigere Niveaus für eADO (Publikation Figure 6C⁵⁵).

Neben dem Einfluss auf den extrazellulären Adosinhaushalt stellt die extrazelluläre IMP-Produktion einen bedeutenden neuen Aspekt der Beschreibung von eAMPD2 als Ektoenzym dar. Um die Bedeutung dieses Metaboliten im Kontext von Entzündung zu untersuchen, präinkubierten wir PBMCs mit verschiedenen Adeninderivaten und bestimmten die TNF- α -Sekretion nach Immunstimulation. Im Vergleich zur unbehandelten Kontrolle war die TNF- α -Konzentration im Überstand nach Behandlung mit IMP reduziert (Publikation Figure 6D⁵⁵).

Diese Untersuchungen zeigen das anti-inflammatorische Potential von extrazellulärem IMP auf humane Immunzellen, während sich eine Reduktion der eADO-Produktion im Kontext einer hohen eAMPD2-Expression nicht nachweisen ließ.

5. Diskussion

Diese Arbeit zeigte erstmals die Bedeutung der AMP-Desaminase 2 im extrazellulären Purinstoffwechsel von Immunzellen. Durch die kombinierte Anwendung von Methoden der Proteomanalytik und Oberflächenfärbungen identifizierten wir eAMPD2 als neues Ektoenzym auf primären humanen Leukozyten mit einer gesteigerten Expression nach Immunstimulation *in vitro* sowie bei RA-Patient*innen. Die erhöhte Expression war nicht mit einer Reduktion des eADO-Gehalts verbunden, während IMP anti-inflammatorische Wirkung zeigte. Mögliche Mechanismen der Membranlokalisation von AMPD2 werden im Diskussionsteil der dieser Dissertationsschrift zugrundeliegenden Publikation⁵⁵ besprochen. In den folgenden Abschnitten

steht die pathophysiologische Rolle der AMP-Desaminierung sowie ihre Einordnung in den extrazellulären Purinmetabolismus im Mittelpunkt.

5.1 Pathophysiologische Bedeutung von AMPD2

Die Erstbeschreibung der Oberflächenexpression von AMPD2 auf humanen Immunzellen ordnet dieses Enzym in den neuen Kontext des extrazellulären Purinmetabolismus ein. Im Rahmen dieser Diskussion soll die Rolle der extrazellulären AMP-Desaminierung umfänglich diskutiert werden. Zu diesem Zweck ist es hilfreich, auch die Physiologie des zytosolischen Enzyms zu berücksichtigen. Mit der Desaminierung von AMP zu IMP katalysiert AMPD einen von drei Schritten des Purinnukleotidzyklus.⁶³ Dieser erstmals 1971 von Lowenstein beschriebene Stoffwechselweg recycelt AMP über zwei Zwischenschritte unter Produktion von Ammoniak und Fumarat.⁶⁴ Damit sichert AMPD einerseits das intrazelluläre Gleichgewicht der Purinnukleotide und ist indirekt über Intermediate am Citratzyklus beteiligt.⁶³ Durch den alternativen Abbau von AMP hat AMPD zudem Einfluss auf die für den zellulären Energiestatus bedeutsame ATP:AMP-Ratio: Plaideau et al. wiesen einen Anstieg von AMP durch pharmakologische Inhibition von AMPD sowie im Skelettmuskel von Mäusen mit einem Knockout des *AMPD1*-Gens nach.⁶⁵ Dieser Anstieg ging mit einer gesteigerten Aktivität der AMP-aktivierten Proteinkinase (AMPK) – dem Energiesensor der Zelle – einher. Die Autor*innen diskutieren in diesem Kontext einen Benefit der AMPD-Inhibition durch vermehrte AMPK-Aktivierung in Energie-depletierten Zellen. Eine Aktivierung der AMPK durch Hemmung von AMPD ist auch als Wirkmechanismus von Metformin diskutiert worden.⁶⁶ Umgekehrt argumentieren Hancock et al., dass die Aktivität von AMPD die Akkumulation von intrazellulärem AMP verhindert und somit die Regeneration von ATP durch die Adenylatkinase ermöglicht.⁶⁷ Diese Ambiguität spiegelt sich auch in den beschriebenen klinischen Konsequenzen einer veränderten AMPD-Aktivität wider. Bereits 1978 wiesen Fishbein et al. einen muskulären AMPD-Mangel bei Patienten mit Muskelschwäche und –krämpfen nach.⁶⁸ Im Gegensatz dazu zeigten Norman et al. die hohe Prävalenz dieses Enzymmangels in Individuen ohne muskuläre Beschwerden.⁶⁹ Untersuchungen am Herzmuskel weisen hingegen auf den potentiellen Nutzen einer reduzierten AMPD-Aktivität hin. Bei Patient*innen mit Herzinsuffizienz war das Vorliegen von Nonsense-Mutationen in *AMPD1*, die mit einer reduzierten Aktivität der AMP-Desaminase einhergehen, mit einer besseren Prognose assoziiert.^{70 71} Smolenski et al. diskutieren die größere Verfügbarkeit von Adenosin und dessen kardioprotektive Effekte als mögliche zugrundeliegende Mechanismen.⁷² Durch Reduktion der AMP-Desaminierung wird AMP vermehrt über 5'-Nukleotidasen zu Adenosin verstoffwechselt. Tatsächlich konnten im Skelettmuskel homozygoter Träger*innen der C34T Nonsense-Mutation erhöhte Adenosinkonzentrationen im Vergleich zu heterozygoten Individuen nachgewiesen werden.⁷³

Während Veränderungen der muskulären AMPD1 somit mit einem milden klinischen Phänotyp einhergehen, führen Mutationen von AMPD2 zu Pontozerebellärer Hypoplasie Typ 9, einem Krankheitsbild mit schwerer neurologischer Entwicklungsstörung.⁷⁴ Pathophysiologisch konnte in Fibroblasten von betroffenen Patient*innen eine Reduktion des GTP-Gehalts nachgewiesen werden, der mit einer Beeinträchtigung der Proteinbiosynthese einhergeht.⁷⁵

Im Mittelpunkt dieser Dissertation steht jedoch im Gegensatz zur bisher geschilderten Pathophysiologie weniger die Bedeutung von AMPD in der Bereitstellung von Zellbausteinen und Energie, sondern vielmehr ihre Relevanz in Bezug auf Entzündungsmediation. In diesem Kontext ist insbesondere der Wirkmechanismus von MTX von Interesse. Neben der Hemmung der Dihydrofolatreduktase wird die Beteiligung eines weiteren Enzyms an der Wirkung des immunmodulatorischen Medikaments diskutiert. MTX-Polyglutamate hemmen die 5-Aminoimidazol-4-carboxamid-Ribonukleotid (AICAR)-Formyltransferase (ATIC).⁷⁶ Cronstein et al. zeigten passend dazu erhöhte Konzentrationen von AICAR unter MTX-Therapie.⁷⁷ Dieser Metabolit steigert durch Hemmung von AMPD und ADA die Verfügbarkeit von anti-entzündlichem Adenosin.⁷⁸ Die Vermittlung der anti-inflammatorischen Wirkung von MTX durch eADO konnte durch Umkehr der Effekte mithilfe von Adenosinrezeptor-Antagonisten bestätigt werden.⁷⁷ Während dieser Mechanismus jedoch auf der Hemmung der zytosolischen Enzyme beruht und den Transport der Adeninmetabolite über die Plasmamembran voraussetzt, beschreiben wir mit eAMPD2 einen neuen direkten Mediator des extrazellulären Adenosinhaushalts von Immunzellen.

5.2 eAMPD2 im Kontext des extrazellulären Purinmetabolismus

Der extrazelluläre Purinmetabolismus stellt ein komplexes System dar, das multiple potentielle pharmakotherapeutische Angriffspunkte bietet. Beispielsweise hemmt Clopidogrel als Antagonist am P2Y₁₂-Rezeptor die ADP-abhängige Thrombozytenaggregation, während Dipyridamol die Aufnahme von eADO über ENT verhindert und eine Adenosin-vermittelte Vasodilatation hervorruft.⁷⁹ Der Nutzen dieser Mechanismen in der Therapie inflammatorischer Erkrankungen wurde kürzlich im Rahmen der TIMERA (Ticagrelor in Methotrexate-Resistant Rheumatoid Arthritis)-Studie untersucht.⁸⁰ Eine kleine Kohorte von Patient*innen mit MTX-resistenter RA erhielt neben MTX über einen Monat Ticagrelor – einen Thrombozytenaggregationshemmer, der neben dem P2Y₁₂-Antagonismus den Adenosintransporter ENT1 hemmt. Es wurde eine Reduktion der Krankheitsaktivität unter der zusätzlichen Therapie beobachtet, die die Autor*innen auf einen Anstieg von anti-inflammatorischem eADO zurückführen. Das bessere Verständnis des extrazellulären Purinhaushalts im Rahmen von Entzündung ist somit auch bedeutsam für die Entwicklung neuer therapeutischer Ansätze.

Die Oberflächenexpression von AMPD2 bietet drei potentielle Einflussmöglichkeiten auf den extrazellulären Purinmetabolismus: (i) durch den beschleunigten Abbau von extrazellulärem ATP, (ii) durch eine Reduktion von eADO durch alternativen Abbau des Ausgangsstoffs AMP und (iii) durch die extrazelluläre Produktion von IMP. Unsere Analysen der Adenosinkonzentration im Überstand weisen darauf hin, dass die Limitation der eADO-Produktion eine untergeordnete Rolle spielt. Mit der Reduktion des extrazellulären ATP-Gehalts hingegen würde eAMPD2 eine synergistische Funktion mit CD39 zukommen. Diese Hypothese ist im Einklang mit dem von uns beschriebenen Expressionsmuster des Ektoenzym. Unsere Analysen zeigten eine ausgeprägte Oberflächenexpression von AMPD2 auf B-Zellen, Monozyten und Granulozyten. Damit ähnelt sie der von CD39.⁸¹⁻⁸⁴ Übereinstimmungen in der Regulation der beiden Ektoenzyme wurden auch in der Korrelation der monozytären Grundexpression (Publikation Supplementary Figure 4B⁵⁵) sowie einer vergleichbaren Modulation durch TLR-Stimulation (Publikation Figure 4B⁵⁵) deutlich. Dieses synchrone Verhalten von eAMPD2 und CD39 könnte auf eine gemeinsame Rolle in der Entzündungskontrolle durch Beschleunigung des ATP-Abbaus hindeuten. Die anti-inflammatorische Funktion von CD39 zeigten Finn et al. 2015, indem sie eine verminderte Sekretion von Entzündungsmediatoren durch Überexpression von CD39 und CD73 in Fibroblasten-artigen Synoviozyten nachwies.⁸⁵ Umgekehrt fallen CD39^{-/-} Mäuse durch Gefäßentzündung auf.⁸⁶ Für eAMPD2 liegen vergleichbare Daten noch nicht vor. Eine Steigerung der intrazellulären AMPD2-Expression unter Einfluss pro-inflammatorischer Zytokine konnten Endo et al. jedoch 2014 in Chondrozyten nachweisen.⁸⁷

CD73 wird neben Immunzellen (dendritische Zellen, B-Zellen, zytotoxische T-Zellen) auch auf mesenchymalen Stromazellen sowie Endothelzellen exprimiert.^{82 83 88-91} Im Gegensatz zu CD39 ist die Expression dieser Ektonukleotidase auf Monozyten jedoch minimal (Publikation Supplementary Figure S4D⁵⁵). Ausgeprägt ist CD73 hingegen auf Makrophagen zu finden.⁹²⁻⁹⁴ Diese vorherrschende Rolle auf gewebeständigen Zelltypen ist vereinbar mit der kurzen Halbwertszeit von Adenosin, die eine Produktion am Ort des Entzündungsgeschehens erforderlich macht.⁹⁵ Im Gegensatz dazu wird mit der Oberflächenexpression von AMPD2 IMP als langlebigerer anti-entzündlicher Mediator eingeführt, der das bestehende System der Ektonukleotidasen ergänzt. Viegas et al. wiesen für Inosinderivate eine Halbwertszeit von 15 Stunden nach.⁹⁶ Zusätzlich zeigten Qiu et al. eine Reduktion der Migration neutrophiler Granulozyten unter Einfluss von IMP.⁹⁷ Unser Nachweis des anti-inflammatorischen Potentials von extrazellulärem IMP unterstützt die Hypothese von eAMPD2 als zusätzlichem Mediator des entzündlichen Milieus. Damit stehen unsere Ergebnisse im Gegensatz zur Aussage von Magalhães-Cardoso et al., die in ihrer Beschreibung von eAMPD an der neuromuskulären Endplatte IMP als „inaktiven Metaboliten [Übersetzung der Autorin]“ (S. 400)⁹⁸ bezeichnen.

Um die klinische Relevanz dieser Hypothese zu überprüfen, analysierten wir die eAMPD2-Expression auf PBMCs von RA-Patient*innen im Vergleich zu gesunden Kontrollspender*innen. Das erhöhte Expressionsniveau der Patientengruppe könnte einen Gegenregulationsmechanismus zur Eindämmung des chronischen Inflammationszustands darstellen, indem einerseits der Abbau von pro-inflammatorischem ATP beschleunigt wird und andererseits vermehrt entzündungshemmendes IMP entsteht. Eine Hochregulation bei chronisch-inflammatorischen Erkrankungen wurde zuvor auch für andere Proteine im extrazellulären Purinstoffwechsel beschrieben. Beispielhaft seien hier die Steigerung der Expression von CD39 und CD73 auf Monozyten von Uveitispatient*innen, von CD73 und dem A2AR auf synovialen neutrophilen Granulozyten und Monozyten im CIA-Mausmodell sowie die synoviale Anreicherung FOXP3+CD39+ Tregs bei RA-Patient*innen genannt.^{33 99 100} Die Regulation des extrazellulären Adenosinhaushalts ist jedoch komplex. So ist für Patient*innen mit ankylosierender Spondylitis und Psoriasis eine Reduktion der Expression von CD39, CD73, A1R und A2BR auf Makrophagen bzw. Tregs beschrieben. Eine signifikante Reduktion der lymphozytären CD39-Expression identifizierten wir auch in unserer RA-Kohorte. Signifikante Veränderungen der CD39- und CD73-Expression auf Monozyten waren nicht nachzuweisen (Abbildung 4.2f). Limitierend ist an dieser Stelle jedoch anzumerken, dass für eine differenzierte Analyse eine größere Patientenzahl sowie die detaillierte Betrachtung der verschiedenen Lymphozytenpopulationen notwendig wäre. Insgesamt lassen sich die beobachteten Veränderungen der Protagonisten des extrazellulären Adenosinstoffwechsels wie folgt interpretieren: Einerseits könnte eine verminderte extrazelluläre Adenosinproduktion einen Entzündungszustand hervorrufen oder aufrechterhalten und somit zur Pathogenese beitragen. Umgekehrt würde eine Hochregulation entsprechend einen Kontrollmechanismus darstellen, der dem Entzündungsprozess entgegenwirkt. Beide Erklärungsansätze legen einen potentiellen therapeutischen Angriffspunkt im extrazellulären Purinstoffwechsel bei der Behandlung chronisch-entzündlicher Zustände nahe. Ein spiegelbildliches Konzept befindet sich zur Therapie von Krebserkrankungen bereits in der klinischen Testung: Durch Blockade der Adenosinproduktion oder –wirkung wird ein Milieu geschaffen, das eine effizientere Anti-Tumor-Immunität erlaubt.³⁵⁻³⁹

5.3 Limitationen und Ausblick

In dieser Arbeit konnten wir erstmals die Oberflächenexpression von AMPD2 auf verschiedenen humanen Leukozytenpopulationen nachweisen und fanden Expressionsunterschiede unter inflammatorischen Bedingungen. Während diese Ergebnisse die Grundlage für die weitere Entschlüsselung der extrazellulären AMP-Desaminierung legen und das System der Ektoenzyme um einen weiteren Baustein ergänzen, sind weitere Analysen erforderlich, um die

Funktionalität und pathophysiologische Bedeutung von eAMPD2 zu verifizieren. Mit der Bestimmung des Adenosingehalts im Überstand CD14+ Monozyten im Zustand niedriger und hoher eAMPD2-Expression zeigten wir, dass eine erhöhte Oberflächenexpression von AMPD2 nicht mit einer Reduktion der extrazellulären Adenosinkonzentration verbunden war. Limitierend ist an dieser Stelle jedoch anzuführen, dass die Aktivität der Ektonukleotidasen CD39 und CD73 und damit deren Einfluss auf die Adenosinproduktion in diesem experimentellen Ansatz nicht eliminiert wurde, sodass die Bedeutung von eAMPD2 nur näherungsweise abgeleitet werden kann. Um diese differenzierter zu analysieren, wäre die isolierte Ausschaltung von eAMPD2 mittels Inhibition oder Gen-Knockout in einem zukünftigen Experiment notwendig.

Ähnlich verhält es sich mit der extrazellulären IMP-Produktion. Während der Nachweis des anti-entzündlichen Effekts von IMP das Modell von eAMPD2 als Modulator des inflammatorischen Milieus unterstützt, setzt diese Annahme die Funktionalität des Enzyms in der Plasmamembran voraus. Ein Funktionsnachweis wäre zur weiteren Beurteilung der physiologischen Relevanz des Ektoenzym folglich essentiell. Dieser würde die Bestimmung von extrazellulärem AMP und IMP im Überstand in An- und Abwesenheit von eAMPD2 erfordern. Aufgrund der molekularen Ähnlichkeit von AMP und IMP ist eine solche Analyse methodisch anspruchsvoll. Folglich werden weitere Studien notwendig sein, um die Funktionalität von eAMPD2 einwandfrei zu belegen.

Ergänzende Untersuchungen sind ebenfalls erforderlich, um die Regulation der eAMPD2-Expression im Detail zu eruieren. Während wir in der Analyse von PBMCs eine Hochregulation von eAMPD2 bei RA-Patient*innen nachweisen konnten, bleibt offen, welche Leukozyten-subpopulationen Anteil an dieser Expressionssteigerung haben. Eine differenzierte Analyse verschiedener Lymphozytengruppen sowie der Co-Expression von CD39 und CD73 wäre wünschenswert, um die Rolle von eAMPD2 im extrazellulären Purinstoffwechsel besser zu verstehen.

Ebenso erlaubt die Größe unserer Patientenkohorte nur eine orientierende Analyse des Einflusses von Krankheitsaktivität und immunmodulierenden Medikamenten auf die Expression von eAMPD2. Wir sahen weder eine Korrelation mit der Höhe des CRP-Werts als Marker für die Entzündungsaktivität noch mit der Höhe der aktuellen Glucocorticoiddosis. Aufgrund der kleinen Patientenzahl schließen diese Ergebnisse einen tatsächlichen Zusammenhang jedoch nicht aus. Weitere Studien, die eine solche Assoziation untersuchen, wären von Interesse, um eAMPD2 in die Pathophysiologie chronischer Entzündung einzuordnen.

In Bezug auf die klinische Einordnung unserer Ergebnisse interessiert eAMDP2 insbesondere als möglicher pharmakologischer Angriffspunkt. Zwar wurde die AMPD-Inhibition in anderem Kontext bereits als therapeutische Zielstruktur untersucht. Jedoch ist bei Hemmung der intrazellulären AMP-Desaminierung stets auch von umfangreichen metabolischen Konsequenzen auszugehen. Das selektive Ansteuern von eAMPD2 böte insofern den Vorteil

der gezielteren Beeinflussung des extrazellulären Purinmetabolismus und seiner Rolle in der Entzündungsmediation. Je nach klinischem Kontext können hier sowohl eine gesteigerte als auch eine reduzierte Wirkung anti-inflammatorischer Purinmetabolite wünschenswert sein. Dies ist vergleichbar mit der Beeinflussung der extrazellulären Adenosinwirkung. Während Inhibitoren von CD73 in der Therapie onkologischer Erkrankungen die Anti-Tumor-Immunität verstärken sollen,³⁵ wird das anti-entzündliche Potential von Adenosinrezeptor-Agonisten in der Therapie inflammatorischer Erkrankungen evaluiert.^{101 102}

Der Nutzen einer selektiven Hemmung von eAMPD2 im Gegensatz zu intrazellulärem AMPD2 lässt sich zudem am Beispiel der Adenosin-Desaminasen verdeutlichen. Im Gegensatz zur intrazellulären ADA1 liegt ADA2 gebunden an CD26 extrazellulär vor. Obwohl beide Enzyme die Desaminierung von Adenosin katalysieren, führen Loss-of-Function-Mutationen der jeweiligen Gene klinisch zu unterschiedlichen Krankheitsbildern.^{103 104} Auch experimentell konnte die Bedeutung der Enzymlokalisierung für die resultierende Pathophysiologie untermauert werden. In Endothelzellen aus humanen Nabelschnurvenen (HUVEC) führte die Reduktion der ADA2-Expression zur vermehrten Expression von Interferon- β trotz unbeeinträchtigter intrazellulärer ADA1-Aktivität. Durch extrazelluläre Zugabe von ADA1 zu siADA2-transfizierten Zellen konnte dieser Anstieg der Zytokinexpression jedoch reduziert werden.¹⁰⁵ Diese Ergebnisse unterstützen die Annahme einer eigenständigen Bedeutung der extrazellulären Enzymfunktion unabhängig von der Aktivität der intrazellulären Varianten. Das Verständnis der Oberflächenexpression von AMPD2 legt somit die Grundlage für die Etablierung eines weiteren therapeutischen Angriffspunkts im extrazellulären Purinmetabolismus.

6. Literaturverzeichnis

1. Burnstock G, Verkhratsky A. Evolutionary origins of the purinergic signalling system. *Acta Physiol (Oxf)* 2009;195(4):415-47. doi: 10.1111/j.1748-1716.2009.01957.x [published Online First: 2009/02/19]
2. Roberts JA, Vial C, Digby HR, Agboh KC, Wen H, Atterbury-Thomas A, Evans RJ. Molecular properties of P2X receptors. *Pflugers Arch* 2006;452(5):486-500. doi: 10.1007/s00424-006-0073-6 [published Online First: 2006/04/12]
3. Idzko M, Ferrari D, Eltzschig HK. Nucleotide signalling during inflammation. *Nature* 2014;509(7500):310-7. doi: 10.1038/nature13085 [published Online First: 2014/05/16]
4. Antonioli L, Blandizzi C, Pacher P, Haskó G. Immunity, inflammation and cancer: a leading role for adenosine. *Nat Rev Cancer* 2013;13(12):842-57. doi: 10.1038/nrc3613 [published Online First: 2013/11/15]
5. Chen JF, Eltzschig HK, Fredholm BB. Adenosine receptors as drug targets--what are the challenges? *Nat Rev Drug Discov* 2013;12(4):265-86. doi: 10.1038/nrd3955 [published Online First: 2013/03/29]
6. Antonioli L, Pacher P, Vizi ES, Haskó G. CD39 and CD73 in immunity and inflammation. *Trends Mol Med* 2013;19(6):355-67. doi: 10.1016/j.molmed.2013.03.005 [published Online First: 2013/04/23]
7. Ferretti E, Horenstein AL, Canzonetta C, Costa F, Morandi F. Canonical and non-canonical adenosinergic pathways. *Immunology letters* 2019;205:25-30. doi: 10.1016/j.imlet.2018.03.007 [published Online First: 2018/03/20]
8. Horenstein AL, Chillemi A, Zaccarello G, Bruzzone S, Quarona V, Zito A, Serra S, Malavasi F. A CD38/CD203a/CD73 ectoenzymatic pathway independent of CD39 drives a novel adenosinergic loop in human T lymphocytes. *Oncoimmunology* 2013;2(9):e26246. doi: 10.4161/onci.26246 [published Online First: 2013/12/10]
9. Dong RP, Kameoka J, Hegen M, Tanaka T, Xu Y, Schlossman SF, Morimoto C. Characterization of adenosine deaminase binding to human CD26 on T cells and its biologic role in immune response. *Journal of immunology (Baltimore, Md : 1950)* 1996;156(4):1349-55. [published Online First: 1996/02/15]
10. Cheleni FB, Elliott MR, Sandilos JK, Walk SF, Kinchen JM, Lazarowski ER, Armstrong AJ, Penuela S, Laird DW, Salvesen GS, Isakson BE, Bayliss DA, Ravichandran KS. Pannexin 1 channels mediate 'find-me' signal release and membrane permeability during apoptosis. *Nature* 2010;467(7317):863-7. doi: 10.1038/nature09413 [published Online First: 2010/10/15]
11. Eltzschig HK, Eckle T, Mager A, Küper N, Karcher C, Weissmüller T, Boengler K, Schulz R, Robson SC, Colgan SP. ATP release from activated neutrophils occurs via connexin 43 and modulates adenosine-dependent endothelial cell function. *Circ Res* 2006;99(10):1100-8. doi: 10.1161/01.res.0000250174.31269.70 [published Online First: 2006/10/14]
12. Qu Y, Misaghi S, Newton K, Gilmour LL, Louie S, Cupp JE, Dubyak GR, Hackos D, Dixit VM. Pannexin-1 is required for ATP release during apoptosis but not for inflammasome activation. *Journal of immunology (Baltimore, Md : 1950)* 2011;186(11):6553-61. doi: 10.4049/jimmunol.1100478 [published Online First: 2011/04/22]
13. Sawada K, Echigo N, Juge N, Miyaji T, Otsuka M, Omote H, Yamamoto A, Moriyama Y. Identification of a vesicular nucleotide transporter. *Proceedings of the National Academy of Sciences of the United States of America* 2008;105(15):5683-6. doi: 10.1073/pnas.0800141105 [published Online First: 2008/04/01]
14. Baldwin SA, Beal PR, Yao SY, King AE, Cass CE, Young JD. The equilibrative nucleoside transporter family, SLC29. *Pflugers Arch* 2004;447(5):735-43. doi: 10.1007/s00424-003-1103-2 [published Online First: 2003/07/03]
15. Gray JH, Owen RP, Giacomini KM. The concentrative nucleoside transporter family, SLC28. *Pflugers Arch* 2004;447(5):728-34. doi: 10.1007/s00424-003-1107-y [published Online First: 2003/07/12]

16. Young JD, Yao SY, Sun L, Cass CE, Baldwin SA. Human equilibrative nucleoside transporter (ENT) family of nucleoside and nucleobase transporter proteins. *Xenobiotica* 2008;38(7-8):995-1021. doi: 10.1080/00498250801927427 [published Online First: 2008/08/01]
17. Drury AN, Szent-Györgyi A. The physiological activity of adenine compounds with especial reference to their action upon the mammalian heart. *The Journal of physiology* 1929;68(3):213-37. doi: 10.1113/jphysiol.1929.sp002608 [published Online First: 1929/11/25]
18. Antonioli L, Csóka B, Fornai M, Colucci R, Kókai E, Blandizzi C, Haskó G. Adenosine and inflammation: what's new on the horizon? *Drug Discov Today* 2014;19(8):1051-68. doi: 10.1016/j.drudis.2014.02.010 [published Online First: 2014/03/13]
19. Antonioli L, Novitskiy SV, Sachsenmeier KF, Fornai M, Blandizzi C, Haskó G. Switching off CD73: a way to boost the activity of conventional and targeted antineoplastic therapies. *Drug Discov Today* 2017;22(11):1686-96. doi: 10.1016/j.drudis.2017.06.005 [published Online First: 2017/07/06]
20. Chen Y, Corriden R, Inoue Y, Yip L, Hashiguchi N, Zinkernagel A, Nizet V, Insel PA, Junger WG. ATP release guides neutrophil chemotaxis via P2Y2 and A3 receptors. *Science (New York, NY)* 2006;314(5806):1792-5. doi: 10.1126/science.1132559 [published Online First: 2006/12/16]
21. Elliott MR, Chekeni FB, Trampont PC, Lazarowski ER, Kadl A, Walk SF, Park D, Woodson RI, Ostankovich M, Sharma P, Lysiak JJ, Harden TK, Leitinger N, Ravichandran KS. Nucleotides released by apoptotic cells act as a find-me signal to promote phagocytic clearance. *Nature* 2009;461(7261):282-6. doi: 10.1038/nature08296 [published Online First: 2009/09/11]
22. Ferrari D, Chiozzi P, Falzoni S, Dal Susino M, Melchiorri L, Baricordi OR, Di Virgilio F. Extracellular ATP triggers IL-1 beta release by activating the purinergic P2Z receptor of human macrophages. *Journal of immunology (Baltimore, Md : 1950)* 1997;159(3):1451-8. [published Online First: 1997/08/01]
23. Parzych K, Zetterqvist AV, Wright WR, Kirkby NS, Mitchell JA, Paul-Clark MJ. Differential role of pannexin-1/ATP/P2X(7) axis in IL-1 β release by human monocytes. *FASEB journal : official publication of the Federation of American Societies for Experimental Biology* 2017;31(6):2439-45. doi: 10.1096/fj.201600256 [published Online First: 2017/03/02]
24. Schenk U, Westendorf AM, Radaelli E, Casati A, Ferro M, Fumagalli M, Verderio C, Buer J, Scanziani E, Grassi F. Purinergic control of T cell activation by ATP released through pannexin-1 hemichannels. *Science signaling* 2008;1(39):ra6. doi: 10.1126/scisignal.1160583 [published Online First: 2008/10/02]
25. Trautmann A. Extracellular ATP in the immune system: more than just a "danger signal". *Science signaling* 2009;2(56):pe6. doi: 10.1126/scisignal.256pe6 [published Online First: 2009/02/06]
26. Csóka B, Himer L, Selmečzy Z, Vizi ES, Pacher P, Ledent C, Deitch EA, Spolarics Z, Németh ZH, Haskó G. Adenosine A2A receptor activation inhibits T helper 1 and T helper 2 cell development and effector function. *FASEB journal : official publication of the Federation of American Societies for Experimental Biology* 2008;22(10):3491-9. doi: 10.1096/fj.08-107458 [published Online First: 2008/07/16]
27. Eltzschig HK, Thompson LF, Karhausen J, Cotta RJ, Ibla JC, Robson SC, Colgan SP. Endogenous adenosine produced during hypoxia attenuates neutrophil accumulation: coordination by extracellular nucleotide metabolism. *Blood* 2004;104(13):3986-92. doi: 10.1182/blood-2004-06-2066 [published Online First: 2004/08/21]
28. Haskó G, Szabó C, Németh ZH, Kvetan V, Pastores SM, Vizi ES. Adenosine receptor agonists differentially regulate IL-10, TNF-alpha, and nitric oxide production in RAW 264.7 macrophages and in endotoxemic mice. *Journal of immunology (Baltimore, Md : 1950)* 1996;157(10):4634-40. [published Online First: 1996/11/15]
29. Yago T, Tsukamoto H, Liu Z, Wang Y, Thompson LF, McEver RP. Multi-Inhibitory Effects of A2A Adenosine Receptor Signaling on Neutrophil Adhesion Under Flow. *Journal of*

- immunology (Baltimore, Md : 1950)* 2015;195(8):3880-9. doi: 10.4049/jimmunol.1500775 [published Online First: 2015/09/12]
30. Botta Gordon-Smith S, Ursu S, Eaton S, Moncrieffe H, Wedderburn LR. Correlation of low CD73 expression on synovial lymphocytes with reduced adenosine generation and higher disease severity in juvenile idiopathic arthritis. *Arthritis Rheumatol* 2015;67(2):545-54. doi: 10.1002/art.38959 [published Online First: 2014/11/25]
 31. Yan K, Xu W, Huang Y, Zhang Z, Huang Q, Xin KZ, Ma Y, Han L. Methotrexate restores the function of peripheral blood regulatory T cells in psoriasis vulgaris via the CD73/AMPK/mTOR pathway. *Br J Dermatol* 2018;179(4):896-905. doi: 10.1111/bjd.16560 [published Online First: 2018/03/25]
 32. Akhtari M, Zargar SJ, Mahmoudi M, Vojdani M, Rezaeimanesh A, Jamshidi A. Ankylosing spondylitis monocyte-derived macrophages express increased level of A2A adenosine receptor and decreased level of ectonucleoside triphosphate diphosphohydrolase-1 (CD39), A1 and A2B adenosine receptors. *Clinical rheumatology* 2018 doi: 10.1007/s10067-018-4055-9 [published Online First: 2018/03/11]
 33. Walscheid K, Neekamp L, Heiligenhaus A, Weinlage T, Holzinger D, Heinz C, Kasper M, Foell D. Peripheral blood monocytes reveal an activated phenotype in pediatric uveitis. *Clinical immunology (Orlando, Fla)* 2017 doi: 10.1016/j.clim.2017.09.014 [published Online First: 2017/09/20]
 34. Antonioli L, Fornai M, Blandizzi C, Pacher P, Hasko G. Adenosine signaling and the immune system: When a lot could be too much. *Immunology letters* 2019;205:9-15. doi: 10.1016/j.imlet.2018.04.006 [published Online First: 2018/04/28]
 35. Allard D, Chrobak P, Allard B, Messaoudi N, Stagg J. Targeting the CD73-adenosine axis in immuno-oncology. *Immunology letters* 2019;205:31-39. doi: 10.1016/j.imlet.2018.05.001 [published Online First: 2018/05/15]
 36. Figueiró F, Mendes FB, Corbelini PF, Janarelli F, Jandrey EH, Russowsky D, Eifler-Lima VL, Battastini AM. A monastrol-derived compound, LaSOM 63, inhibits ecto-5'nucleotidase/CD73 activity and induces apoptotic cell death of glioma cell lines. *Anticancer Res* 2014;34(4):1837-42. [published Online First: 2014/04/03]
 37. Häusler SF, Del Barrio IM, Diessner J, Stein RG, Strohschein J, Hönig A, Dietl J, Wischhusen J. Anti-CD39 and anti-CD73 antibodies A1 and 7G2 improve targeted therapy in ovarian cancer by blocking adenosine-dependent immune evasion. *Am J Transl Res* 2014;6(2):129-39. [published Online First: 2014/02/04]
 38. Stagg J, Divisekera U, McLaughlin N, Sharkey J, Pommey S, Denoyer D, Dwyer KM, Smyth MJ. Anti-CD73 antibody therapy inhibits breast tumor growth and metastasis. *Proceedings of the National Academy of Sciences of the United States of America* 2010;107(4):1547-52. doi: 10.1073/pnas.0908801107 [published Online First: 2010/01/19]
 39. Young A, Ngiow SF, Barkauskas DS, Sult E, Hay C, Blake SJ, Huang Q, Liu J, Takeda K, Teng MWL, Sachsenmeier K, Smyth MJ. Co-inhibition of CD73 and A2AR Adenosine Signaling Improves Anti-tumor Immune Responses. *Cancer Cell* 2016;30(3):391-403. doi: 10.1016/j.ccell.2016.06.025 [published Online First: 2016/09/14]
 40. Lowenstein JM. Ammonia production in muscle and other tissues: the purine nucleotide cycle. *Physiol Rev* 1972;52(2):382-414. doi: 10.1152/physrev.1972.52.2.382 [published Online First: 1972/04/01]
 41. Sabina RL, Mahnke-Zizelman DK. Towards an understanding of the functional significance of N-terminal domain divergence in human AMP deaminase isoforms. *Pharmacol Ther* 2000;87(2-3):279-83. doi: 10.1016/s0163-7258(00)00040-1 [published Online First: 2000/09/29]
 42. Ogasawara N, Goto H, Yamada Y, Watanabe T. Distribution of AMP deaminase isozymes in various human blood cells. *Int J Biochem* 1984;16(3):269-73. doi: 10.1016/0020-711x(84)90099-5 [published Online First: 1984/01/01]
 43. Ogasawara N, Goto H, Yamada Y, Watanabe T, Asano T. AMP deaminase isozymes in human tissues. *Biochimica et biophysica acta* 1982;714(2):298-306. doi: 10.1016/0304-4165(82)90337-3 [published Online First: 1982/02/02]

44. Zabielska MA, Borkowski T, Slominska EM, Smolenski RT. Inhibition of AMP deaminase as therapeutic target in cardiovascular pathology. *Pharmacol Rep* 2015;67(4):682-8. doi: 10.1016/j.pharep.2015.04.007 [published Online First: 2015/09/01]
45. Hohl CM. AMP deaminase in piglet cardiac myocytes: effect on nucleotide metabolism during ischemia. *The American journal of physiology* 1999;276(5):H1502-10. doi: 10.1152/ajpheart.1999.276.5.H1502 [published Online First: 1999/05/18]
46. Sabina RL, Swain JL, Olanow CW, Bradley WG, Fishbein WN, DiMauro S, Holmes EW. Myoadenylate deaminase deficiency. Functional and metabolic abnormalities associated with disruption of the purine nucleotide cycle. *The Journal of clinical investigation* 1984;73(3):720-30. doi: 10.1172/jci111265 [published Online First: 1984/03/01]
47. Atkinson DE. Regulation of Enzyme Activity. *Annual Review of Biochemistry* 1966;35(1):85-124. doi: 10.1146/annurev.bi.35.070166.000505
48. Chapman AG, Atkinson DE. Stabilization of adenylate energy charge by the adenylate deaminase reaction. *J Biol Chem* 1973;248(23):8309-12. [published Online First: 1973/12/10]
49. Dunkley CR, Manery JF, Dryden EE. The conversion of ATP to IMP by muscle surface enzymes. *Journal of Cellular Physiology* 1966;68(3):241-47. doi: 10.1002/jcp.1040680305
50. Manery JF, Riordan JR, Dryden EE. Characteristics of nucleotide-converting enzymes at muscle surfaces with special reference to ion sensitivity. *Can J Physiol Pharmacol* 1968;46(3):537-47. doi: 10.1139/y68-078 [published Online First: 1968/05/01]
51. Rao SN, Hara L, Askari A. Alkali cation-activated AMP deaminase of erythrocytes: some properties of the membrane-bound enzyme. *Biochimica et biophysica acta* 1968;151(3):651-4. doi: 10.1016/0005-2744(68)90012-0 [published Online First: 1968/03/25]
52. Pipoly GM, Nathans GR, Chang D, Deuel TF. Regulation of the interaction of purified human erythrocyte AMP deaminase and the human erythrocyte membrane. *The Journal of clinical investigation* 1979;63(5):1066-76. doi: 10.1172/jci109376 [published Online First: 1979/05/01]
53. Binkley PF, Auseon A, Cooke G. A polymorphism of the gene encoding AMPD1: clinical impact and proposed mechanisms in congestive heart failure. *Congest Heart Fail* 2004;10(6):274-78; quiz 79-80. doi: 10.1111/j.1527-5299.2004.02017.x [published Online First: 2004/12/14]
54. Borkowski T, Slominska EM, Orlewska C, Chlopicki S, Siondalski P, Yacoub MH, Smolenski RT. Protection of mouse heart against hypoxic damage by AMP deaminase inhibition. *Nucleosides, nucleotides & nucleic acids* 2010;29(4-6):449-52. doi: 10.1080/15257771003741364 [published Online First: 2010/06/15]
55. Ehlers L, Kuppe A, Damerau A, Wilantri S, Kirchner M, Mertins P, Strehl C, Buttgerit F, Gaber T. Surface AMP deaminase 2 as a novel regulator modifying extracellular adenine nucleotide metabolism. *The FASEB Journal* 2021;35(7):e21684. doi: <https://doi.org/10.1096/fj.202002658RR>
56. Uhlen M, Bandrowski A, Carr S, Edwards A, Ellenberg J, Lundberg E, Rimm DL, Rodriguez H, Hiltke T, Snyder M, Yamamoto T. A proposal for validation of antibodies. *Nat Methods* 2016;13(10):823-7. doi: 10.1038/nmeth.3995 [published Online First: 2016/09/07]
57. Perez-Riverol Y, Csordas A, Bai J, Bernal-Llinares M, Hewapathirana S, Kundu DJ, Inuganti A, Griss J, Mayer G, Eisenacher M, Pérez E, Uszkoreit J, Pfeuffer J, Sachsenberg T, Yilmaz S, Tiwary S, Cox J, Audain E, Walzer M, Jarnuczak AF, Ternent T, Brazma A, Vizcaíno JA. The PRIDE database and related tools and resources in 2019: improving support for quantification data. *Nucleic acids research* 2019;47(D1):D442-d50. doi: 10.1093/nar/gky1106 [published Online First: 2018/11/06]
58. Cossarizza A, Chang HD, Radbruch A, Akdis M, Andrä I, Annunziato F, Bacher P, Barnaba V, Battistini L, Bauer WM, Baumgart S, Becher B, Beisker W, Berek C, Blanco A, Borsellino G, Boulais PE, Brinkman RR, Büscher M, Busch DH, Bushnell TP, Cao X, Cavani A, Chattopadhyay PK, Cheng Q, Chow S, Clerici M, Cooke A, Cosma A, Cosmi L, Cumano A, Dang VD, Davies D, De Biasi S, Del Zotto G, Della Bella S, Dellabona P,

- Deniz G, Dessing M, Diefenbach A, Di Santo J, Dieli F, Dolf A, Donnenberg VS, Dörner T, Ehrhardt GRA, Endl E, Engel P, Engelhardt B, Esser C, Everts B, Dreher A, Falk CS, Fehniger TA, Filby A, Fillatreau S, Follo M, Förster I, Foster J, Foulds GA, Frenette PS, Galbraith D, Garbi N, García-Godoy MD, Geginat J, Ghoreschi K, Gibellini L, Goettlinger C, Goodyear CS, Gori A, Grogan J, Gross M, Grützkau A, Grummitt D, Hahn J, Hammer Q, Hauser AE, Haviland DL, Hedley D, Herrera G, Herrmann M, Hiepe F, Holland T, Hombrink P, Houston JP, Hoyer BF, Huang B, Hunter CA, Iannone A, Jäck HM, Jávega B, Jonjic S, Juelke K, Jung S, Kaiser T, Kalina T, Keller B, Khan S, Kienhöfer D, Kroneis T, Kunkel D, Kurts C, Kvistborg P, Lannigan J, Lantz O, Larbi A, LeibundGut-Landmann S, Leipold MD, Levings MK, Litwin V, Liu Y, Lohoff M, Lombardi G, Lopez L, Lovett-Racke A, Lubberts E, Ludewig B, Lugli E, Maecker HT, Martrus G, Matarese G, Maueröder C, McGrath M, McInnes I, Mei HE, Melchers F, Melzer S, Mielenz D, Mills K, Mirrer D, Mjösberg J, Moore J, Moran B, Moretta A, Moretta L, Mosmann TR, Müller S, Müller W, Münz C, Multhoff G, Munoz LE, Murphy KM, Nakayama T, Nasi M, Neudörfel C, Nolan J, Nourshargh S, O'Connor JE, Ouyang W, Oxenius A, Palankar R, Panse I, Peterson P, Peth C, Petriz J, Philips D, Pickl W, Piconese S, Pinti M, Pockley AG, Podolska MJ, Pucillo C, Quataert SA, Radstake T, Rajwa B, Rebhahn JA, Recktenwald D, Remmerswaal EBM, Rezvani K, Rico LG, Robinson JP, Romagnani C, Rubartelli A, Ruckert B, Ruland J, Sakaguchi S, Sala-de-Oyanguren F, Samstag Y, Sanderson S, Sawitzki B, Scheffold A, Schiemann M, Schildberg F, Schimisky E, Schmid SA, Schmitt S, Schober K, Schüler T, Schulz AR, Schumacher T, Scotta C, Shankey TV, Shemer A, Simon AK, Spidlen J, Stall AM, Stark R, Stehle C, Stein M, Steinmetz T, Stockinger H, Takahama Y, Tarnok A, Tian Z, Toldi G, Tornack J, Traggiai E, Trotter J, Ulrich H, van der Braber M, van Lier RAW, Veldhoen M, Vento-Asturias S, Vieira P, Voehringer D, Volk HD, von Volkman K, Waisman A, Walker R, Ward MD, Warnatz K, Warth S, Watson JV, Watzl C, Wegener L, Wiedemann A, Wienands J, Willimsky G, Wing J, Wurst P, Yu L, Yue A, Zhang Q, Zhao Y, Ziegler S, Zimmermann J. Guidelines for the use of flow cytometry and cell sorting in immunological studies. *European journal of immunology* 2017;47(10):1584-797. doi: 10.1002/eji.201646632 [published Online First: 2017/10/13]
59. Ziegler-Heitbrock L, Ancuta P, Crowe S, Dalod M, Grau V, Hart DN, Leenen PJ, Liu YJ, MacPherson G, Randolph GJ, Scherberich J, Schmitz J, Shortman K, Sozzani S, Strobl H, Zembala M, Austyn JM, Lutz MB. Nomenclature of monocytes and dendritic cells in blood. *Blood* 2010;116(16):e74-80. doi: 10.1182/blood-2010-02-258558 [published Online First: 2010/07/16]
60. Thul PJ, Akesson L, Wiking M, Mahdessian D, Geladaki A, Ait Blal H, Alm T, Asplund A, Bjork L, Breckels LM, Backstrom A, Danielsson F, Fagerberg L, Fall J, Gatto L, Gnann C, Hober S, Hjelmare M, Johansson F, Lee S, Lindskog C, Mulder J, Mulvey CM, Nilsson P, Oksvold P, Rockberg J, Schutten R, Schwenk JM, Sivertsson A, Sjostedt E, Skogs M, Stadler C, Sullivan DP, Tegel H, Winsnes C, Zhang C, Zwahlen M, Mardinoglu A, Ponten F, von Feilitzen K, Lilley KS, Uhlen M, Lundberg E. A subcellular map of the human proteome. *Science (New York, NY)* 2017;356(6340) doi: 10.1126/science.aal3321 [published Online First: 2017/05/13]
61. Peterson RE, Pierce CE, Wyngaarden JB, Bunim JJ, Brodie BB. The physiological disposition and metabolic fate of cortisone in man. *The Journal of clinical investigation* 1957;36(9):1301-12. doi: 10.1172/jci103528 [published Online First: 1957/09/01]
62. Webel ML, Ritts RE, Jr., Taswell HF, Danadio JV, Jr., Woods JE. Cellular immunity after intravenous administration of methylprednisolone. *J Lab Clin Med* 1974;83(3):383-92. [published Online First: 1974/03/01]
63. Gross M. Molecular biology of AMP deaminase deficiency. *Pharmacy world & science : PWS* 1994;16(2):55-61. [published Online First: 1994/04/15]
64. Lowenstein J, Tornheim K. Ammonia production in muscle: the purine nucleotide cycle. *Science (New York, NY)* 1971;171(3969):397-400. doi: 10.1126/science.171.3969.397
65. Plaideau C, Lai YC, Kviklyte S, Zanou N, Löfgren L, Andersén H, Vertommen D, Gailly P, Hue L, Bohlooly YM, Hallén S, Rider MH. Effects of pharmacological AMP deaminase

- inhibition and Ampd1 deletion on nucleotide levels and AMPK activation in contracting skeletal muscle. *Chem Biol* 2014;21(11):1497-510. doi: 10.1016/j.chembiol.2014.09.013 [published Online First: 2014/12/03]
66. Ouyang J, Parakhia RA, Ochs RS. Metformin activates AMP kinase through inhibition of AMP deaminase. *J Biol Chem* 2011;286(1):1-11. doi: 10.1074/jbc.M110.121806 [published Online First: 2010/11/10]
 67. Hancock CR, Brault JJ, Terjung RL. Protecting the cellular energy state during contractions: role of AMP deaminase. *J Physiol Pharmacol* 2006;57 Suppl 10:17-29. [published Online First: 2007/01/24]
 68. Fishbein WN, Armbrustmacher VW, Griffin JL. Myoadenylate deaminase deficiency: a new disease of muscle. *Science (New York, NY)* 1978;200(4341):545-8. doi: 10.1126/science.644316
 69. Norman B, Glenmark B, Jansson E. Muscle AMP deaminase deficiency in 2% of a healthy population. *Muscle Nerve* 1995;18(2):239-41. doi: 10.1002/mus.880180216 [published Online First: 1995/02/01]
 70. Loh E, Rebbeck TR, Mahoney PD, DeNofrio D, Swain JL, Holmes EW. Common variant in AMPD1 gene predicts improved clinical outcome in patients with heart failure. *Circulation* 1999;99(11):1422-5. doi: 10.1161/01.cir.99.11.1422 [published Online First: 1999/03/23]
 71. Kalsi KK, Yuen AH, Johnson PH, Birks EJ, Yacoub MH, Smolenski RT. AMPD1 C34T mutation selectively affects AMP-deaminase activity in the human heart. *Nucleosides, nucleotides & nucleic acids* 2005;24(4):287-8. doi: 10.1081/ncn-59721
 72. Smolenski RT, Rybakowska I, Turyn J, Romaszko P, Zabielska M, Taegtmeyer A, Słomińska EM, Kaletha KK, Barton PJ. AMP deaminase 1 gene polymorphism and heart disease—a genetic association that highlights new treatment. *Cardiovasc Drugs Ther* 2014;28(2):183-9. doi: 10.1007/s10557-013-6506-5 [published Online First: 2014/01/17]
 73. Norman B, Sabina RL, Jansson E. Regulation of skeletal muscle ATP catabolism by AMPD1 genotype during sprint exercise in asymptomatic subjects. *J Appl Physiol (1985)* 2001;91(1):258-64. doi: 10.1152/jappl.2001.91.1.258
 74. Accogli A, Iacomino M, Pinto F, Orsini A, Vari MS, Selmi R, Torella A, Nigro V, Minetti C, Severino M, Striano P, Capra V, Zara F. Novel AMPD2 mutation in pontocerebellar hypoplasia, dysmorphisms, and teeth abnormalities. *Neurology Genetics* 2017;3(5):e179. doi: 10.1212/nxg.0000000000000179 [published Online First: 20170809]
 75. Akizu N, Cantagrel V, Schroth J, Cai N, Vaux K, McCloskey D, Naviaux RK, Van Vleet J, Fenstermaker AG, Silhavy JL, Scheliga JS, Toyama K, Morisaki H, Sonmez FM, Celep F, Oraby A, Zaki MS, Al-Baradie R, Faqeih EA, Saleh MA, Spencer E, Rosti RO, Scott E, Nickerson E, Gabriel S, Morisaki T, Holmes EW, Gleeson JG. AMPD2 regulates GTP synthesis and is mutated in a potentially treatable neurodegenerative brainstem disorder. *Cell* 2013;154(3):505-17. doi: 10.1016/j.cell.2013.07.005 [published Online First: 2013/08/06]
 76. Allegra CJ, Drake JC, Jolivet J, Chabner BA. Inhibition of phosphoribosylaminoimidazolecarboxamide transformylase by methotrexate and dihydrofolic acid polyglutamates. *Proceedings of the National Academy of Sciences of the United States of America* 1985;82(15):4881-5. doi: 10.1073/pnas.82.15.4881 [published Online First: 1985/08/01]
 77. Cronstein BN, Naime D, Ostad E. The antiinflammatory mechanism of methotrexate. Increased adenosine release at inflamed sites diminishes leukocyte accumulation in an in vivo model of inflammation. *The Journal of clinical investigation* 1993;92(6):2675-82. doi: 10.1172/jci116884 [published Online First: 1993/12/01]
 78. Cronstein BN, Aune TM. Methotrexate and its mechanisms of action in inflammatory arthritis. *Nature reviews Rheumatology* 2020;16(3):145-54. doi: 10.1038/s41584-020-0373-9 [published Online First: 20200217]
 79. Eltzschig HK, Sitkovsky MV, Robson SC. Purinergic signaling during inflammation. *The New England journal of medicine* 2012;367(24):2322-33. doi: 10.1056/NEJMra1205750

80. Garshick MS, Rosenthal PB, Luttrell-Williams E, Cronstein BN, Berger JS. Ticagrelor added to methotrexate improves rheumatoid arthritis disease severity. *Rheumatology (Oxford, England)* 2021 doi: 10.1093/rheumatology/keab481 [published Online First: 20210617]
81. Pulte ED, Broekman MJ, Olson KE, Drosopoulos JH, Kizer JR, Islam N, Marcus AJ. CD39/NTPDase-1 activity and expression in normal leukocytes. *Thromb Res* 2007;121(3):309-17. doi: 10.1016/j.thromres.2007.04.008 [published Online First: 2007/06/09]
82. Saze Z, Schuler PJ, Hong CS, Cheng D, Jackson EK, Whiteside TL. Adenosine production by human B cells and B cell-mediated suppression of activated T cells. *Blood* 2013;122(1):9-18. doi: 10.1182/blood-2013-02-482406 [published Online First: 2013/05/17]
83. Silva-Vilches C, Ring S, Mahnke K. ATP and Its Metabolite Adenosine as Regulators of Dendritic Cell Activity. *Front Immunol* 2018;9:2581. doi: 10.3389/fimmu.2018.02581 [published Online First: 2018/11/27]
84. Yu N, Li X, Song W, Li D, Yu D, Zeng X, Li M, Leng X. CD4(+)CD25 (+)CD127 (low/-) T cells: a more specific Treg population in human peripheral blood. *Inflammation* 2012;35(6):1773-80. doi: 10.1007/s10753-012-9496-8 [published Online First: 2012/07/04]
85. Finn JD, Snoek S, van Ittersum J, Broekstra N, Braam C, Kramer E, van Geldorp M, Tak PP, Vervoordeldonk MJ. A8.12 AAV mediated expression of CD39 and CD73 is effective in reducing inflammation in the air pouch synovial inflammation model. *Annals of the rheumatic diseases* 2015;74(Suppl 1):A86. doi: 10.1136/annrheumdis-2015-207259.197
86. Sun X, Cárdenas A, Wu Y, Enyoji K, Robson SC. Vascular stasis, intestinal hemorrhage, and heightened vascular permeability complicate acute portal hypertension in cd39-null mice. *Am J Physiol Gastrointest Liver Physiol* 2009;297(2):G306-11. doi: 10.1152/ajpgi.90703.2008 [published Online First: 2009/06/13]
87. Endo W, Arito M, Sato T, Kurokawa MS, Omoteyama K, Iizuka N, Okamoto K, Suematsu N, Nakamura H, Beppu M, Kato T. Effects of sulfasalazine and tofacitinib on the protein profile of articular chondrocytes. *Modern rheumatology* 2014;24(5):844-50. doi: 10.3109/14397595.2013.864225 [published Online First: 2013/12/18]
88. Gourdin N, Bossennec M, Rodriguez C, Vigano S, Machon C, Jandus C, Bauché D, Faget J, Durand I, Chopin N, Tredan O, Marie JC, Dubois B, Guitton J, Romero P, Caux C, Ménétrier-Caux C. Autocrine Adenosine Regulates Tumor Polyfunctional CD73(+)CD4(+) Effector T Cells Devoid of Immune Checkpoints. *Cancer research* 2018;78(13):3604-18. doi: 10.1158/0008-5472.can-17-2405 [published Online First: 2018/03/22]
89. Ohta M, Toyama K, Gutterman DD, Campbell WB, Lemaître V, Teraoka R, Miura H. Ecto-5'-nucleotidase, CD73, is an endothelium-derived hyperpolarizing factor synthase. *Arterioscler Thromb Vasc Biol* 2013;33(3):629-36. doi: 10.1161/atvbaha.112.300600 [published Online First: 2013/01/05]
90. Quarona V, Ferri V, Chillemi A, Bolzoni M, Mancini C, Zaccarello G, Roato I, Morandi F, Marimpietri D, Faccani G, Martella E, Pistoia V, Giuliani N, Horenstein AL, Malavasi F. Unraveling the contribution of ectoenzymes to myeloma life and survival in the bone marrow niche. *Annals of the New York Academy of Sciences* 2015;1335:10-22. doi: 10.1111/nyas.12485 [published Online First: 2014/07/23]
91. Thomson LF, Ruedi JM, Glass A, Moldenhauer G, Moller P, Low MG, Klemens MR, Massaia M, Lucas AH. Production and characterization of monoclonal antibodies to the glycosyl phosphatidylinositol-anchored lymphocyte differentiation antigen ecto-5'-nucleotidase (CD73). *Tissue Antigens* 1990;35(1):9-19. doi: 10.1111/j.1399-0039.1990.tb01750.x [published Online First: 1990/01/01]
92. Zanin RF, Braganhol E, Bergamin LS, Campesato LF, Filho AZ, Moreira JC, Morrone FB, Sévigny J, Schetinger MR, de Souza Wyse AT, Battastini AM. Differential macrophage activation alters the expression profile of NTPDase and ecto-5'-nucleotidase. *PLoS one* 2012;7(2):e31205. doi: 10.1371/journal.pone.0031205 [published Online First: 2012/02/22]

93. Eichin D, Laurila JP, Jalkanen S, Salmi M. CD73 Activity is Dispensable for the Polarization of M2 Macrophages. *PloS one* 2015;10(8):e0134721. doi: 10.1371/journal.pone.0134721 [published Online First: 2015/08/11]
94. Ohradanova-Repic A, Machacek C, Charvet C, Lager F, Le Roux D, Platzner R, Leksa V, Mitulovic G, Burkard TR, Zlabinger GJ, Fischer MB, Feuillet V, Renault G, Blüml S, Benko M, Suchanek M, Huppa JB, Matsuyama T, Cavaco-Paulo A, Bismuth G, Stockinger H. Extracellular Purine Metabolism Is the Switchboard of Immunosuppressive Macrophages and a Novel Target to Treat Diseases With Macrophage Imbalances. *Front Immunol* 2018;9:852. doi: 10.3389/fimmu.2018.00852 [published Online First: 2018/05/22]
95. Möser GH, Schrader J, Deussen A. Turnover of adenosine in plasma of human and dog blood. *The American journal of physiology* 1989;256(4 Pt 1):C799-806. doi: 10.1152/ajpcell.1989.256.4.C799 [published Online First: 1989/04/01]
96. Viegas TX, Omura GA, Stoltz RR, Kisicki J. Pharmacokinetics and pharmacodynamics of peldesine (BCX-34), a purine nucleoside phosphorylase inhibitor, following single and multiple oral doses in healthy volunteers. *J Clin Pharmacol* 2000;40(4):410-20. doi: 10.1177/00912700022008991 [published Online First: 2000/04/13]
97. Qiu FH, Wada K, Stahl GL, Serhan CN. IMP and AMP deaminase in reperfusion injury down-regulates neutrophil recruitment. *Proceedings of the National Academy of Sciences of the United States of America* 2000;97(8):4267-72. doi: 10.1073/pnas.97.8.4267 [published Online First: 2000/04/13]
98. Magalhães-Cardoso MT, Pereira MF, Oliveira L, Ribeiro JA, Cunha RA, Correia-de-Sá P. Ecto-AMP deaminase blunts the ATP-derived adenosine A2A receptor facilitation of acetylcholine release at rat motor nerve endings. *The Journal of physiology* 2003;549(Pt 2):399-408. doi: 10.1113/jphysiol.2003.040410 [published Online First: 2003/04/08]
99. Flögel U, Burghoff S, van Lent PL, Temme S, Galbarz L, Ding Z, El-Tayeb A, Huels S, Bönner F, Borg N, Jacoby C, Müller CE, van den Berg WB, Schrader J. Selective activation of adenosine A2A receptors on immune cells by a CD73-dependent prodrug suppresses joint inflammation in experimental rheumatoid arthritis. *Sci Transl Med* 2012;4(146):146ra08. doi: 10.1126/scitranslmed.3003717 [published Online First: 2012/08/10]
100. Herrath J, Chemin K, Albrecht I, Catrina AI, Malmström V. Surface expression of CD39 identifies an enriched Treg-cell subset in the rheumatic joint, which does not suppress IL-17A secretion. *European journal of immunology* 2014;44(10):2979-89. doi: 10.1002/eji.201344140 [published Online First: 2014/07/06]
101. Silverman MH, Strand V, Markovits D, Nahir M, Reitblat T, Molad Y, Rosner I, Rozenbaum M, Mader R, Adawi M, Caspi D, Tishler M, Langevitz P, Rubinow A, Friedman J, Green L, Tanay A, Ochaion A, Cohen S, Kerns WD, Cohn I, Fishman-Furman S, Farbstein M, Yehuda SB, Fishman P. Clinical evidence for utilization of the A3 adenosine receptor as a target to treat rheumatoid arthritis: data from a phase II clinical trial. *The Journal of rheumatology* 2008;35(1):41-8. [published Online First: 2007/12/01]
102. Fishman P, Cohen S. The A3 adenosine receptor (A3AR): therapeutic target and predictive biological marker in rheumatoid arthritis. *Clinical rheumatology* 2016;35(9):2359-62. doi: 10.1007/s10067-016-3202-4 [published Online First: 2016/02/18]
103. Hirschhorn R. Adenosine deaminase deficiency: molecular basis and recent developments. *Clin Immunol Immunopathol* 1995;76(3 Pt 2):S219-27. doi: 10.1016/s0090-1229(95)90288-0
104. Zhou Q, Yang D, Ombrello AK, Zavialov AV, Toro C, Stone DL, Chae JJ, Rosenzweig SD, Bishop K, Barron KS, Kuehn HS, Hoffmann P, Negro A, Tsai WL, Cowen EW, Pei W, Milner JD, Silvin C, Heller T, Chin DT, Patronas NJ, Barber JS, Lee CC, Wood GM, Ling A, Kelly SJ, Kleiner DE, Mullikin JC, Ganson NJ, Kong HH, Hambleton S, Candotti F, Quezado MM, Calvo KR, Alao H, Barham BK, Jones A, Meschia JF, Worrall BB, Kasner SE, Rich SS, Goldbach-Mansky R, Abinun M, Chalom E, Gotte AC, Punaro M, Pascual V, Verbsky JW, Torgerson TR, Singer NG, Gershon TR, Ozen S, Karadag O, Fleisher TA, Remmers EF, Burgess SM, Moir SL, Gadina M, Sood R, Hershfield MS, Boehm M,

- Kastner DL, Aksentijevich I. Early-onset stroke and vasculopathy associated with mutations in ADA2. *The New England journal of medicine* 2014;370(10):911-20. doi: 10.1056/NEJMoa1307361 [published Online First: 2014/02/21]
105. Dhanwani R, Takahashi M, Mathews IT, Lenzi C, Romanov A, Watrous JD, Pieters B, Hedrick CC, Benedict CA, Linden J, Nilsson R, Jain M, Sharma S. Cellular sensing of extracellular purine nucleosides triggers an innate IFN- β response. *Sci Adv* 2020;6(30):eaba3688. doi: 10.1126/sciadv.aba3688 [published Online First: 2020/08/04]

Eidesstattliche Versicherung

„Ich, Lisa Ehlers, versichere an Eides statt durch meine eigenhändige Unterschrift, dass ich die vorgelegte Dissertation mit dem Thema: *Oberflächenexpression der AMP-Desaminase 2 auf humanen Immunzellen und ihre Rolle im extrazellulären Purinmetabolismus / Surface expression of AMP deaminase 2 on human immune cells and its role in extracellular purine metabolism* selbstständig und ohne nicht offengelegte Hilfe Dritter verfasst und keine anderen als die angegebenen Quellen und Hilfsmittel genutzt habe.

Alle Stellen, die wörtlich oder dem Sinne nach auf Publikationen oder Vorträgen anderer Autor*innen beruhen, sind als solche in korrekter Zitierung kenntlich gemacht. Die Abschnitte zu Methodik (insbesondere praktische Arbeiten, Laborbestimmungen, statistische Aufarbeitung) und Resultaten (insbesondere Abbildungen, Graphiken und Tabellen) werden von mir verantwortet.

Ich versichere ferner, dass ich die in Zusammenarbeit mit anderen Personen generierten Daten, Datenauswertungen und Schlussfolgerungen korrekt gekennzeichnet und meinen eigenen Beitrag sowie die Beiträge anderer Personen korrekt kenntlich gemacht habe (siehe Anteilserklärung). Texte oder Textteile, die gemeinsam mit anderen erstellt oder verwendet wurden, habe ich korrekt kenntlich gemacht.

Meine Anteile an etwaigen Publikationen zu dieser Dissertation entsprechen denen, die in der untenstehenden gemeinsamen Erklärung mit dem Erstbetreuer, angegeben sind. Für sämtliche im Rahmen der Dissertation entstandenen Publikationen wurden die Richtlinien des ICMJE (International Committee of Medical Journal Editors; www.icmje.org) zur Autorenschaft eingehalten. Ich erkläre ferner, dass ich mich zur Einhaltung der Satzung der Charité – Universitätsmedizin Berlin zur Sicherung Guter Wissenschaftlicher Praxis verpflichte.

Weiterhin versichere ich, dass ich diese Dissertation weder in gleicher noch in ähnlicher Form bereits an einer anderen Fakultät eingereicht habe.

Die Bedeutung dieser eidesstattlichen Versicherung und die strafrechtlichen Folgen einer unwahren eidesstattlichen Versicherung (§§156, 161 des Strafgesetzbuches) sind mir bekannt und bewusst.“

Datum

Unterschrift

Anteilserklärung an der erfolgten Publikation

Lisa Ehlers hatte folgenden Anteil an der folgenden Publikation:

Publikation 1: **Ehlers L**, Kuppe A, Damerau A, Wilantri S, Kirchner M, Mertins P, Strehl C, Buttgerit F, Gaber T. Surface AMP deaminase 2 as a novel regulator modifying extracellular adenine nucleotide metabolism. The FASEB Journal 2021;35(7):e21684. doi: <https://doi.org/10.1096/fj.202002658RR>

Beitrag im Einzelnen:

Lisa Ehlers war als Erstautorin dieser Publikation maßgeblich verantwortlich für die Planung, Durchführung und Auswertung der Experimente, den Einschluss der Patient*innen und gesunden Spender*innen sowie das Verfassen des wissenschaftlichen Manuskripts und dessen Überarbeitung im Rahmen des Revisions- und Veröffentlichungsprozesses. Ihr Beitrag zu dieser Publikation beläuft sich auf etwa 90% der Arbeit. Im Folgenden sind ihre Leistungen im Detail aufgeführt:

Projektplanung

Die Projektplanung inklusive des experimentellen Aufbaus sowie der Rekrutierung von Patient*innen und gesunden Spender*innen erfolgte selbstständig durch Lisa Ehlers in Zusammenarbeit mit den Promotionsbetreuern Prof. Dr. Frank Buttgerit und Dr. Timo Gaber. Lisa Ehlers etablierte die Zusammenarbeit der Arbeitsgruppe mit der MDC Proteomics Platform. Beim Einschluss der Patient*innen wurde Lisa Ehlers durch Gabriele May unterstützt.

Experimentelle Arbeit

Folgende experimentelle Arbeiten wurden von Lisa Ehlers eigenständig geplant und durchgeführt:

- Etablierung der experimentellen Methoden anhand von Zelllinien
- Isolation von humanen Leukozyten mittels Erythrolyse und von PBMCs mittels Dichtegradientenzentrifugation
- Anreicherung von Immunzellpopulationen mittels magnetischer Zellseparation, Ausschluss von Zellen mit eingeschränkter Vitalität mittels Dead Cell Removal
- Zellkultur inklusive Etablierung verschiedener Methoden der Immunstimulation und Inhibition des sekretorischen Wegs
- Reduktion der Genexpression von AMPD2 mittels RNA-Interferenz in verschiedenen Zelllinien: Transfektion zur Herstellung eines transienten Knockdowns, Produktion lentiviraler Partikel, Transduktion und Selektion erfolgreich transduzierter Zellen, Überprüfung der Proteinexpression mittels Western Blot

- Anreicherung von Oberflächenprotein mittels Membranfraktionierung und Oberflächenbiotinylierung mit Streptavidin-basiertem Pulldown
- Bestimmung der Proteinkonzentration mittels BCA Assay
- Proteinanreicherung durch Immunpräzipitation
- Proteinnachweis mittels SDS-PAGE und Western Blot
- Vorbereitung der angereicherten Proben für die massenspektrometrische Analyse
- Etablierung und Durchführung einer Oberflächenfärbung von AMPD2 sowie anschließende durchflusszytometrische Messung der Zellen, Entwicklung eines durchflusszytometrischen Panels zur parallelen Analyse mehrerer Oberflächenproteine
- fluorometrische Bestimmung der Adenosinkonzentration

Folgende Experimente wurden unter Beteiligung der Co-Autor*innen durchgeführt:

- Immunfluoreszenzmikroskopie in Zusammenarbeit mit Alexandra Damerau
- durchflusszytometrische Analyse der T-Zell-Populationen in Zusammenarbeit mit Siska Wilantri
- Bestimmung von TNF- α im Überstand mittels ELISA in Zusammenarbeit mit Alexandra Damerau
- massenspektrometrische Analysen durch Dr. Marieluse Kirchner

Datenauswertung

Lisa Ehlers führte selbstständig die Auswertung der Daten durch. Dies umfasste die folgenden Analysen:

- Auswertung der klinischen Parameter der RA-Kohorte
- Analyse der Aminosäuresequenz von AMPD2 in Bezug auf das Vorliegen möglicher Membrandomänen mithilfe der Server UniProt, TMHMM und PSIPRED
- Auswertung des Proteinsignals im Western Blot mittels ImageJ
- Analyse der durchflusszytometrischen Daten mittels FlowJo
- Zusammenstellung der Ergebnisse in Microsoft Excel sowie deren statistische Auswertung mit GraphPad Prism

Die Auswertung der massenspektrometrischen Ergebnisse wurde durch Dr. Marieluse Kirchner vorgenommen.

Verfassung und Veröffentlichung des wissenschaftlichen Manuskripts

Die strukturelle Planung des Manuskripts erfolgte in Zusammenarbeit mit dem Promotionsbetreuer Dr. Timo Gaber. Lisa Ehlers verfasste eigenständig das wissenschaftliche Manuskript mit Ausnahme der Abschnitte 2.10 und 2.11, die von Dr. Marieluse Kirchner beigetragen wurden.

Mit Ausnahme der Figure 2D (Dr. Marieluse Kirchner) wurden alle Abbildungen und Tabellen durch Lisa Ehlers erstellt. Figure 3B entstand in Zusammenarbeit mit Alexandra Damerau und Figure S1A in Zusammenarbeit mit Siska Wilantri. Generiert wurden die Abbildungen unter Verwendung von GraphPad Prism.

Lisa Ehlers war hauptverantwortlich für den Einreichungs- und Veröffentlichungsprozess des wissenschaftlichen Manuskripts. Dies beinhaltet das Verfassen des Anschreibens, die Überarbeitung des Manuskripts im Rahmen des Revisionsprozesses und die Durchführung der dafür erforderlichen Experimente sowie das Verfassen des Antwortschreibens an die Gutachter*innen.

Unterschrift, Datum und Stempel des erstbetreuenden Hochschullehrers

Unterschrift der Doktorandin

Auszug aus der Journal Summary List

Journal Data Filtered By: **Selected JCR Year: 2019** Selected Editions: SCIE,SSCI
 Selected Categories: **"BIOLOGY"** Selected Category Scheme: WoS

Gesamtanzahl: 93 Journale

Rank	Full Journal Title	Total Cites	Journal Impact Factor	Eigenfactor Score
1	Physics of Life Reviews	1,627	14.789	0.003150
2	BIOLOGICAL REVIEWS	13,490	10.701	0.019440
3	CURRENT BIOLOGY	63,256	9.601	0.133170
4	BIOSCIENCE	19,069	8.282	0.014250
5	eLife	46,775	7.080	0.287130
6	PLOS BIOLOGY	31,650	7.076	0.060300
7	BMC BIOLOGY	6,440	6.765	0.018830
8	PHILOSOPHICAL TRANSACTIONS OF THE ROYAL SOCIETY B- BIOLOGICAL SCIENCES	46,796	5.680	0.063840
9	FASEB JOURNAL	43,126	4.966	0.043730
10	BIOELECTROCHEMISTRY	4,944	4.722	0.004950
11	PROCEEDINGS OF THE ROYAL SOCIETY B- BIOLOGICAL SCIENCES	55,054	4.637	0.075820
12	BIOESSAYS	10,189	4.627	0.016560
13	Science China-Life Sciences	3,248	4.611	0.006650
14	Current Opinion in Insect Science	2,247	4.565	0.008900
15	QUARTERLY REVIEW OF BIOLOGY	4,227	4.389	0.001130
16	Geobiology	2,390	4.385	0.004450
17	Communications Biology	1,326	4.165	0.004260
18	ASTROBIOLOGY	4,070	4.091	0.006180
19	Biology-Basel	1,424	3.796	0.003350
20	YALE JOURNAL OF BIOLOGY AND MEDICINE	2,230	3.549	0.003170
21	Interface Focus	2,218	3.514	0.005060
22	COMPUTERS IN BIOLOGY AND MEDICINE	6,737	3.434	0.010660
23	JOURNAL OF BIOLOGICAL RHYTHMS	3,258	3.122	0.003220
24	BIOLOGICAL RESEARCH	1,736	3.092	0.002210
25	JOURNAL OF EXPERIMENTAL BIOLOGY	34,195	3.014	0.032180
26	Life-Basel	1,260	2.991	0.004150
27	Biology Letters	10,299	2.869	0.017320
28	EXCLI Journal	1,622	2.837	0.002840
29	BIOCELL	346	2.821	0.000160
30	SAUDI JOURNAL OF BIOLOGICAL SCIENCES	3,994	2.802	0.005800
31	AEROBIOLOGIA	1,565	2.708	0.001250
32	RADIATION RESEARCH	8,707	2.657	0.005340
33	Life Science Alliance	310	2.622	0.001050

1

Selected JCR Year: 2019; Selected Categories: "BIOLOGY"

Abgerufen am 17.07.2021.

Mit Rang 9 von 93 (10%) befindet sich The FASEB Journal unter den oberen 25 Prozent der nach Impact Factor gelisteten Fachzeitschriften im Bereich Biologie und erfüllt damit die Definition eines Top-Journals.

Druckexemplar der ausgewählten Publikation

RESEARCH ARTICLE

Surface AMP deaminase 2 as a novel regulator modifying extracellular adenine nucleotide metabolism

Lisa Ehlers^{1,2}  | Aditi Kuppe^{1,2} | Alexandra Damerau^{1,2} | Siska Wilantri^{1,2} | Marieluise Kirchner³ | Philipp Mertins³ | Cindy Strehl^{1,2} | Frank Buttgereit^{1,2} | Timo Gaber^{1,2}

¹Department of Rheumatology and Clinical Immunology, Charité-Universitätsmedizin Berlin, Corporate Member of Freie Universität Berlin, Humboldt-Universität zu Berlin, Berlin, Germany

²Deutsches Rheuma-Forschungszentrum (DRFZ) Institute of the Leibniz Association, Berlin, Germany

³BIH Core Unit Proteomics, Berlin Institute of Health (BIH) and Max-Delbrück-Centrum für Molekulare Medizin (MDC), Berlin, Germany

Correspondence

Lisa Ehlers, Department of Rheumatology and Clinical Immunology, Charité-Universitätsmedizin Berlin, Corporate Member of Freie Universität Berlin, Humboldt-Universität zu Berlin, Berlin Institute of Health (BIH), Charitéplatz 1, 10117 Berlin, Germany.
Email: lisa.ehlers@charite.de

Funding information

Horizon Pharma, Grant/Award Number: 112517; Studienstiftung des Deutschen Volkes (Studienstiftung); Alexandra Damerau; Deutsche Forschungsgemeinschaft (DFG), Grant/Award Number: 353142848

Abstract

Adenine nucleotides represent crucial immunomodulators in the extracellular environment. The ectonucleotidases CD39 and CD73 are responsible for the sequential catabolism of ATP to adenosine via AMP, thus promoting an anti-inflammatory milieu induced by the “adenosine halo”. AMPD2 intracellularly mediates AMP deamination to IMP, thereby both enhancing the degradation of inflammatory ATP and reducing the formation of anti-inflammatory adenosine. Here, we show that this enzyme is expressed on the surface of human immune cells and its predominance may modify inflammatory states by altering the extracellular milieu. Surface AMPD2 (eAMPD2) expression on monocytes was verified by immunoblot, surface biotinylation, mass spectrometry, and immunofluorescence microscopy. Flow cytometry revealed enhanced monocytic eAMPD2 expression after TLR stimulation. PBMCs from patients with rheumatoid arthritis displayed significantly higher levels of eAMPD2 expression compared with healthy controls. Furthermore, the product of AMPD2—IMP—exerted anti-inflammatory effects, while the levels of extracellular adenosine were not impaired by an increased eAMPD2 expression. In summary, our study identifies eAMPD2 as a novel regulator of the extracellular ATP-adenosine balance adding to the immunomodulatory CD39-CD73 system.

KEYWORDS

adenosine, inflammation, nucleotidases, purines, rheumatoid arthritis, RRIDs

Abbreviations: A1R, adenosine A1 receptor; A2AR, adenosine A2A receptor; A2BR, adenosine A2B receptor; A3R, adenosine A3 receptor; AMPD2, AMP deaminase 2; BFA, brefeldin A; BL, B lymphocyte; DC, dendritic cell; Dex, dexamethasone; eADO, extracellular adenosine; eAMPD2, surface AMP deaminase 2; eATP, extracellular ATP; FDR, false discovery rate; iBAQ, intensity-based absolute quantification; IP, immunoprecipitation; LFQ, label-free quantification; MN, monensin; MSC, mesenchymal stromal cell; MTX, methotrexate; PBMC, peripheral blood mononuclear cell; scr, scrambled; T_H cell, T helper cell; TLR, Toll-like receptor; Treg, regulatory T cell.

This is an open access article under the terms of the Creative Commons Attribution-NonCommercial-NoDerivs License, which permits use and distribution in any medium, provided the original work is properly cited, the use is non-commercial and no modifications or adaptations are made.

© 2021 The Authors. The FASEB Journal published by Wiley Periodicals LLC on behalf of Federation of American Societies for Experimental Biology.

1 | INTRODUCTION

In recent years, extracellular adenosine (eADO) has emerged as an important factor in the pathogenesis of immune-mediated and neoplastic diseases.^{1,2} eADO is mainly provided by the degradation of extracellular ATP (eATP) through the subsequent action of different ectonucleotidases.³ The process of enzymatic ADO production is subdivided into two interacting pathways: the more prominent canonical pathway and the alternative pathway. The canonical pathway consists of the rate-limiting ectonucleoside triphosphate diphosphohydrolase-1 (CD39) and the ecto-5'-nucleotidase (CD73). While CD39 catalyzes the dephosphorylation of ATP and ADP to AMP, CD73 mediates the phosphorolytic cleavage of the latter, thereby producing ADO.⁴ On the other hand, the alternative pathway involves the conversion of extracellular NAD⁺ to ADP ribose by CD38, followed by AMP production by CD203a/PC-1.^{5,6} These pathways of ADO generation are completed by an additional ectoenzyme—adenosine deaminase—that terminates ADO action by deamination to inosine.⁷ Beyond ectoenzyme activity, extracellular adenine nucleotide levels are determined by cellular uptake and release via channel proteins and nucleoside transporters.⁸⁻¹¹

Extracellular purine metabolites signal via two major classes of receptors: P2 receptors mediate the action of purine nucleotides like ATP. The P1 receptor family, on the other hand, consists of four ADO receptors (A1R, A2AR, A2BR, A3R) that signal via different G-proteins.¹² Purinergic receptors are expressed ubiquitously throughout different tissues and elicit a myriad of effects.¹³ Our work focuses on the role of adenine nucleotides in the context of inflammation.

The increasing understanding of the regulation of eADO production as well purinergic signaling has enhanced the development of therapeutic concepts involving adenosinergic pathways.^{1,12,14,15} eATP is released from cells under conditions of stress and inflammation, thereby functioning as an alarm in provoking a pro-inflammatory reaction.¹⁶⁻²³ In contrast, eADO represents a potent anti-inflammatory agent.²⁴⁻³³ Anti-inflammatory effects of eADO have mainly been attributed to the activation of A2R and A3R and agonists of these receptors are currently being evaluated as therapeutic agents to treat inflammatory conditions.³⁴⁻³⁸

Besides ADO receptors, leukocytes are also equipped with ectonucleotidases permitting a regulation of the inflammatory environment by both ATP breakdown and ADO generation. CD39 and CD73 are differentially expressed on distinct immune cell subsets. While CD39 expression is present in the majority of neutrophils, dendritic cells (DC), monocytes and B lymphocytes (BL) as well as a subset of regulatory T cells (Treg), CD73 is expressed by DCs, BLs, cytotoxic T cells, and several non-immune cells like mesenchymal stromal cells (MSC) and endothelial cells.³⁹⁻⁴⁶ In contrast, only a small subset of CD4⁺ T helper (T_H) cells is characterized by CD39 or CD73

expression.⁴⁷ Recent research has revealed a dysregulation of the adenosinergic system in many autoimmune diseases.⁴⁸⁻⁵¹

Conversely, enhanced tumor growth has been ascribed to a surplus of anti-inflammatory eADO.⁵²⁻⁵⁵ Therefore, blocking eADO generation or ADO receptor signaling might eliminate the protective “adenosine halo” and restore an environment permitting an effective anti-tumor immune response.^{2,12,56} Recent approaches examining this therapeutic concept have yielded promising results.⁵⁷⁻⁶¹ These findings demonstrate the clinical relevance of adenosinergic signaling and highlight the importance of a deep understanding of extracellular purine metabolism.

In this context, we noticed that the ensemble of ectoenzymes implicated in the regulation of extracellular adenine nucleotides is incomplete compared with the complex network of reactions involved in intracellular purine metabolism.⁶² While AMP deamination substantially modifies cytosolic purine content, it has hitherto not been recognized as an essential reaction in the extracellular space. Although previous studies have reported attachment of AMP deaminases (AMPDs) to the muscle surface and the inner erythrocyte membrane,⁶³⁻⁶⁶ surface expression of AMPD in human leukocytes has not yet been described. AMPDs are responsible for the conversion of AMP to IMP by hydrolyzing the amino group from the 6-position of the adenine nucleotide ring. In contrast to adenine nucleotides, the immunomodulatory role of IMP in the extracellular space remains unclear. AMP deamination facilitates the removal of AMP that accumulates in states of energy depletion. By increasing the ATP:AMP ratio, AMPDs promote energy yield from ATP hydrolysis.^{62,67-69} At the same time, AMPDs compete with 5'-nucleotidases for AMP supply, thereby impeding the formation of anti-inflammatory ADO. Conversely, loss of function mutations in the AMPD genes as well as the development of AMPD inhibitors have shown that reduced AMP deamination is associated with an increase in ADO levels.⁷⁰⁻⁷² We hypothesized that this principle might be equally relevant to the modification of extracellular purine levels under inflammatory conditions. Therefore, we examined AMPD expression on the outer plasma membrane of immune cells.

Here, we demonstrate that AMPD2 is expressed on the cell surface of primary human leukocytes and may function as a novel regulator of extracellular purine metabolism, thereby modifying the ATP-adenosine balance controlled by the CD39-CD73 ectonucleotidase system (Figure 1).

2 | MATERIALS AND METHODS

2.1 | Subjects

Fifteen patients with a diagnosis of rheumatoid arthritis (RA) were recruited as part of the Charité Rh-GIOP

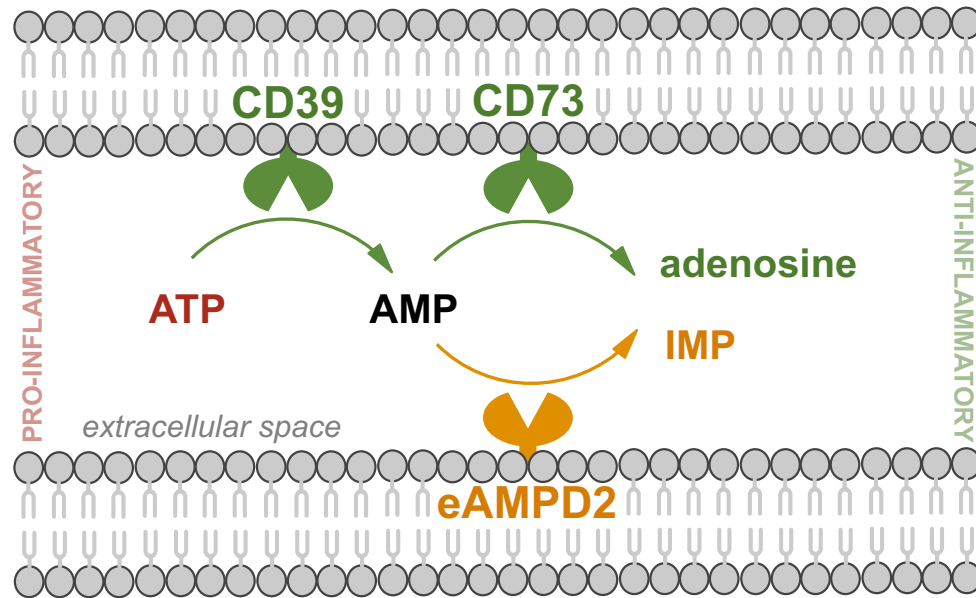


FIGURE 1 Possible role of eAMPD2 as a novel regulator of extracellular purine metabolism

study at the Department of Rheumatology and Clinical Immunology at Charité-Universitätsmedizin Berlin, Germany. Patients with active disease and in remission were considered for the study. Patients were included irrespective of their current immunosuppressive therapy. Thirteen healthy donors were matched for sex and age. The study was performed in accordance with the Declaration of Helsinki and ethical approval was obtained from the local ethics committee (Charité-Universitätsmedizin Berlin, approval number EA1/207/17). All participants gave informed written consent.

2.2 | Preparation of peripheral blood leukocytes and magnetic cell separation

Peripheral venous blood was collected in lithium heparin tubes. Isolation of polymorphonuclear leukocytes was preceded by red blood cell lysis using erythrocyte lysis buffer (0.01 M KHCO_3 , 0.155 M NH_4Cl , 0.1 mM EDTA, pH 7.5). CD15+ neutrophil granulocytes were purified by magnetic activated cell sorting (MACS) with anti-CD15-microbeads (Miltenyi Biotec, Bergisch Gladbach, Germany, Cat# 130-094-530, RRID:AB_2814656). Peripheral blood mononuclear cells (PBMCs) were isolated from the blood samples by Ficoll-Paque PLUS (GE Healthcare, Chicago, Illinois) density gradient centrifugation. CD14+ monocytes were isolated from PBMCs by MACS using anti-CD14-microbeads provided by Miltenyi Biotec (Cat# 130-050-201, RRID:AB_2665482). Cell preparations were performed according to the manufacturer's instructions. Purity of isolated CD14+ monocytes and CD15+ neutrophils exceeded 97% as verified by flow cytometry (Figure S1B+C).

2.3 | Chemicals and reagents

Dulbecco's Modified Eagle Medium (DMEM), Roswell Park Memorial Institute 1640 Medium (RPMI), MCDB 131 Medium, penicillin, streptomycin, and L-glutamine were obtained from Gibco (Thermo Fisher Scientific, Waltham, Massachusetts). Fetal calf serum (FCS), human AB serum, β -mercaptoethanol (2-ME), Accutase solution, brefeldin A (BFA), monensin (MN), lipopolysaccharide (LPS), flagellin (FliC), phytohemagglutinin-L (PHA-L), Phorbol 12-myristate 13-acetate (PMA), ionomycin, dexamethasone (Dex), hydrocortisone, Epidermal Growth Factor (EGF), ATP, ADO, IMP, and inosine were purchased from Sigma-Aldrich (St. Louis, Missouri). Miltenyi Biotec provided Poly (I:C) and ODN 2006. Pam3CSK4, FSL-1, and Resiquimod (R848) were purchased from Tocris (Bristol, United Kingdom).

2.4 | Antibodies

Staining for flow cytometry was performed using antibodies against AMPD2 (unconjugated, 1:50, rabbit polyclonal, Thermo Fisher Scientific, Cat# PA5-26127, RRID:AB_2543627), CD3 (Brilliant Violet 510, 1:20, OKT3, BioLegend, San Diego, California, Cat# 317332, RRID:AB_2561943), CD3 (Alexa Fluor 594, 1:20, UCHT1, DRFZ, Cat# UCHT1, RRID:AB_2619695), CD4 (APC-Vio 770, 1:10, M-T321, Miltenyi Biotec, Cat# 130-100-357, RRID:AB_2657994), CD8 (Alexa Fluor 647, 1:200 and Alexa Fluor 700, 1:1600, GN11/134D7, DRFZ), CD14 (FITC, 1:400, TM1, DRFZ), CD14 (Brilliant Violet 650, 1:20, M5E2, BioLegend, Cat# 301835, RRID:AB_11204241), CD15 (FITC, 1:10, VIMC6, Miltenyi Biotec, Cat# 130-081-101,

RRID:AB_244217), CD16 (APC/Cyanin7, 1:50, 3G8, BioLegend, Cat# 302018, RRID:AB_314218), CD19 (PerCP/Cyanine5.5, 1:100, HIB19, BioLegend, Cat# 302230, RRID:AB_2073119), CD25 (Brilliant Violet 785, 1:20, BC96, BioLegend, Cat# 302637, RRID:AB_11219197), CD39 (APC, 1:100, REA739, Miltenyi Biotec, Cat# 130-110-789, RRID:AB_2657891), CD45 (FITC, 1:20, HI30, BioLegend, Cat# 304006, RRID:AB_314394), CD45RA (Pacific Orange, 1:50, 4G11, DRFZ), CD73 (Brilliant Violet 421, 1:50, AD2, BioLegend, Cat# 344008, RRID:AB_11204424), CD127 (PE, 1:25, REA614, Miltenyi Biotec, Cat# 130-109-514, RRID:AB_2654831), CD127 (FITC, 1:10, MB15-18C9, Miltenyi Biotec, Cat# 130-098-093, RRID:AB_2659850), CCR4 (Brilliant Violet 605, 1:20, L291H4, BioLegend, Cat# 359418, RRID:AB_2562483), CCR6 (APC, 1:20, REA190, Miltenyi Biotec, Cat# 130-100-373, RRID:AB_2655933), and CXCR3 (PE-Vio 770, 1:50, REA232, Miltenyi Biotec, Cat# 130-101-382, RRID:AB_2655739). Goat anti-rabbit IgG (PE, 1:200, Invitrogen, Cat# P2771MP, RRID:AB_221651), streptavidin (PE, 1:200, Life Technologies, Cat# S866) and streptavidin (APC/Cyanine7, 1:300, BioLegend Cat# 405208) were used as secondary reagents. The following isotype controls were utilized to verify the staining: rabbit IgG (unconjugated, 1:125, Invitrogen, Carlsbad, California, Cat# 02-6102, RRID:AB_2532938), REA Control (S) (APC, 1:10, Miltenyi Biotec, Cat# 130-113-434, RRID:AB_2733447), and Mouse IgG1, κ Isotype Ctrl Antibody (Brilliant Violet 421, 1:50, MOPC-21, BioLegend, Cat# 400157, RRID:AB_10897939). The following antibodies were used for immunofluorescence microscopy: anti-AMPD2 antibody (unconjugated, 1:50, rabbit polyclonal, Thermo Fisher Scientific, Cat# PA5-26127, RRID:AB_2543627) and goat anti-rabbit IgG (Alexa Fluor Plus 488, 1:500, Thermo Fisher Scientific, Cat# A32731, RRID:AB_2633280). Antibodies against AMPD2 (1:500, QQ13, SCBT, Dallas, Texas, Cat# sc-100504, RRID:AB_2258261), beta Actin (1:10 000, BA3R, Invitrogen, Cat# MA5-15739, RRID:AB_10979409), glyceraldehyde 3-phosphate dehydrogenase (GAPDH) (1:100, 6C5, Merck Millipore, Burlington, Massachusetts, Cat# MAB374, RRID:AB_2107445), alpha Tubulin (100 ng/mL, rabbit polyclonal, abcam, Cambridge, United Kingdom, Cat# ab4074, RRID:AB_2288001), pan Cadherin (1:500, CH-19, abcam, Cat# ab6528, RRID:AB_305544), CD14 (Biotin, 1:50, TM1, DRFZ), lamin B1 (1:200, B-10, SCBT, Cat# sc-374015, RRID:AB_10947408), cytochrome b (1:200, SCBT, Cat# sc-11436, RRID:AB_2088887), calreticulin (1:2000, Thermo Fisher Scientific, Cat# PA1-902A, RRID:AB_2069607), mouse IgG (HRP, 1:10 000, Promega, Madison, Wisconsin, Cat# W4021, RRID:AB_430834), rabbit IgG (HRP, 1:10 000, Promega, Cat# W4011, RRID:AB_430833), chicken IgY (HRP, 1:5000, Thermo Fisher Scientific Cat# A16054, RRID:AB_2534727) and streptavidin (HRP, 1:1000, R&D Systems, Minneapolis,

Minnesota, Cat# DY998) were used for western blot analysis. Mouse monoclonal (2 μ L, QQ13, SCBT, Cat# sc-100504, RRID:AB_2258261) and rabbit polyclonal (3 μ L, Thermo Fisher Scientific, Cat# PA5-26127, RRID:AB_2543627) anti-AMPD2 antibodies were applied to realize immunoprecipitation (IP) of AMPD2, while mouse IgG1 (1:10, 2 μ L, Invitrogen, Cat# 02-6100, RRID:AB_2532935) and rabbit IgG (1,2 μ L, Invitrogen, Cat# 02-6102, RRID:AB_2532938) served as isotype controls.

2.5 | Cell culture

Human embryonic kidney 293 (HEK293) cells (Cat# CRL-1573, RRID:CVCL_0045) were purchased from ATCC (Manassas, Virginia) and cultured in DMEM supplemented with 10% (v/v) FCS. Jurkat (ATCC, Cat# TIB-152, RRID:CVCL_0367), THP-1 (ATCC, Cat# TIB-202, RRID:CVCL_0006) and U-937 (ATCC, Cat# CRL-1593, RRID:CVCL_0007) cells were cultured in RPMI supplemented with 10% (v/v) FCS. Human microvascular endothelial cells-1 (HMEC-1) (ATCC, Cat# CRL-10636, RRID:CVCL_0307) were cultured in MCDB 131 Medium supplemented with 25% (v/v) FCS, 2 mM L-glutamine, 10 ng/mL EGF and 0.3 μ g/mL hydrocortisone. Human primary immune cells were cultured in RPMI supplemented with 10% (v/v) human AB serum. 100 U/mL penicillin, 100 μ g/mL streptomycin and 50 μ M 2-ME were added to all media used. Cells were incubated in a humidified atmosphere at 5% CO₂ and approximately 18% O₂. Hypoxia was established by placing the cells in a hypoxic chamber (Binder) at 1% O₂. Incubation with either 1 μ g/mL Pam3CSK4, 10 μ g/mL Poly (I:C), 1 μ g/mL LPS, 100 ng/mL FliC, 1 μ g/mL FSL-1, 1 μ g/mL R848, 0.5 μ M ODN 2006, 5 μ g/mL PHA-L, or 10 ng/mL PMA and 1 μ g/mL ionomycin was performed as indicated to provoke immunostimulation. Inhibition of the golgi apparatus was achieved by incubation with 1 μ g/mL BFA or 0.5 μ g/mL MN. Dex was applied at concentrations of 10⁻⁵ M or 10⁻⁸ M as indicated while methotrexate (MTX) (medac, Wedel, Germany) was utilized at 0.8 μ M. Adherent cells were detached with the help of Accutase solution for 5 minutes at 37°C.

2.6 | Transfection of HEK293 cells with short hairpin RNA (shRNA)

Bacterial stocks containing shRNA plasmids cloned into the pLKO.1 puro vector were purchased from Sigma-Aldrich (MISSION shRNA). Hairpin sequences are provided in Table 1. The empty lentiviral backbone of pLKO.1 puro was provided by Bob Weinberg (Addgene plasmid #8453; <http://n2t.net/addgene:8453>; RRID:Addgene_8453)

TABLE 1 shRNA sequences targeting AMPD2

sh1	CCGGCCAAGGCCAAATATCCCTTTACTCGAGTAAAGGGATATTTGGCCTTGGTTTTTG
sh2	CCGGGCGCTTCATCAAGCGGGCAATCTCGAGATTGCCCGCTTGATGAAGCGCTTTTTG
sh3	CCGGGGGTATCTGGGAAGTACTTTGCTCGAGCAAAGTACTTCCCAGATACCCTTTTTTG
sh4	CCGGCATCGCTTTGACAAGTTAATCTCGAGATTAACTTGTCAAAGCGATGTTTTTG
sh5	CCGGGCACGCTATGGATGGCAAATCTCGAGATTGGCCATCCATAGACGTGCTTTTTG
sh6	CCGGATGTGCTGGAACGGGAGTTTCTCGAGGAACTCCCGTCCAGCACATTTTTTTG
sh7	CCGGGCCTCTTTGATGTGTACCGTACTCGAGTACGGTACACATCAAAGAGGCTTTTTG
sh8	CCGGTCATGCTGGCTGAGAACATTTCTCGAGAAATGTTCTCAGCCAGCATGATTTTTTG

whereas the plasmid containing scrambled shRNA was a gift from David Sabatini (Addgene plasmid #1864; <http://n2t.net/addgene:1864>; RRID:Addgene_1864).^{73,74} Bacterial colonies were cultured according to the manufacturer's instructions and plasmid DNA was prepared using NucleoBond Xtra EF (Macherey-Nagel, Düren, Germany). HEK293 cells were transfected with 30 µg of each plasmid to achieve transient knockdown of AMPD2.

2.7 | Lentivirus production and transduction of HEK293 and U-937 cells

Viral particles were produced by co-transfecting HEK293 cells with packaging plasmids pPAX2 and pVSVG by means of calcium phosphate precipitation. Viral supernatants were harvested after 48 hours and supplemented with 10 µg/mL polybrene (Sigma-Aldrich). Infection of HEK293 and U-937 cells was achieved by centrifugation for 2 hours at 700 g and 32°C. Successfully transduced cells were selected for at least 10 days by adding 1 µg/mL puromycin (InvivoGen, San Diego, California) to the culture medium.

2.8 | Sample preparation for protein analysis

Whole cell protein was prepared by lysing 10⁶ cells in 20 µL Laemmli sample buffer (Bio-Rad, Hercules, California, Cat# 1610747). IP lysis buffer (10 mM Tris HCl pH 7.5, 10 mM NaCl, 2 mM EDTA, 0.1% (v/v) Triton X-100, 1 mM PMSF, 2 µg/mL aprotinin) supplemented with protease and phosphatase inhibitor (Thermo Fisher Scientific, Cat# 78440) yielded whole cell lysates suitable for IP: 10 × 10⁶ cells were lysed in 300 µL IP lysis buffer for 5 minutes on ice. 12 µL 3 M NaCl were added for another 10 minutes prior to centrifugation for 15 minutes at 16 000 g and 4°C, yielding a clear supernatant. Cytosolic and membrane fractions were prepared using the Mem-PER Plus Membrane Protein Extraction Kit (Thermo Fisher Scientific, Cat# 89842). Additionally, surface protein enriched samples were obtained

by surface biotinylation followed by streptavidin-based pull-down (Pierce Cell Surface Protein Isolation Kit, Thermo Fisher Scientific). The manufacturer's protocols were followed for both procedures. In order to concentrate cytosolic and membrane fractions prior to sodium dodecyl sulfate polyacrylamide gel electrophoresis (SDS-PAGE), the lysates were concentrated using Amicon Ultra-0.5 mL Centrifugal Filters (50K, Merck Millipore Ltd., Ireland). Prior to IP or SDS-PAGE, respectively, protein concentrations of the lysates were determined by bicinchoninic acid assay (BCA assay, Interchim, Montluçon, France) and equal protein amounts were applied to the subsequent procedure. Before IP, the lysates were precleared with 20 µL protein A/G plus agarose (SCBT, Cat# sc-2003, RRID:AB_10201400) for 30 minutes at 4°C. IP of AMPD2 was performed by incubating 1 mL lysate with either antibody against AMPD2 or isotype control overnight. Pull-down was achieved by adding 20 µL protein A/G plus agarose and four 5-minute washing steps with 1 mL IP buffer (0.15 M NaCl, 0.05 M Tris-HCl pH 8, 1% (v/v) NP40) supplemented with protease and phosphatase inhibitor (Thermo Fisher Scientific, Cat# 78440) followed by centrifugation at 1000 g for one minute. Agarose pellets were prepared for SDS-PAGE by adding 6.5 µL 4× Laemmli sample buffer (Bio-Rad, Cat# 1610747) or directly digested for mass spectrometric analysis (see *Protein Digest* below).

2.9 | Western blot analysis

Samples were separated by SDS-PAGE and subsequently blotted onto PVDF membranes (Merck Millipore). PVDF membranes were block with 5% (w/v) nonfat dry milk (AppliChem GmbH, Darmstadt, Germany) in TBS/0.05% Tween 20 (Sigma-Aldrich) for 90 minutes followed by three 10-minute washing steps with TBS/0.05% Tween 20. Protein detection was accomplished with the aforementioned antibodies diluted in TBS/0.05% Tween 20: the membranes were incubated with the primary antibody for 2 hours at room temperature (RT) or overnight at 4°C. The secondary antibody was added for 1 hour at RT. Each step was followed by three 10-minute washing steps with TBS/0.05% Tween

20. Visualization was accomplished by enzymatic chemiluminescence (PerkinElmer, GE Healthcare) in an ImageQuant LAS 4000 imager (GE Healthcare).

2.10 | Protein digest

Antibody pull-down samples were processed for mass spectrometry as follows: Dry beads were resuspended in 20 μ L urea buffer (6 M urea, 2 M thiourea, 10 mM HEPES, pH 8.0) and reduced for 30 minutes at RT in 12 mM dithiothreitol solution, followed by alkylation by 40 mM chloroacetamide for 20 minutes in the dark at RT. The samples were first digested using 1 μ g endopeptidase LysC (Wako, Osaka, Japan) for 4 hours, followed by dilution in 4 volumes of 50 mM ammonium bicarbonate buffer (pH = 8.5) and digestion with 1 μ g sequence-grade trypsin (Promega) for 16h. The digestion was stopped by acidifying each sample to pH < 2.5 by adding trifluoroacetic acid solution (final concentration 1%). The peptides were extracted and desalted using the StageTip protocol.⁷⁵ Samples from streptavidin pull-down experiments were processed using the SP3 protein clean-up and digestion protocol.⁷⁶ Peptides were collected, extracted, and desalted using the StageTip protocol.⁷⁵ Proteins from total cell lysate, cytosolic and membrane fraction (input samples) were extracted with 6 M Guanidinium chloride/50 mM ammonium bicarbonate buffer (pH = 8.5) and reduced for 30 minutes at RT in 12 mM dithiothreitol solution, followed by alkylation by 40 mM chloroacetamide for 20 minutes in the dark at RT. The samples were digested and desalted as described above.

2.11 | LC-MS/MS analyses

For LC-MS/MS analyses peptides were eluted with 80% Acetonitrile/0.1% formic acid, dried and resolved in 3% acetonitrile/0.1% formic acid. Peptides were separated on a reversed-phase column (20 cm fritless silica microcolumns with an inner diameter of 75 μ m, packed with ReproSil-Pur C18-AQ 1.9 μ m resin (Dr Maisch GmbH, Ammerbuch-Entringen, Germany)) with a 250 nL/min flow rate of increasing Buffer B concentration (from 2% to 60%) on a High Performance Liquid Chromatography (HPLC) system (Thermo Fisher Scientific). A 90-minute gradient was applied for antibody-based and streptavidin-based pull-down samples, whereas a 202-minute gradient was applied for input samples. Peptides from pull-down samples were analyzed on a Q Exactive Plus or HF-X Hybrid Quadrupole-Orbitrap instrument (Thermo Fisher Scientific). Input sample measurements were performed with an Orbitrap Fusion Tribrid instrument (Thermo Fisher Scientific). The Q Exactive Plus instrument was run in data dependent mode selecting the Top 10 most intense ions in the MS full scans, selecting ions from

350 to 2000 m/z , using 70K resolution with a 3×10^6 ion count target and 50 ms injection time. Tandem MS was performed by isolation at 1.6 m/z with the quadrupole, HCD fragmentation with normalized collision energy of 26 and resolution of 17.5K. The MS² ion count target was set to 5×10^4 with a maximum injection time of 250 ms For measurements with the HF-X instrument the Top 20 most intense ions in the MS full scans from 350 to 1800 m/z were selected, using 60K resolution with a 3×10^6 ion count target and 10 ms injection time. Tandem MS was performed by isolation at 1.3 m/z with the quadrupole, HCD fragmentation with normalized collision energy of 27 and resolution of 15K. The MS² ion count target was set to 1×10^5 with a maximum injection time of 22 ms The Orbitrap Fusion Tribrid instrument was run in data dependent mode selecting the top 20 most intense ions in the MS full scans, selecting ions from 350 to 2000 m/z , using 60K resolution with a 4×10^5 ion count target and 50 ms injection time. Tandem MS was performed by isolation at 0.7 m/z with the quadrupole, HCD fragmentation with normalized collision energy of 32 and resolution of 15K. The MS² ion count target was set to 5×10^4 with a maximum injection time of 250 ms For all measurements only precursors with charge state 2-7 were sampled for MS². The dynamic exclusion duration was set to 30 seconds with a 10 ppm tolerance around the selected precursor and its isotopes. Data were analyzed using the MaxQuant software package (v1.6.0.1). The internal Andromeda search engine was used to search MS² spectra against a decoy human UniProt database (HUMAN.2017, HUMAN.2019) containing forward and reverse sequences. The search included variable modifications of methionine oxidation and N-terminal acetylation, deamidation (N and Q) and fixed modification of carbamidomethyl cysteine. Minimal peptide length was set to seven amino acids and a maximum of 3 missed cleavages was allowed. The FDR (false discovery rate) was set to 1% for peptide and protein identifications. Unique and razor peptides were considered for quantification. Retention times were recalibrated based on the built-in nonlinear time-rescaling algorithm. MS² identifications for technical replicates were transferred between runs with the "Match between runs" option. iBAQ values and LFQ (label-free quantification) intensities were calculated using the in-built algorithms. The resulting text files were filtered to exclude reverse database hits, potential contaminants, and proteins only identified by site. The mass spectrometry proteomics data have been deposited to the ProteomeXchange Consortium via the PRIDE partner repository with the dataset identifier PXD022350.⁷⁷

2.12 | Flow cytometry

Staining for flow cytometry was performed on ice. Dead cell removal (Miltenyi Biotec) was performed prior to

the staining as indicated. The cells were resuspended in PBS/0.5% BSA/0.05% sodium azide (PBA). 10% (v/v) human IgG (Kiovig [100 mg/mL, 1:2 dilution], Baxter AG, Wien, Austria) was added to block unspecific binding of Fc receptors. Specificity was ensured by incubating the cells with 25-fold excess unconjugated antibody for 10 minutes prior to the staining procedure to block binding of the primary antibody. Cells were incubated with a combination of the aforementioned antibodies for 10 minutes followed by two 3-minute washing steps with PBA at 300 g and 4°C. Where applicable, cells were subsequently incubated with a secondary antibody for 10 minutes and washed as before. Apoptotic cells were identified using annexin V (Cy5, 1:100, BD, Franklin Lakes, New Jersey, Cat# 559934, RRID:AB_2869267), while 7-AAD (1:100, BD, Cat# 559925, RRID:AB_2869266) and DAPI (1 µg/mL, Sigma-Aldrich) where applied to exclude dead cells. Cells were fixed and permeabilized with -20°C cold 90% (v/v) methanol to complete intracellular stainings. The samples were measured using a MACSQuant Analyzer 10 (Miltenyi Biotec) and an LSRFortessa cell analyzer (BD) and analyzed with FlowJo software (version 7.6.4 and 10.7.1, BD). eAMPD2, CD39 and CD73 expression was recorded by determining geometric mean fluorescence intensity (gMFI). Results are provided as the ratio (*r* gMFI) of staining to either block or secondary antibody control. Lymphocyte subsets were analyzed as follows: CD4+ T cell subsets were subdivided into Type 1 helper (T_H1) cells, Type 2 helper (T_H2) cells and IL-17-producing T helper (T_H17) cells. T_H1 cells were identified by the expression of CXCR3 in the absence of CCR4 and CCR6. T_H2 cells were defined as CCR4+CXCR3-CCR6-, while T_H17 cells co-expressed CCR4 and CCR6 in the absence of CXCR3. CD4+CD25+CD127low cells were defined as regulatory T cells (Treg).⁷⁸ Cytotoxic T cells and B cells were identified by the expression of CD8 and CD19, respectively. Monocytes were subanalyzed according to CD14 and CD16 surface expression as follows: classical (CD14^{hi}, CD16-), intermediate (CD14^{hi}, CD16+) and non-classical (CD14^{low}, CD16^{hi}).⁷⁹ The gating strategy is depicted in Figure S1A,E.

2.13 | Immunofluorescence microscopy

Human PBMCs were seeded onto 8-well chamber slides directly after isolation, while U-937 cells were stained in a 48-well plate and subsequently centrifuged onto a glass slide at 500 g for 1 minute with the help of a Cytospin 4 cytocentrifuge (Thermo Fisher Scientific). The cells were fixed with 4% paraformaldehyde for 8 minutes followed by three 3-minute washing steps with PBS. In order to achieve intracellular staining the cells were permeabilized prior to the staining procedure with PBS/0.1% Tween 20 (Qbiogene Inc, Carlsbad, CA, USA) for 10 minutes. This step was

omitted for all extracellular stainings. Unspecific binding sites were blocked by incubation with 5% (v/v) FCS in PBS. Staining was achieved by overnight incubation with anti-AMPD2 antibody diluted in PBS at 4°C in the dark followed by a goat anti-rabbit secondary antibody diluted in PBS for two hours at RT. Actin was visualized using TRITC-conjugated phalloidin (1:50, Sigma-Aldrich, Cat# P1951, RRID:AB_2315148) diluted in PBS/5% FCS for 40 minutes, whereas DAPI (1 µg/mL in PBS/5% FCS, 10-minute incubation) was applied to detect the nuclei. After three 3-minute washing steps with PBS images were acquired with an LSM 880 confocal laser scanning microscope (ZEISS, Germany, RRID:SCR_020925) and a Bioevo BZ-9000 microscope (Keyence, RRID:SCR_015486) and analyzed with ZEN (ZEISS) and ImageJ.

2.14 | Purine nucleoside measurements

CD14+ monocytes purified by MACS technology were incubated in RPMI without phenol red supplemented with 10% (v/v) human AB serum and 1 µg/mL LPS ±1 µg/mL BFA as indicated for 24 hours. Supernatants were collected and immediately stored at -80°C. Extracellular adenosine levels were determined enzymatically with the help of a fluorometric adenosine assay (abcam, Cat# ab211094) performed according to the manufacturer's instructions.

2.15 | Cytokine measurements

PBMCs were cultured in a 24-well plate in RPMI supplemented with 10% (v/v) heat-inactivated human AB serum at 10⁶ cells per well. Incubation with either 100 µM / 1 mM ATP, 1 µM / 50 µM ADO, 100 µM / 1 mM IMP, or 100 µM / 1 mM inosine for 30 minutes was followed by immunostimulation with 1 µg/mL LPS for another two hours. Subsequently, supernatants were collected and TNF-alpha release was measured by ELISA (R&D Systems, Minneapolis, Minnesota, Cat# DY210, RRID:AB_2848160).

2.16 | Statistical analysis

Statistical data analysis of mass spectrometric measurements was performed using Perseus software (v1.6.2.1). Technical and biological replicates for each condition were defined as groups and intensity values were filtered for "minimum value of 3" per group. After log2 transformation missing values were imputed with random noise simulating the detection limit of the mass spectrometer. Imputed values are taken from a log normal distribution with 0.25× the standard deviation of the measured, logarithmized values, down-shifted by

1.8 standard deviations. Differential protein abundance was calculated using two-sample Student's *t* test, applying a permutation based FDR (false discovery rate) cut-off of 5%.

Statistical analyses of all other samples were performed using GraphPad Prism. In order to assess differences between paired samples Wilcoxon matched-pairs signed rank test was applied. Mann Whitney test was used to compare different groups.

2.17 | Search for potential membrane domains

UniProt and TMHMM servers were consulted to screen AMPD2 for potential transmembrane domains.^{80,81} Subsequently, we followed the decision tree suggested by HeliQuest: The secondary protein structure was determined using the PSIPRED server.^{82,83} The identified helical regions were then submitted to the HeliQuest webserver to calculate the hydrophobicity $\langle H \rangle$, the hydrophobic moment $\langle \mu H \rangle$ and the net charge z . Based on these data, the discriminant factor D was then determined as follows: $D = 0.944(\langle \mu H \rangle) + 0.33(z)$. $D > 1.34$ defined a lipid-binding helix, while helices with $0.68 < D < 1.34$ were classified as possible lipid-binding helices.^{83,84}

3 | RESULTS

3.1 | AMPD2 is differentially expressed in primary immune cells and various cell lines and is selectively detected on the cell surface

As AMPDs are encoded by three different genes, AMPD1, AMPD2, and AMPD3,⁸⁵ we initially aimed to determine the most abundant isoform in human immune cells. Data from the Human Protein Atlas reveals that AMPD2 represents the most common variant of AMPDs in human leukocytes (Figure 2A).⁸⁶ Consequently, we focused on this isoform in the following experiments. In order to identify a suitable model system to examine AMPD2 surface expression, we first analyzed cytoplasmic AMPD2 expression in different cell lines. Flow cytometric analysis following intracellular staining showed similar expression levels of AMPD2 in all examined cell lines, namely HEK293, HMEC-1, Jurkat, THP-1, and U-937 cells (Figure S2A, upper row). Cell lines generally displayed low eAMPD2 expression (Figure S2A, lower row). However, HEK293 cells and U-937 presented appreciable surface expression (r gMFI = 2.03 and 2.19) and a successful blocking of surface staining by an excess of unconjugated antibody and were thus chosen to further verify the presence of AMPD2 on the cell surface. Western blot analysis of AMPD2 immunoprecipitated from HEK293 and

U-937 membrane fractions additionally demonstrated the localization of AMPD2 in the cell membrane (Figure 2B). In order to confirm the identity of the immunoprecipitated target protein, mass spectrometric analyses of immunoprecipitated samples from HEK293 membrane fractions using a mouse monoclonal anti-AMPD2 antibody (QQ13) were performed. AMPD2 was found to be the top abundant protein (TopX) and was significantly enriched compared with isotype control ($\log_2(\text{enrichment factor}) = 5.82$; $-\log_{10}(P\text{-value}) = 3.85$ (LFQ)) (Figure S2C, Table S1). IP from HEK293 whole cell lysates using the staining antibody anti-AMPD2 (PA5) was performed in addition in order to validate antibody specificity by IP-MS (Table S1).⁸⁷ By concentrating the cytosolic and membrane lysates subsequently analyzed by SDS-PAGE, we were able to increase the amount of AMPD2 detected on western blot (Figure S2B). As our membrane protein purification procedure does not explicitly differentiate between plasma membrane and subcellular membranes, we conducted further experiments to characterize the membrane fraction: we detected both lamin B1 and calreticulin—markers of the nuclear membrane and the endoplasmic reticulum, respectively—in the purified membrane lysates (Figure S2D). Contamination by cytosolic protein indicated by GAPDH was, however, minimal (Figure S2D). As the presence of AMPD2 in the membrane fraction is, therefore, not clearly attributable to its presence in the plasma membrane, we performed surface biotinylation to verify the localization of AMPD2 at the cell surface. AMPD2 was detected in biotin-enriched samples isolated from HMEC-1 and U-937 cells as well as CD14+ monocytes by a surface biotinylation assay (Figure 2C). For HMEC-1 cells this result was verified with the help of mass spectrometry showing significant enrichment compared with non-biotinylated streptavidin-based pull-down controls ($\log_2(\text{enrichment factor}) = 3.70$; $-\log_{10}(P\text{-value}) = 2.00$ (LFQ)) (Figure 2D, Table S2). The top abundant proteins enriched by streptavidin-based pull-down following surface biotinylation are listed in Table S2 as proof of efficient surface protein enrichment. Figure S2E additionally shows flow-through samples to display surface abundance compared with the overall protein content. Surface biotinylation was also verified by flow cytometry demonstrating eAMPD2 expression on surface-biotinylated cells (Figure S2F). As Eltzhig et al previously demonstrated increased surface expression of adenosine deaminase in HMEC-1 cells exposed to hypoxia,⁸⁸ we additionally evaluated this scenario with respect to AMPD2. Interestingly, surface biotinylation of HMEC-1 cells cultured under hypoxic conditions revealed a slight decrease in AMPD2 surface expression (Figure S2G). Mass spectrometric analysis confirmed these results ($\log_2(\text{enrichment factor}) = -0.44$ (LFQ); $-\log_{10}(P\text{-value}) = 3.38$ (LFQ)). These data corresponded to flow cytometric analyses of the AMPD2 surface staining performed

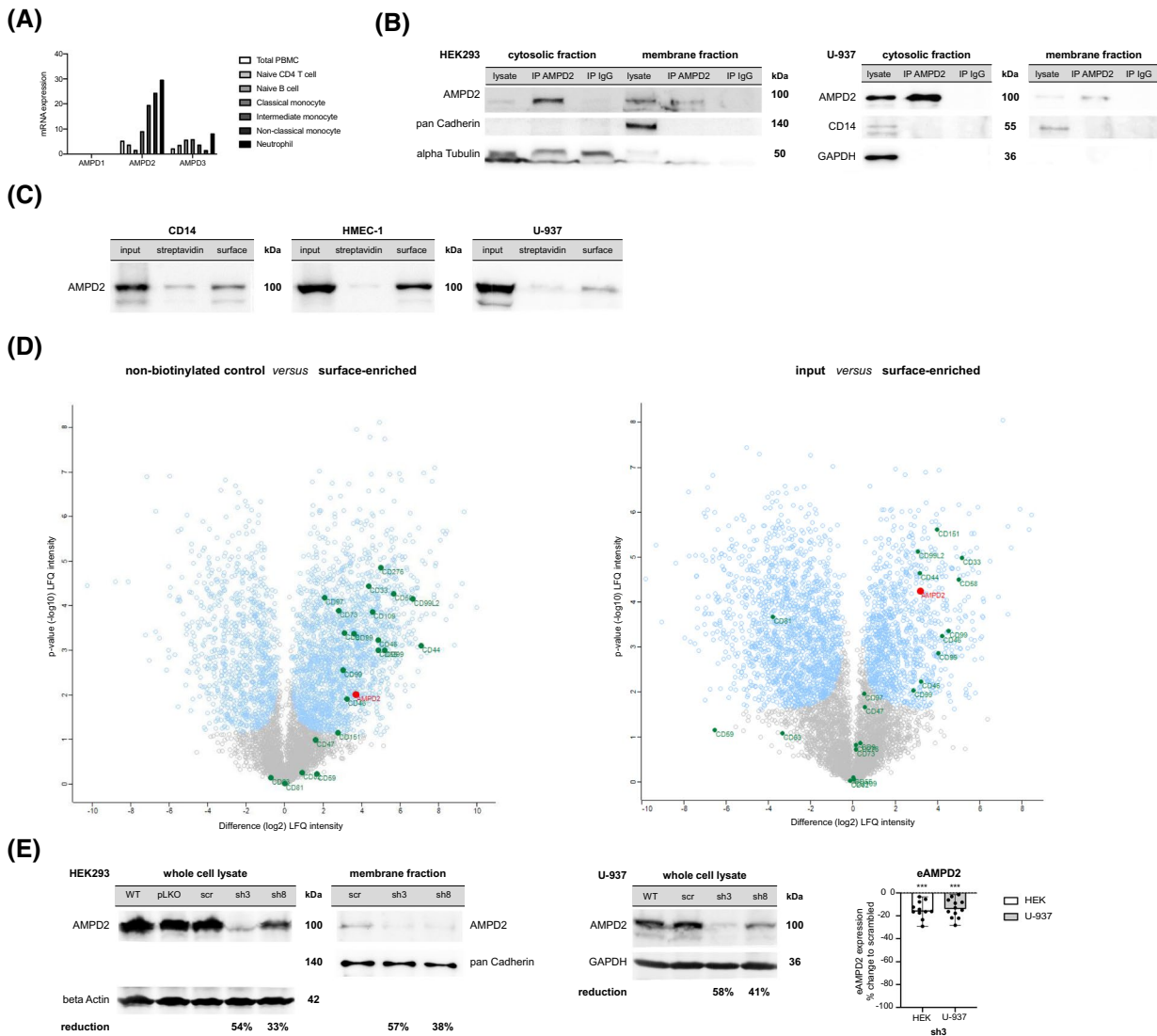


FIGURE 2 Differential AMPD expression in primary human immune cells and cell lines and detection of AMPD2 in the cell membrane. A, mRNA expression of AMPD isoforms in human leukocyte populations according to the Human Protein Atlas.⁸⁶ The values represent normalized expression and were extracted from the Consensus dataset. B, Western blot analysis of AMPD2 pulled down from HEK293 and U-937 cytosolic and membrane fractions by IP using a mouse monoclonal antibody against human AMPD2 (IP AMPD2) compared to isotype control (IP IgG). Purity of cytosolic and membrane fractions was verified by analyzing pan Cadherin as well as alpha Tubulin and GAPDH, respectively. Uncropped images are provided in Figure S7. C, Western blot analysis of CD14⁺ monocytes, HMEC-1 and U-937 cells after surface protein enrichment. Surface biotinylation was performed followed by streptavidin-based pull-down (surface). A non-biotinylated control sample was run in parallel (streptavidin). Input samples represent cell lysates after surface biotinylation prior to streptavidin-based enrichment. D, Mass spectrometric analysis of surface-enriched protein obtained from HMEC-1 cells by streptavidin-based pull-down following surface biotinylation. Presence of AMPD2 in the surface-enriched fraction is displayed compared to streptavidin-based pull-down of non-biotinylated samples (non-biotinylated control) and biotinylated whole cell lysate without streptavidin-based pull-down (input), respectively. Differential protein abundance was determined using two-sample Student's *t* test and blue circles represent significance with an FDR cut-off of 5%. E, AMPD2 protein expression was quantified by western blot and flow cytometry. Western blot analysis of AMPD2 protein expression in HEK293 and U-937 whole cell lysates and HEK293 membrane fractions after AMPD2 knockdown by lentiviral transduction of shRNA particles and 10-day selection with 1 μ g/mL puromycin is shown on the left. AMPD2 protein expression was semiquantified relative to beta Actin, pan Cadherin and GAPDH, respectively, by image analysis and reduction by shRNA transduction is depicted in relation to a lentiviral negative control vector containing scrambled shRNA. BCA assay was utilized for protein quantification of membrane fractions. Uncropped images are provided in Figure S7. Reduced eAMPD2 surface expression in HEK293 and U-937 cells after lentiviral knockdown by shRNA sh3 was reproducible by surface staining and flow cytometric analysis ($n = 11-12$). Doublets and dead cells were excluded for analysis as shown in Figure S1F. The data are depicted as change in *r* gMFI (geometric mean fluorescence intensity of staining to secondary antibody control) in relation to a lentiviral negative control vector containing scrambled shRNA. Bar graphs depict median and range. *** $P < .001$, compared to scrambled shRNA; Wilcoxon matched-pairs signed rank test. WT, wild type; pLKO, pLKO.1 puro; scr, scrambled

in parallel (Figure S2G). Similarly, changes in CD73 expression observed under normoxic and hypoxic conditions measured by flow cytometry (Figure S2G) were consistent with the mass spectrometric analyses ($\log_2(\text{enrichment factor}) = 0.566$ (LFQ); $-\log_{10}(P\text{-value}) = 3.96$ (LFQ)). In summary, AMPD2 surface expression was confirmed by three independent methods in various cell lines.

3.2 | AMPD2 surface expression is reduced after AMPD2 knockdown in HEK293 and U-937 cells

In order to further substantiate surface staining specificity and verify eAMPD2 expression, we performed AMPD2 knockdown in HEK293 and U-937 cells. Knockdown efficiency was examined by transiently transfecting HEK293 cells with plasmids containing shRNA sequences targeting AMPD2. The corresponding sequences are listed in Table 1. Western blot analysis of whole cell lysates demonstrated that shRNA constructs 3 and 8 efficiently reduced AMPD2 protein expression. Thus, these shRNA sequences were used to produce viral particles and subsequently obtain stable gene silencing of AMPD2 by infecting HEK293 and U-937 cells. Successfully transduced cells were selected by puromycin and protein expression was analyzed by western blotting of whole cell lysates. Image analysis demonstrated that lentiviral knockdown with shRNA constructs 3 and 8 reduced AMPD2 protein expression by 54% and 33% in HEK293, and by 58% and 41% in U-937 cells (Figure 2E). In the following, AMPD2 protein levels were examined in membrane fractions from HEK293 cells stably expressing the viral constructs. Western blot analysis revealed that the reduction of AMPD2 in the membrane after stable gene silencing was similar to the changes observed with respect to the overall expression (Figure 2E). This reduction in membrane expression was reproduced by flow cytometric analysis following surface staining of successfully transduced HEK293 and U-937 cells (Figure 2E).

3.3 | AMPD2 contains lipid-binding regions and AMPD2 surface expression is reduced by inhibitors of the secretory pathway

After verifying AMPD2 surface expression in different cell lines, we screened the proteins for potential membrane domains. UniProt and TMHMM servers did not identify any transmembrane domains in the protein sequence.^{80,81} In order to search for lipid-binding regions that are characteristic of amphitropic proteins—proteins that localize both to the cytosol and to the plasma membrane—we identified helical regions with the help of the PSIPRED server.⁸² The results of this search are displayed in Figure S2H. A total of 143 helical sequences were subsequently submitted to the HeliQuest webserver analyzing sequences containing 18 amino acids at a time in accordance with the server's requirements.⁸³ We identified five lipid-binding helices and 35 possible lipid-binding helices, although the identified sequences were overlapping due to the character of the search. Therefore, the five lipid-binding helices likely form part of one single lipid-binding region. The results are shown in Table 2 and Table S3. Additionally, we aimed to evaluate possible mechanisms of membrane trafficking experimentally: we verified whether changes in eAMPD2 expression could be provoked by disrupting protein transport via the Golgi apparatus. eAMPD2 expression was indeed reduced after treating HEK293 and U-937 cells with either 1 $\mu\text{g/mL}$ BFA or 0.5 $\mu\text{g/mL}$ MN for 24 hours (Figure S2I). Thus, we provide evidence that AMPD2 contains lipid-binding regions and that the secretory pathway is directly or indirectly involved in membrane trafficking of eAMPD2.

3.4 | AMPD2 is expressed on the cell surface of peripheral immune cells

Having successfully established a surface staining procedure in HEK293 and U-937 cells as model systems, we were particularly interested in examining its role in primary

Sequence	H	μH	z	D
³⁶⁸ NGPIKSFYRRLQYLSSK ₃₈₅	0.346	0.232	4	1.539008
³⁶⁹ GPIKSFYRRLQYLSSKF ₃₈₆	0.479	0.338	4	1.639072
³⁷⁰ PIKSFYRRLQYLSSKFQ ₃₈₇	0.467	0.346	4	1.646624
³⁷¹ IKSFYRRLQYLSSKFQM ₃₈₈	0.495	0.329	4	1.630576
³⁷² KSFYRRLQYLSSKFQM ₃₈₉	0.402	0.248	4	1.554112

TABLE 2 Predicted lipid-binding region within the AMPD2 protein sequence

Note: Amino acids 368–389 of the AMPD2 protein sequence: H, μH and z were provided by the HeliQuest webserver.⁸³ D was calculated as follows: $D = 0.944((\mu\text{H})) + 0.33(z)$. A lipid-binding helix was defined by $D > 1.34$.

Abbreviations: D, discrimination factor; H, hydrophobicity; z, net charge; μH , hydrophobic moment.

human immune cells. As expression of ectonucleotidases CD39 and CD73 has been described in a variety of immune cell populations,⁴ our first endeavor was to screen different leukocyte subsets for eAMPD2 expression. Flow

cytometric analysis revealed that eAMPD2 was predominantly expressed on the cell surface of B cells, monocytes and granulocytes (Figure 3A). With respect to monocyte subpopulations, AMPD2 staining intensity did not differ

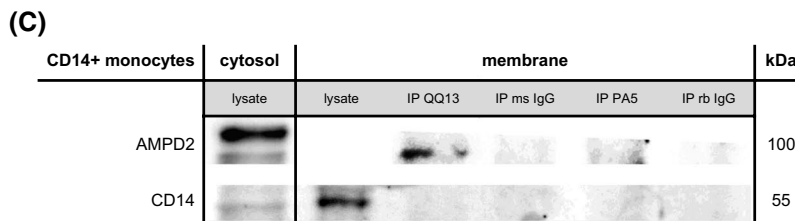
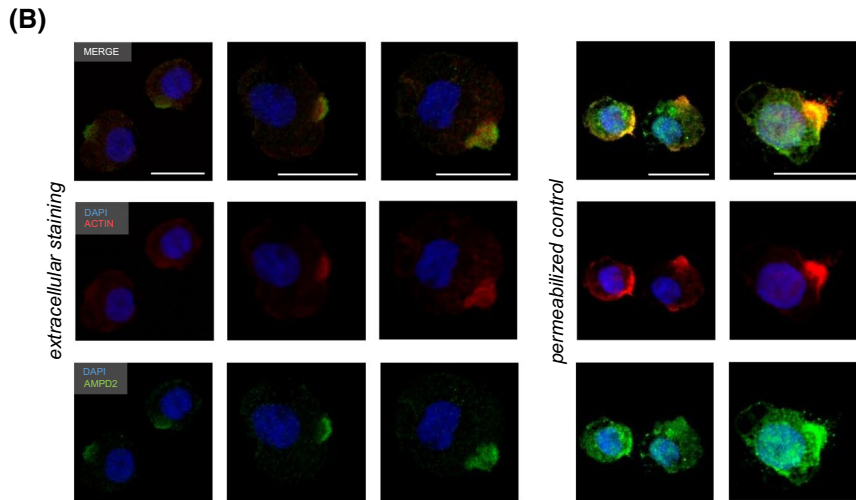
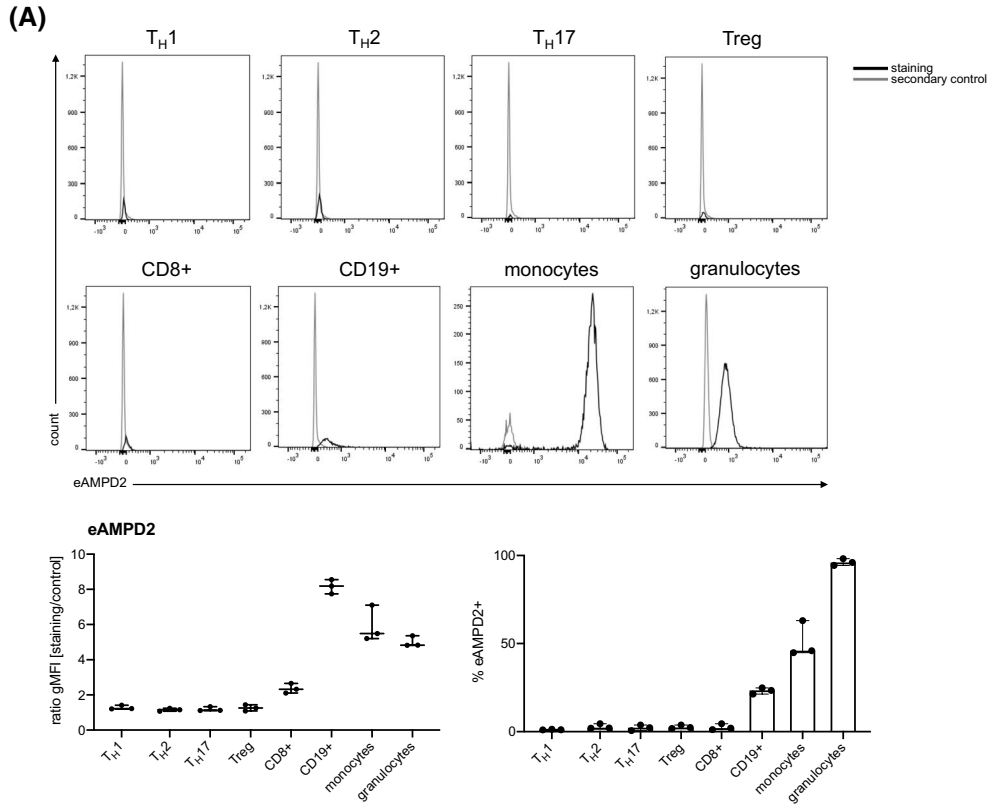


FIGURE 3 AMPD2 surface expression on primary human immune cells. A, Human leukocytes were isolated by red blood cell lysis and analyzed for AMPD2 surface expression on different leukocyte subsets by flow cytometry ($n = 3$). The gating strategy is displayed in Figure S1A. ratio gMFI represents the ratio of geometric mean fluorescence intensity of staining to secondary antibody control. B, Localization of AMPD2 on the cell surface of U-937 cells identified by immunofluorescence microscopy. Cells were stained for AMPD2 (green), actin (red) and DAPI (blue). The scale bar represents 20 μm . The images show two independent experiments. Extracellular staining for eAMPD2 was performed on intact cells, while the cells were permeabilized to achieve intracellular staining. C, Western blot analysis of AMPD2 pulled down from membrane fractions of sorted CD14+ monocytes by IP using a mouse monoclonal antibody (QQ13) and a rabbit polyclonal antibody (PA5) against human AMPD2 compared to isotype control. CD14 was detected as a membrane marker. Uncropped images are provided in Figure S7. Boxplots show median and minimum or maximum values, respectively, while bar graphs depict median and range

between classical, intermediate and non-classical monocytes (Figure S1E). On the other hand, we did not observe significant expression of eAMPD2 in the different T cell populations examined, namely T_{H1} , T_{H2} , T_{H17} cells, Tregs and CD8+ T cells. Incubation with 25-fold excess unconjugated anti-AMPD2 antibody for 10 minutes completely prevented staining of the target protein, thus rebutting the possibility of the staining antibody inaccurately adhering to the cell surface (Figure S1E). Additionally, eAMPD2 expression on U-937 cells and PBMCs was confirmed by immunofluorescence microscopy as depicted in Figure 3B and Figure S3A. Actin as part of the cytoskeleton was visualized with the help of TRITC-conjugated phalloidin, while DAPI was applied to detect the cell nuclei. Incubation with rabbit IgG isotype control did not result in a signal (Figure S3A), whereas a distinct surface staining was achieved by adding anti-AMPD2 antibody. Furthermore, membrane fractions were prepared from isolated CD14+ monocytes. AMPD2 was successfully pulled down from the lysates by IP and detected by western blotting (Figure 3C). In comparison with equivalent samples incubated with corresponding isotype controls, AMPD2 was strongly enriched by IP performed with anti-AMPD2 antibodies (Figure 3C). The comparatively weak signal produced after pull-down with the polyclonal antibody “PA5” can be explained by the fact that this product is designed for flow cytometry. Significant enrichment of AMPD2 by IP from monocytic membrane fractions with mouse monoclonal anti-AMPD2 (QQ13) compared with isotype control was additionally confirmed by mass spectrometry ($\log_2(\text{enrichment factor}) = 4.2$; $-\log_{10}(P\text{-value}) = 2.87$ (LFQ)) (Table S4).

After verifying AMPD2 surface expression in primary immune cells and establishing a reliable surface staining, we proceeded to examine whether surface expression was modifiable by immunostimulation. As we could not refer to any previous data regarding eAMPD2 expression, we initially incubated PBMCs with 5 $\mu\text{g}/\text{mL}$ PHA-L and 1 $\mu\text{g}/\text{mL}$ LPS activating T lymphocytes and monocytes, respectively, and examined the kinetics of eAMPD2 expression for 30 hours. While eAMPD2 expression on lymphocytes tended to be reduced after incubation with PHA-L, we observed an increase in eAMPD2 on the cell surface of monocytes stimulated with LPS that reached a maximum after

20-24 hours (Figure S3E). In contrast, eAMPD2 expression was not enhanced in neutrophils activated by LPS stimulation (Figure S3B). Similarly, activating lymphocytes with a combination of PMA and ionomycin did not alter eAMPD2 expression (Figure S3C). Successful T cell stimulation was demonstrated by flow cytometric analysis of CD25 and CD69 (Figure S3D). Since we were specifically seeking conditions that augmented eAMPD2 expression to understand the role of this enzyme on the cell surface, we focused on monocytes in PBMC co-culture after 21-24 hours incubation in the following experiments. To guarantee that the enhanced surface staining after LPS stimulation was not caused by unspecific attachment of staining antibodies to dying monocytes upon activation, apoptotic and dead cells were excluded by dead cell removal as well as co-staining with annexin V. Both procedures did not affect the intensity of eAMPD2 expression measured by flow cytometry (Figure S3F). Therefore, we concluded that surface expression was in fact enhanced distinctively in stimulated monocytes, suggesting a possible role of eAMPD2 as a novel pro- or anti-inflammatory switch actively regulated by immune cells in states of inflammation.

3.5 | eAMPD2 and CD39 display a similar surface expression pattern

Following this first indication of its relevance, we aimed to further understand AMPD2 surface expression in the context of other ectoenzymes. Since we hypothesized a role in the ectonucleotidase-driven metabolism of extracellular purine nucleotides, we initially examined surface expression of eAMPD2, CD39 and CD73 by flow cytometry on human PBMCs at baseline (Figure S4A+B). Interestingly, CD73 was scarcely detectable on monocytes directly after isolation. Instead, we observed that CD73 expression was restricted to distinct lymphocyte subsets. CD73+ lymphocytes were predominantly identified as CD8+ T cells and CD19+ B cells (Figure S4D). Similar to eAMPD2, CD39 was predominantly expressed on monocytes, while only a small fraction of lymphocytes was CD39+. Indeed, eAMPD2 expression on monocytes tended to correlate with CD39 expression at baseline ($r_{\text{Sp}} = 0.6788$, $P = .0255$) (Figure S4B).

3.6 | TLR stimulation enhances AMPD2 surface expression on monocytes

In order to identify stimuli that enhance eAMPD2 expression, we next performed toll-like receptor (TLR) stimulation at TLRs 1-9 in PBMC co-culture. Except for Poly (I:C) and ODN 2006 that are agonists at TLR3 and TLR9, respectively, all reagents significantly enhanced eAMPD2 expression on human monocytes. The greatest increase in eAMPD2 expression compared with the untreated control was observed after stimulation of TLR4 and TLR7/8 (Figure 4B). A similar pattern was found regarding CD39 expression on monocytes, although agonists of TLR3 and TLR9 effectively enhanced CD39 surface expression as well (Figure 4B). Besides a slight reduction in CD73 surface expression on monocytes after incubation with the TLR9 agonist ODN 2006, CD73 expression was not significantly affected by TLR activation (Figure 4B). Lymphocytes were analyzed simultaneously and were largely unaffected by TLR stimulation. Although a significant reduction in CD73 expression was observed for each TLR agonist, these changes were minute (Figure 4A). Having confirmed LPS as the strongest trigger of eAMPD2 expression in monocytes, we proceeded to examine whether this increase could be prevented by Golgi transport inhibition; in order to confirm our prior hypothesis that the secretory pathway mediated AMPD2 surface expression. We observed that concomitant incubation with BFA significantly reduced eAMPD2 expression after 24 hours compared to LPS alone. This was true for both lymphocytes and monocytes in PBMC co-culture (Figure 4C+D). CD73 showed similar changes in monocytes, whereas surface expression proved to be more stable in lymphocytes (Figure 4C+D). Strikingly, disruption of the Golgi apparatus significantly increased monocytic CD39 surface expression (Figure 4D). Importantly, these effects were also observed for Golgi transport inhibition in the absence of concomitant immunostimulation (Figure 4C+D). Incubation with MN yielded similar results as BFA (Figure S4E+F). The effects observed in PBMC co-culture were successfully reproduced in a monoculture of isolated CD14+ monocytes (Figure 4E). Simultaneously, membrane fractions were generated from CD14+ monocytes and analyzed for AMPD2 protein expression by western blotting (Figure 4F). In accordance with the data acquired by flow cytometry, western blot analysis revealed an increase of approximately 35% in AMPD2 expression in membrane fractions of CD14+ monocytes stimulated with LPS. Of note, analysis of whole cell protein simultaneously demonstrated a decrease of total AMPD2 after LPS stimulation. Overall, we observed a significant increase in eAMPD2 expression on monocytes by TLR activation. This effect might either indicate a pro-inflammatory function of AMPD2 on the cell surface, maintaining a pro-inflammatory

environment by impeding adenosine production through CD73 in the extracellular space. On the other hand, similar to CD39, the upregulation by immunostimulation might equally represent a counter-regulatory mechanism to contain the state of inflammation.

3.7 | Dexamethasone inversely affects AMPD2 surface expression in lymphocytes and monocytes

Assuming that the enhancement of eAMPD2 expression by TLR agonism in monocytes constitutes a distinct immune cell response to immunoactivation, we hypothesized that these effects might be attenuated by the application of immunomodulatory drugs. First, we examined the impact of glucocorticoids (GC) as versatile anti-inflammatory agents broadly affecting various immune cell functions.^{89,90} PBMCs were incubated with LPS as before and concomitantly treated with either 10^{-8} M or 10^{-5} M Dex. Contrary to our expectation, Dex treatment did not significantly prevent the increase in monocytic eAMPD2 expression by LPS stimulation (Figure 5A+B). The same was true with respect to CD39. However, 10^{-5} M Dex tended to attenuate the enhancement of eAMPD2 ($P = .05$). In order to adequately interpret these results, we also studied the effects of GC treatment in isolation. Flow cytometric analysis revealed that eAMPD2 expression was not affected by treatment with 10^{-8} M Dex, a concentration that is equivalent to physiological glucocorticoid doses.^{91,92} Notably, incubation with 10^{-5} M Dex (corresponding to high-dose GC therapy)^{93,94} resulted in a significant increase in eAMPD2 expression on monocytes while causing the opposite effect in lymphocytes in co-culture (Figure S5). A similar pattern was observed analyzing CD39 surface expression although the lower Dex concentration interestingly caused a decrease in CD39 in both populations. In contrast, CD73 surface expression was uniformly reduced by Dex. This effect was stronger in the presence of the lower concentration of Dex. Instead of reversing the effects of immunostimulation on monocytes, incubation with high doses of Dex consequently promoted a similar increase in the surface expression of both AMPD2 and CD39. We thus concluded that this upregulation might indeed represent an anti-inflammatory mechanism supported by GC treatment. As the immunomodulatory effects of MTX have been described to be partly modulated by changes in ectonucleotidase function,⁹⁵⁻⁹⁷ we exploratorily examined PBMCs after incubation with $0.8 \mu\text{M}$ MTX (corresponding to plasma levels achieved by weekly application of 15 mg MTX)⁹⁸ for 24 hours in comparison with untreated control samples or in the presence of LPS. We found that ectoenzyme expression remained unaffected by MTX treatment (Figure 5C+D).

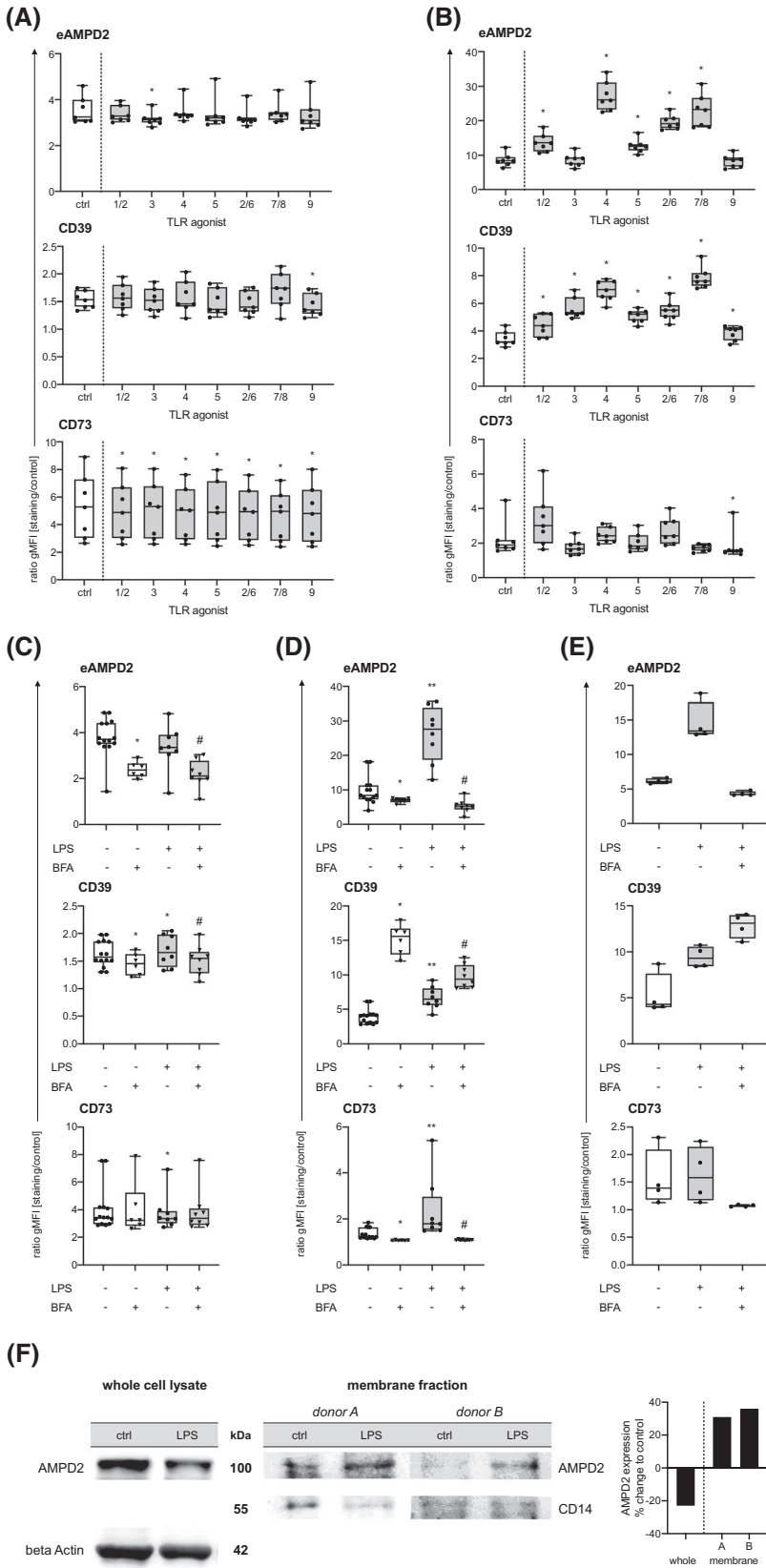


FIGURE 4 AMPD2 surface expression on human PBMCs is altered by TLR stimulation and Golgi transport inhibition. Cells were incubated for 21-24 hours and surface expression of eAMPD2, CD39 and CD73 was measured by flow cytometry. TLR agonism was achieved using 1 $\mu\text{g}/\text{mL}$ Pam3SCK4 at TLR1/2, 10 $\mu\text{g}/\text{mL}$ Poly (I:C) at TLR3, 1 $\mu\text{g}/\text{mL}$ LPS at TLR4, 100 ng/mL Flagellin at TLR5, 1 $\mu\text{g}/\text{mL}$ FSL-1 at TLR2/6, 1 $\mu\text{g}/\text{mL}$ at TLR7/8, and 0.5 μM ODN 2006 at TLR9. 1 $\mu\text{g}/\text{mL}$ BFA was added simultaneously as indicated to inhibit Golgi transport. Lymphocytes (A,C) and monocytes (B,D) were incubated in co-culture and gated according to Figure S1E for analysis ($n = 7-8$). E, CD14+ monocytes were sorted by magnetic cell separation and incubated in monoculture ($n = 4$). The applied gating strategy is depicted in Figure S1B. ratio gMFI represents the ratio of geometric mean fluorescence intensity of staining to secondary antibody control. F, AMPD2 protein expression in sorted CD14+ monocytes was detected by western blotting of whole cell lysates and membrane fractions after 24-hour incubation with 1 $\mu\text{g}/\text{mL}$ LPS. AMPD2 protein expression was semiquantified relative to beta Actin and CD14 respectively by image analysis and modification by LPS stimulation is depicted in relation to a untreated control samples. All boxplots show median, interquartile range, and minimum or maximum values, respectively. * $P < .05$, ** $P < .01$, compared to untreated control; # $P < .01$, compared to LPS; Wilcoxon matched-pairs signed rank test

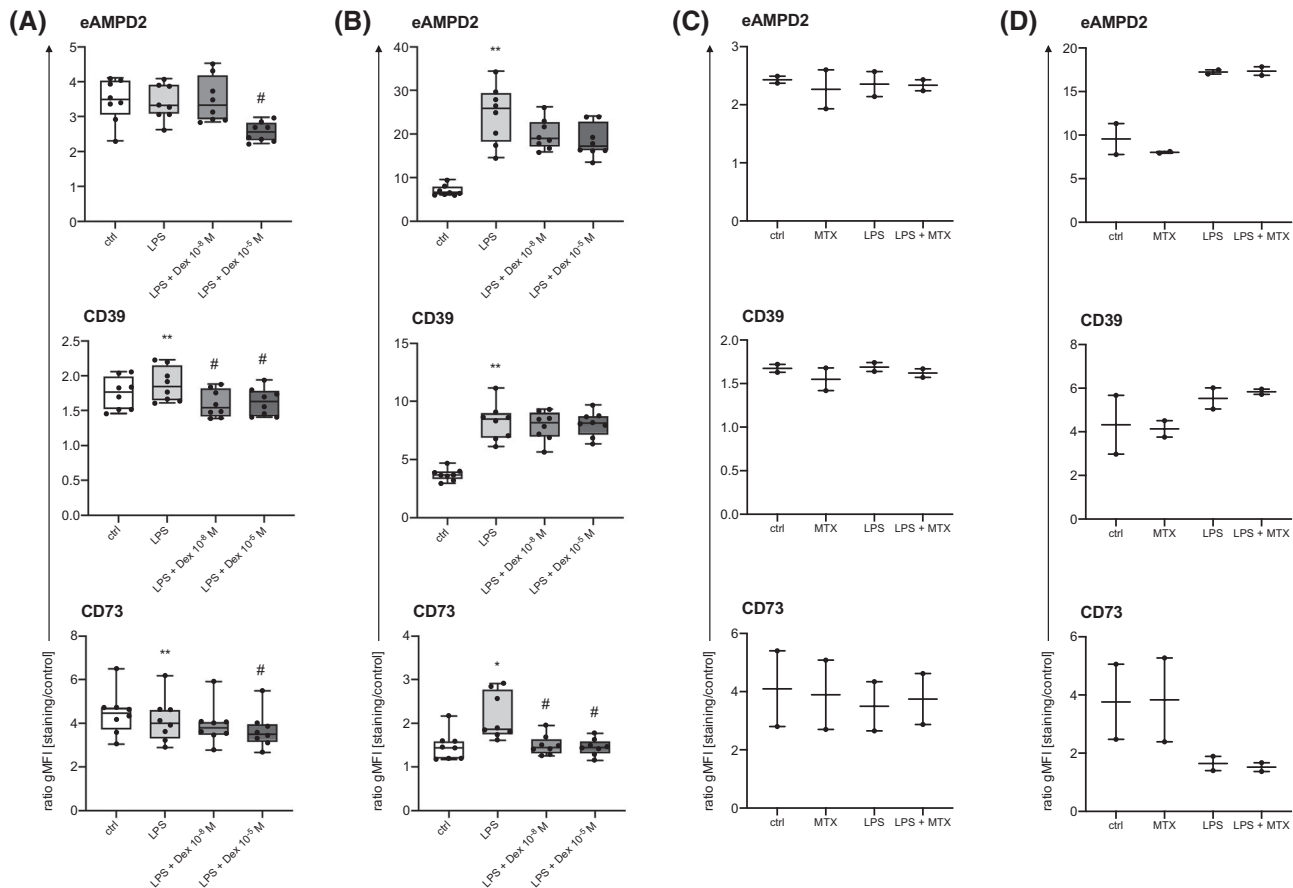


FIGURE 5 AMPD2 surface expression on human PBMCs following immunomodulation. Cells were incubated for 21–24 hours and surface expression of eAMPD2, CD39 and CD73 was measured by flow cytometry. Lymphocytes (A,C) and monocytes (B,D) were incubated in co-culture and gated according to Figure S1E for analysis. ratio gMFI represents the ratio of geometric mean fluorescence intensity of staining to secondary antibody control. A,B, PBMCs were treated with 1 $\mu\text{g}/\text{mL}$ LPS $\pm 10^{-8}$ and 10^{-5} M dexamethasone, respectively ($n = 8$). C,D, PBMC co-cultures were incubated with 0.8 μM methotrexate and 1 $\mu\text{g}/\text{mL}$ LPS, respectively, and a combination of both ($n = 2$). All boxplots show median, interquartile range, and minimum or maximum values, respectively. * $P < .05$, ** $P < .01$, compared to untreated control; # $P < .01$, compared to LPS; Wilcoxon matched-pairs signed rank test

3.8 | Patients with rheumatoid arthritis show increased AMPD2 surface expression in peripheral blood lymphocytes and monocytes

Having confirmed that eAMPD2 expression was distinctively modified by immunoactivation *in vitro*, we investigated whether eAMPD2 was equally affected by inflammatory conditions *in vivo*. Therefore, we isolated PBMCs from peripheral blood samples from patients with RA and healthy controls. Patient characteristics are provided in Table 3. The majority of patients were under immunosuppressive therapy. Sex and age distribution in the healthy control group did not differ significantly from the patient group (Table 3). Surface expression of AMPD2, CD39 and CD73 was examined by flow cytometry. Comparing PBMCs at baseline, we observed that eAMPD2 expression in RA patients was significantly elevated compared with healthy controls (Figure 6A). Remarkably, this was true for both lymphocytes and monocytes. This enhancement did not correlate with CRP levels

indicating inflammatory activity nor with the current GC dose, although a reliable correlation analysis would require a greater sample size. Contrary to our previous results, CD39 expression in monocytes was not correspondent with eAMPD2 in this experiment where no differences between RA patients and healthy controls were apparent (Figure 6A). Lymphocytes, on the other hand, showed significantly lower levels of CD39 expression (Figure 6A) although the overall expression was low and lymphocyte subsets would have to be analyzed separately to properly evaluate the relevance of this finding. CD73 expression was not significantly different between the two groups (Figure 6A). Regarding CD73, we found that monocytic expression was generally very low at baseline immediately after isolation and increased in cell culture. These findings are discussed more thoroughly in the Appendix.

After confirming differences in baseline expression of eAMPD2, we were interested whether expression patterns in PBMCs from RA patients also differed from healthy controls

TABLE 3 Patient characteristics

Patients, n	15
<i>Healthy controls</i>	13
Female, n (%)	11 (73)
<i>Healthy controls</i>	8 (62)
Age [years], median (IQR)	61 (54-73)
<i>Healthy controls</i>	56 (51-75)
Disease duration [years], median (IQR)	17 (8.5-32)
RF-positive, n (%)	10 (67)
Anti-CCP-positive, n (%)	10 (67)
CRP [mg/L], median (IQR)	5 (1.1-6.5) ^a
ESR 1st hour [mm/h], median (IQR)	18 (9.5-35) ^b
SJC [n/28], median (IQR)	2 (0.5-3.5) ^b
TJC [n/28], median (IQR)	1 (0-4.5) ^b
Receiving DMARDs, n (%)	12 (80)
Receiving GCs, n (%)	11 (73)
Current GC dose [mg/d PE], median (IQR)	5 (3-10) ^c

Abbreviations: CCP, cyclic citrullinated peptide; CRP, C-reactive protein; DMARDs, disease-modifying anti-rheumatic drugs; ESR, erythrocyte sedimentation rate; GC, glucocorticoids; IQR, interquartile range; PE, prednisone equivalent; RF, rheumatoid factor; SJC, swollen joint count; TJC, tender joint count.

^aInformation available for 12/15.

^bInformation available for 9/15.

^cCalculated only for patients receiving glucocorticoids.

in response to *in vitro* stimulation. Cells were incubated with LPS as before and surface expression of AMPD2, CD39 and CD73 was assessed by flow cytometry after 24 hours. Overall, the response to LPS in PBMCs from RA patients resembled that of healthy controls (Figure 6B). However, contrary to corresponding samples from healthy controls, several patients did not exhibit an increase in monocytic surface expression of AMPD2 ($P = .14$) and CD39 ($P = .05$). With respect to eAMPD2, we concluded that elevated surface expression in monocytes at baseline represents a counter-regulatory mechanism in response to the inflammatory state prevalent in RA. We assumed that this permanent upregulation impedes any further increase in eAMPD2 expression upon *in vitro* stimulation. While changes in CD73 expression did not differ between stimulated monocytes from healthy controls and RA patients, we did nevertheless observe a striking difference compared with the expression pattern in our previous measurements where LPS stimulation generally increased monocytic CD73 expression (Figure 4D). Comparing the characteristics of healthy donors in these experiments, it became evident that the age distribution was significantly different between the two groups ($P = .003$). For this reason, we reanalyzed our data by dividing the healthy donors into two groups (≤ 40 years and ≥ 50 years) (Table S5). Interestingly, we found that ectoenzyme expression in monocytes stimulated with LPS was indeed regulated significantly differently

in young and old donors (Figure S6B). In comparison with the younger group, monocytes from older individuals showed a significantly weaker upregulation of AMPD2, CD39 and CD73 surface expression. Differences between the two groups were also apparent at baseline (Figure S6A).

In conclusion, our data showed that eAMPD2 was differentially regulated in both RA and aging—two states associated with distinct patterns of inflammation. We thus concluded that eAMPD2 might indeed exert an immunoregulatory function by modifying the extracellular balance of purine metabolites.

3.9 | Increased AMPD2 surface expression does not prevent extracellular adenosine production

According to our initial hypothesis, we assumed that eAMPD2 might in fact exhibit either a pro-inflammatory or an anti-inflammatory role in the extracellular space. By metabolizing AMP to IMP, the deaminase processes the product of CD39 action, thereby shifting the balance of this reaction and enabling further degradation of ATP by the ectonucleotidase. This reduction of pro-inflammatory ATP favors a predominantly anti-inflammatory role of surface AMPD2. On the other hand, AMP also represents the substrate of ADO generation by CD73. AMP depletion by AMPD2 might therefore equally cause a reduction in eADO—a very potent anti-inflammatory molecule.⁵⁶ In order to evaluate the likelihood of either scenario, we isolated CD14+ monocytes from PBMCs by magnetic cell separation and incubated the cells with 1 $\mu\text{g}/\text{mL}$ LPS \pm 1 $\mu\text{g}/\text{mL}$ BFA for 24 hours. Supernatants were collected after 24 hours and surface expression of eAMPD2, CD39 and CD73 was determined by flow cytometry (Figure 4E). Fluorometric measurements of ADO in the supernatant revealed that an increase in eAMPD2 expression was not associated with a decrease in eADO (Figure 6C). In contrast, stimulation with LPS demonstrated maximal eAMPD2 expression (Figure 4E) and the highest levels of ADO in the supernatant (Figure 6C). CD73 expression was also at the maximum under these conditions and certainly contributed to the increase in eADO production. Similarly, a decrease in the ecto-5'-nucleotidase was presumably responsible for the reduction in eADO observed after Golgi transport inhibition. Moreover, immune cell activation and death considerably affect extracellular purine metabolite levels so that immunostimulation might cause changes in eADO levels independent of ectoenzyme expression.^{9,16,18,19,99} However, the percentage of dead cells did not differ between cells stimulated with LPS only or a combination of LPS and BFA. While this assay is consequently not suitable to exclusively measure eAMPD2 action, the results nevertheless refute the hypothesis that enhanced expression of eAMPD2 on the cell

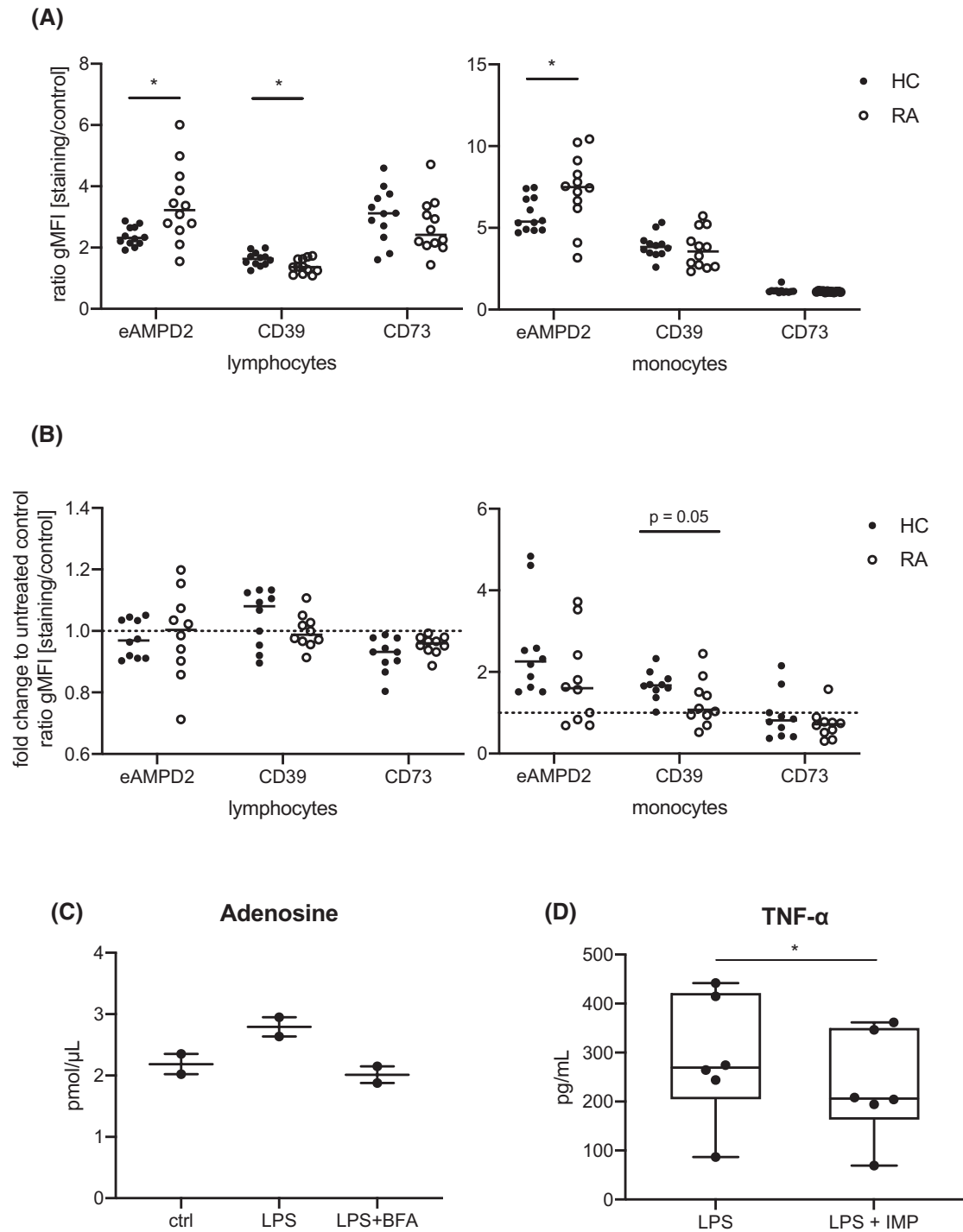


FIGURE 6 eAMPD2 expression on PBMCs from RA patients and functional assays suggest an anti-inflammatory potential of AMPD2 surface expression. A, eAMPD2, CD39 and CD73 surface expression was analyzed by flow cytometry directly after isolation ($n = 12$). PBMCs were gated according to Figure S1E for analysis. ratio gMFI represents the ratio of geometric mean fluorescence intensity of staining to secondary antibody control. B, Flow cytometric analysis of eAMPD2, CD39 and CD73 surface expression after incubation with 1 μ g/mL LPS for 21-24 hours in co-culture ($n = 10$). PBMCs were gated according to Figure S1E for analysis. Modification by LPS stimulation is depicted in relation to untreated control samples. C, CD14+ monocytes were purified from human PBMCs by MACS technology and incubated with 1 μ g/mL LPS \pm 1 μ g/mL BFA for 24 hours. The concentration of adenosine in the supernatant was determined using a fluorometric assay ($n = 2$). D, TNF-alpha release determined by ELISA. PBMCs were preincubated with 100 μ M IMP for 30 minutes, 1 μ g/mL LPS was added for another 2 hours ($n = 6$). Lines on scatter dot plot represent median. Boxplots show median, interquartile range, and minimum or maximum values, respectively. * $P < .05$, Mann Whitney test (A+B) and Wilcoxon matched-pairs signed rank test (C+D). IMP, inosine 5'-monophosphate

surface prevents production of anti-inflammatory ADO in the extracellular space.

3.10 | Inosine monophosphate—the product of AMPD2 action—exerts anti-inflammatory effects

In the system of extracellular purine metabolism regulated by the ectonucleotidases CD39 and CD73, the element that is newly introduced by the discovery of AMPD2 surface expression is the extracellular production of IMP. While the role of eATP and eADO has been studied in detail, the function of inosine derivatives in the interstitial space is less certain.^{6,13,56,100,101} For this reason, we aimed to examine the potential of excess extracellular IMP in balancing inflammation. PBMCs were primed with low and high supraphysiological concentrations of different purine metabolites and subsequently stimulated with 1 µg/mL LPS for two hours. Purine metabolites were applied at concentrations detected in the extracellular space under inflammatory conditions as described previously.¹⁰²⁻¹¹¹ The ADO concentrations applied also corresponded with the levels measured in our own experiments in the supernatant of cultured immune cells (Figure 6C). TNF-alpha was measured in the supernatants as an indicator of inflammatory activity. Prior incubation with 100 µM IMP significantly reduced TNF-alpha release from PBMCs after LPS stimulation (Figure 6D). We therefore concluded that eAMPD2 exerts anti-inflammatory effects by production of extracellular IMP and is upregulated upon immunoactivation to contain the inflammatory environment. As expected, ADO also exhibited highly efficient anti-inflammatory activity ($P = .03$). In comparison, inosine was less potent in reducing TNF-alpha release ($P = .22$). Surprisingly, ATP resulted in the strongest decrease in TNF-alpha release ($P = .03$). This effect was contrary to the pro-inflammatory activity usually attributed to eATP.¹⁰² Considering the ample expression of ectoenzymes in PBMCs, this finding can nevertheless be accounted for by an increase in ADO and IMP production by supplying ATP as a substrate.

4 | DISCUSSION

In this study, we verified AMPD2 surface expression in primary human immune cells and assessed differences in expression in patients with RA. Through a combination of mass spectrometry from membrane fractions and surface staining procedures, we identified eAMPD2 as a novel ectoenzyme involved in the extracellular purine metabolism. Immunostimulation increased monocytic eAMPD2 expression and RA patients exhibited higher surface expression

levels at baseline. This upregulation was not associated with a decrease in eADO levels in cell culture, while IMP exerted anti-inflammatory effects on immune cells.

By confirming AMPD2 surface expression in immune cells, we pursued a concept that was first discussed over 50 years ago in muscle tissue.^{63,64} Contrary to Rao and Pipoly who described attachment of AMPD to the inner erythrocyte membrane,^{65,66} we found that AMPD2 is indeed expressed on the outer surface and consequently potentially relevant to the extracellular milieu. While CD39 and CD73 are integrated into the plasma membrane by transmembrane domains and a GPI anchor, respectively,^{112,113} UniProt and TMHMM queries revealed no corresponding motifs in the AMPD2 protein sequence.^{80,81} In order to further elucidate membrane trafficking of eAMPD2, we analyzed surface expression after Golgi transport inhibition and observed a significant reduction suggesting involvement of the secretory pathway in the surface localization of eAMPD2. These results are in line with previous data locating AMPD in subcellular membrane fractions.^{114,115} Sims et al identified pleckstrin homology domains that might mediate membrane-association via phosphoinositide binding in both AMPD2 and AMPD3.¹¹⁶ Similarly, our search identified a lipid-binding region in the AMPD2 protein sequence. These helical domains are characteristic of amphitropic proteins—a class first described by Burn in 1988.^{84,117} This group of cytosolic proteins displays structural features that enable a reversible interaction with the plasma membrane.^{118,119} The presence of a lipid-binding helix therefore represents a potential mechanism permitting eAMPD2 to associate with the membrane. Further work will be needed to understand this process in detail.

Since the expression pattern of CD39 and CD73 differs between immune cell subsets, we determined eAMPD2 expression in various leukocyte populations.⁴ We found that eAMPD2 expression intensities resembled the distribution of CD39 described previously. These findings suggest that eAMPD2 might assist CD39 activity by shifting the ATP:AMP ratio and hence promoting hydrolysis of pro-inflammatory ATP by CD39. This theory is further supported by the fact that monocytic eAMPD2 expression correlated with CD39. Similarly, we observed an upregulation in both eAMPD2 and CD39 in monocytes upon TLR stimulation. According to our hypothesis, this upregulation under inflammatory conditions might be beneficial by containing ATP signaling and thereby attenuating a potentially detrimental inflammatory response. In accordance with this concept, CD39 deficient mice exhibited increased levels of vascular inflammation.¹²⁰ Conversely, transducing fibroblast-like synoviocytes with CD39 and CD73 resulted in reduced secretion of pro-inflammatory cytokines.¹²¹ Moreover, an induction of AMPD2 had been previously described in chondrocytes upon exposure to IL-1β.¹²² Since these changes in overall AMPD2 protein expression were reversed by incubation with immunomodulatory

agents, we evaluated whether eAMPD2 upregulation was also mitigated by anti-inflammatory therapeutics. Although Dex slightly attenuated the increase in eAMPD2 expression in monocytes upon stimulation with LPS, these changes were however not significant. Interestingly, exposure to therapeutic concentrations of Dex alone significantly increased monocytic eAMPD2 expression. We concluded that eAMPD2 upregulation might thus mediate anti-inflammatory effects of Dex in the extracellular space. Indeed, AMPD2 and AMPD3 have previously been recognized as genes addressed by glucocorticoid receptor signaling.^{123,124} The discrepant effects of Dex on monocytic eAMPD2 expression observed in the presence and absence of concomitant immunostimulation might reflect the attenuation of the inflammatory stimuli in the first scenario as opposed to the direct impact of Dex on AMPD2 surface expression in the latter. A reduction in eAMPD2, CD39 and CD73 expression was observed in the lymphocyte population. In contrast, previous studies of specific lymphocyte subsets demonstrated an increase in both CD39 and CD73 expression caused by Dex treatment.¹²⁵⁻¹²⁸ Likewise, the mechanism of action of MTX has been attributed to changes in AMPD activity.^{129,130} However, contrary to Dex, the anti-inflammatory effect in this context is not ascribed to a facilitation of ATP degradation, but rather to an inhibition of AMPD causing increased levels of eADO.⁹⁵ Correspondingly, polymorphisms causing reduced AMPD activity were associated with enhanced responsiveness to MTX, while low CD39 expression in Tregs caused the opposite.^{131,132} Bossennec et al found that MTX treatment was indeed associated with increased ADO production by T_H cells from RA patients.⁹⁶ Nevertheless, we did not observe changes in eAMPD2 expression after incubation with MTX. Importantly, it has to be considered that—in vivo—several immunomodulatory effects only manifest after up to three months of MTX therapy.¹³³ Also, the proposed mechanism of MTX action only refers to cytosolic AMPD activity. While we focused on eAMPD2 expression, it would be desirable to perform analyses of eAMPD2 function under MTX treatment in the future.

Differences in ectonucleotidase expression have been observed in various immune-mediated diseases. On the one hand, an elevated expression of CD39, CD73 and A2AR, respectively, has been described in neutrophils and monocytes from the synovial fluid of mice with collagen-induced arthritis and the peripheral blood of patients with uveitis.^{38,51} Also, FOXP3+CD39+ Tregs were found to be enriched in the synovial tissue of RA patients.¹³⁴ On the other hand, decreased expression of CD39, A1R and A2BR was detected in patients with ankylosing spondylitis and CD73 was downregulated on Tregs from psoriasis patients.^{49,50} Likewise, a reduction in ADO formation was observed in the synovial fluid of patients with juvenile idiopathic arthritis.⁴⁸ These diverging results indicate both a potential dysregulation of

ectonucleotidase expression enhancing inflammation by impaired eADO production and a counter-regulatory increase in CD39 and CD73 expression to attenuate the pro-inflammatory response in autoimmune diseases. Compared with sex- and age-matched healthy controls we observed higher levels of eAMPD2 expression in both lymphocytes and monocytes from RA patients. Interestingly, monocytic CD39 expression did not differ in our cohort. In response to TLR4 stimulation, upregulation of eAMPD2 in monocytes was not significantly different in the two groups, although it tended to be lower in RA patients. This is in line with the increased baseline levels, preventing further upregulation following a pro-inflammatory stimulus. As stated before, increased levels of eAMPD2 expression might constitute a counter-regulatory mechanism, promoting the removal of immunostimulatory ATP and providing anti-inflammatory IMP. AMPD activity has indeed been shown to correlate inversely with ATP levels.¹³⁵⁻¹³⁷ Importantly, our RA cohort comprises a diverse population that does not allow for the differential assessment of the impact of disease activity and current immunosuppressive therapy. Similarly, further experiments will be necessary to determine the relevance of the age-related differences observed in our cohort and ensure that the results were not caused by confounding factors like comorbidities. On the other hand, eAMPD2 may equally represent an ambiguous mediator of the extracellular ATP-adenosine balance by simultaneously reducing AMP supply and thereby impairing eADO generation. In fact, contrary to our findings in RA patients, Guo et al detected decreased overall AMPD2 protein levels in SLE patients.¹³⁸

Consequently, we aimed to evaluate whether modifying eAMPD2 expression was indeed associated with changes in extracellular eADO content. We did not observe a reduction in eADO concentrations under conditions of increased eAMPD2 expression. Thus, we concluded that impairing anti-inflammatory ectonucleotidase function does not seem to be the dominant role of eAMPD2. However, our approach only represents an approximation of eAMPD2 activity and does not exclude the action of other ectoenzymes present in the experimental setup. A more precise analysis of eAMPD2 function will be advantageous to define the exact role of eAMPD2 in the extracellular purine metabolism: direct measurements of extracellular AMP and IMP levels and the use of specific inhibitors will be necessary to characterize the enzymatic function on the cell surface. In order to provide an initial concept of the immunoregulatory capacity of extracellular AMP deamination, we exploratorily examined the anti-inflammatory effects of IMP and inosine in comparison to adenine nucleotides. IMP was indeed capable of reducing TNF- α secretion from PBMCs upon TLR4 stimulation, supporting the immunomodulatory potential of extracellular AMPD2 activity. Our results are in agreement with previous findings highlighting the anti-inflammatory

potency of inosine. Inosine has been shown to signal via ADO receptors.^{111,139-141} Immunosuppressive effects of inosine have been observed in multiple leukocyte populations including T cells, monocytes, neutrophils and macrophages.^{109,142,143} Moreover, Qiu et al demonstrated that IMP exhibited anti-inflammatory potential by inhibiting neutrophil accumulation.¹⁴⁴ The additional benefit of inosine derivatives in the extracellular space might consist in their longevity. Compared with the very short-lived ADO (half-life: 10 seconds), the half-life of inosine has been defined as 15 hours.^{145,146} While ADO might serve as an immediate regulator with strong anti-inflammatory potential, inosine nucleotides might permit a more prolonged modulation of the inflammatory environment.

In conclusion, we provide evidence of AMPD2 surface expression in human primary immune cells for the first time and thereby introduce a novel regulator of the extracellular purine metabolism that is differentially regulated under inflammatory conditions. We propose that an upregulation of eAMPD2 might enhance the removal of pro-inflammatory ATP from the extracellular space, although further work will be required to elucidate the precise function of this novel ectoenzyme in the inflammatory microenvironment. Considering the promising role of therapeutic agents in advancing the treatment of both immune-mediated and oncological diseases, we regard our findings as an important advancement expanding the system of immunoregulatory ectonucleotidases.

ACKNOWLEDGMENTS

We acknowledge funding provided by an unrestricted grant from Horizon Pharma plc. (112517). This work was supported by grants from Horizon Pharma plc. (112517) for LE, Studienstiftung des deutschen Volkes (Alexandra Damerau) for AD, and Deutsche Forschungsgemeinschaft (353142848) for TG.

CONFLICT OF INTEREST

The authors have no financial conflicts of interest.

AUTHOR CONTRIBUTIONS

We declare that all authors included on this paper fulfill the criteria of authorship. L. Ehlers, C. Strehl, F. Buttgerit and T. Gaber designed the research agenda; L. Ehlers, A. Kuppe, A. Damerau and S. Wilantri performed the experiments and analyzed the data; M. Kirchner and P. Mertins performed the mass spectrometric analyses; L. Ehlers wrote the paper. All authors have read and approved the final manuscript.

ORCID

Lisa Ehlers  <https://orcid.org/0000-0001-8737-001X>

REFERENCES

1. Antonioli L, Csóka B, Fornai M, et al. Adenosine and inflammation: what's new on the horizon? *Drug Discov Today*. 2014;19(8):1051-1068.
2. Antonioli L, Novitskiy SV, Sachsenmeier KF, Fornai M, Blandizzi C, Haskó G. Switching off CD73: a way to boost the activity of conventional and targeted antineoplastic therapies. *Drug Discov Today*. 2017;22(11):1686-1696.
3. Reutershan J, Vollmer I, Stark S, Wagner R, Ngamsri KC, Eltzschig HK. Adenosine and inflammation: CD39 and CD73 are critical mediators in LPS-induced PMN trafficking into the lungs. *FASEB J*. 2009;23(2):473-482.
4. Antonioli L, Pacher P, Vizi ES, Haskó G. CD39 and CD73 in immunity and inflammation. *Trends Mol Med*. 2013;19(6):355-367.
5. Horenstein AL, Chillemi A, Zaccarello G, et al. A CD38/CD203a/CD73 ectoenzymatic pathway independent of CD39 drives a novel adenosinergic loop in human T lymphocytes. *OncoImmunology*. 2013;2(9):e26246.
6. Ferretti E, Horenstein AL, Canzonetta C, Costa F, Morandi F. Canonical and non-canonical adenosinergic pathways. *Immunol Lett*. 2019;205:25-30.
7. Dong RP, Kameoka J, Hegen M, et al. Characterization of adenosine deaminase binding to human CD26 on T cells and its biologic role in immune response. *J Immunol*. 1996;156(4):1349-1355.
8. Eltzschig HK, Eckle T, Mager A, et al. ATP release from activated neutrophils occurs via connexin 43 and modulates adenosine-dependent endothelial cell function. *Circ Res*. 2006;99(10):1100-1108.
9. Qu Y, Misaghi S, Newton K, et al. Pannexin-1 is required for ATP release during apoptosis but not for inflammasome activation. *J Immunol*. 2011;186(11):6553-6561.
10. Baldwin SA, Beal PR, Yao SY, King AE, Cass CE, Young JD. The equilibrative nucleoside transporter family, SLC29. *Pflugers Arch*. 2004;447(5):735-743.
11. Gray JH, Owen RP, Giacomini KM. The concentrative nucleoside transporter family, SLC28. *Pflugers Arch*. 2004;447(5):728-734.
12. Antonioli L, Blandizzi C, Pacher P, Haskó G. Immunity, inflammation and cancer: a leading role for adenosine. *Nat Rev Cancer*. 2013;13(12):842-857.
13. Dou L, Chen YF, Cowan PJ, Chen XP. Extracellular ATP signaling and clinical relevance. *Clin Immunol*. 2018;188:67-73.
14. Cronstein BN, Sitkovsky M. Adenosine and adenosine receptors in the pathogenesis and treatment of rheumatic diseases. *Nat Rev Rheumatol*. 2017;13(1):41-51.
15. Antonioli L, Colucci R, La Motta C, et al. Adenosine deaminase in the modulation of immune system and its potential as a novel target for treatment of inflammatory disorders. *Curr Drug Targets*. 2012;13(6):842-862.
16. Elliott MR, Chekeni FB, Trampont PC, et al. Nucleotides released by apoptotic cells act as a find-me signal to promote phagocytic clearance. *Nature*. 2009;461(7261):282-286.
17. Trautmann A. Extracellular ATP in the immune system: more than just a "danger signal". *Sci Signal*. 2009;2(56):pe6.
18. Chen Y, Corriden R, Inoue Y, et al. ATP release guides neutrophil chemotaxis via P2Y2 and A3 receptors. *Science*. 2006;314(5806):1792-1795.
19. Schenk U, Westendorf AM, Radaelli E, et al. Purinergic control of T cell activation by ATP released through pannexin-1 hemichannels. *Sci Signal*. 2008;1(39):ra6.

20. Ferrari D, Chiozzi P, Falzoni S, et al. Extracellular ATP triggers IL-1 beta release by activating the purinergic P2Z receptor of human macrophages. *J Immunol.* 1997;159(3):1451-1458.
21. MacKenzie A, Wilson HL, Kiss-Toth E, Dower SK, North RA, Surprenant A. Rapid secretion of interleukin-1beta by microvesicle shedding. *Immunity.* 2001;15(5):825-835.
22. Pelegrin P, Barroso-Gutierrez C, Surprenant A. P2X7 receptor differentially couples to distinct release pathways for IL-1beta in mouse macrophage. *J Immunol.* 2008;180(11):7147-7157.
23. Parzych K, Zetterqvist AV, Wright WR, Kirkby NS, Mitchell JA, Paul-Clark MJ. Differential role of pannexin-1/ATP/P2X(7) axis in IL-1 β release by human monocytes. *FASEB J.* 2017;31(6):2439-2445.
24. Szabó C, Scott GS, Virág L, et al. Suppression of macrophage inflammatory protein (MIP)-1alpha production and collagen-induced arthritis by adenosine receptor agonists. *Br J Pharmacol.* 1998;125(2):379-387.
25. McWhinney CD, Dudley MW, Bowlin TL, et al. Activation of adenosine A3 receptors on macrophages inhibits tumor necrosis factor-alpha. *Eur J Pharmacol.* 1996;310(2-3):209-216.
26. Eltzschig HK, Thompson LF, Karhausen J, et al. Endogenous adenosine produced during hypoxia attenuates neutrophil accumulation: coordination by extracellular nucleotide metabolism. *Blood.* 2004;104(13):3986-3992.
27. Yago T, Tsukamoto H, Liu Z, Wang Y, Thompson LF, McEver RP. Multi-inhibitory effects of A2A adenosine receptor signaling on neutrophil adhesion under flow. *J Immunol.* 2015;195(8):3880-3889.
28. Frasson AP, Menezes CB, Goelzer GK, Gnoatto SCB, Garcia SC, Tasca T. Adenosine reduces reactive oxygen species and interleukin-8 production by *Trichomonas vaginalis*-stimulated neutrophils. *Purinergic Signal.* 2017;13(4):569-577.
29. Sun WC, Moore JN, Hurley DJ, Vandenplas ML, Murray TF. Effects of stimulation of adenosine A2A receptors on lipopolysaccharide-induced production of reactive oxygen species by equine neutrophils. *Am J Vet Res.* 2007;68(6):649-656.
30. Lappas CM, Rieger JM, Linden J. A2A adenosine receptor induction inhibits IFN-gamma production in murine CD4+ T cells. *J Immunol.* 2005;174(2):1073-1080.
31. Csóka B, Himer L, Selmeczy Z, et al. Adenosine A2A receptor activation inhibits T helper 1 and T helper 2 cell development and effector function. *FASEB J.* 2008;22(10):3491-3499.
32. Le Vraux V, Chen YL, Masson I, et al. Inhibition of human monocyte TNF production by adenosine receptor agonists. *Life Sci.* 1993;52(24):1917-1924.
33. Haskó G, Szabó C, Németh ZH, Kvetan V, Pastores SM, Vizi ES. Adenosine receptor agonists differentially regulate IL-10, TNF-alpha, and nitric oxide production in RAW 264.7 macrophages and in endotoxemic mice. *J Immunol.* 1996;157(10):4634-4640.
34. Silverman MH, Strand V, Markovits D, et al. Clinical evidence for utilization of the A3 adenosine receptor as a target to treat rheumatoid arthritis: data from a phase II clinical trial. *J Rheumatol.* 2008;35(1):41-48.
35. Fishman P, Cohen S. The A3 adenosine receptor (A3AR): therapeutic target and predictive biological marker in rheumatoid arthritis. *Clin Rheumatol.* 2016;35(9):2359-2362.
36. Milne GR, Palmer TM. Anti-inflammatory and immunosuppressive effects of the A2A adenosine receptor. *ScientificWorldJournal.* 2011;11:320-339.
37. Jacobson KA, Tosh DK, Jain S, Gao ZG. Historical and current adenosine receptor agonists in preclinical and clinical development. *Front Cell Neurosci.* 2019;13:124.
38. Flögel U, Burghoff S, van Lent PL, et al. Selective activation of adenosine A2A receptors on immune cells by a CD73-dependent prodrug suppresses joint inflammation in experimental rheumatoid arthritis. *Sci Transl Med.* 2012;4(146):146ra108.
39. Pulte ED, Broekman MJ, Olson KE, et al. CD39/NTPDase-1 activity and expression in normal leukocytes. *Thromb Res.* 2007;121(3):309-317.
40. Silva-Vilches C, Ring S, Mahnke K. ATP and its metabolite adenosine as regulators of dendritic cell activity. *Front Immunol.* 2018;9:2581.
41. Saze Z, Schuler PJ, Hong CS, Cheng D, Jackson EK, Whiteside TL. Adenosine production by human B cells and B cell-mediated suppression of activated T cells. *Blood.* 2013;122(1):9-18.
42. Gourdin N, Bossennec M, Rodriguez C, et al. Autocrine adenosine regulates tumor polyfunctional CD73(+)/CD4(+) effector T cells devoid of immune checkpoints. *Can Res.* 2018;78(13):3604-3618.
43. Yu N, Li X, Song W, et al. CD4(+)/CD25 (+)/CD127 (low/-) T cells: a more specific Treg population in human peripheral blood. *Inflammation.* 2012;35(6):1773-1780.
44. Thomson LF, Ruedi JM, Glass A, et al. Production and characterization of monoclonal antibodies to the glycosyl phosphatidylinositol-anchored lymphocyte differentiation antigen ecto-5'-nucleotidase (CD73). *Tissue Antigens.* 1990;35(1):9-19.
45. Quarona V, Ferri V, Chillemi A, et al. Unraveling the contribution of ectoenzymes to myeloma life and survival in the bone marrow niche. *Ann N Y Acad Sci.* 2015;1335:10-22.
46. Ohta M, Toyama K, Gutterman DD, et al. Ecto-5'-nucleotidase, CD73, is an endothelium-derived hyperpolarizing factor synthase. *Arterioscler Thromb Vasc Biol.* 2013;33(3):629-636.
47. Schuler PJ, Saze Z, Hong CS, et al. Human CD4+ CD39+ regulatory T cells produce adenosine upon co-expression of surface CD73 or contact with CD73+ exosomes or CD73+ cells. *Clin Exp Immunol.* 2014;177(2):531-543.
48. Botta Gordon-Smith S, Ursu S, Eaton S, Moncrieffe H, Wedderburn LR. Correlation of low CD73 expression on synovial lymphocytes with reduced adenosine generation and higher disease severity in juvenile idiopathic arthritis. *Arthritis Rheumatol.* 2015;67(2):545-554.
49. Yan K, Xu W, Huang Y, et al. Methotrexate restores the function of peripheral blood regulatory T cells in psoriasis vulgaris via the CD73/AMPK/mTOR pathway. *Br J Dermatol.* 2018;179(4):896-905.
50. Akhtari M, Zargar SJ, Mahmoudi M, Vojdani M, Rezaeimanesh A, Jamshidi A. Ankylosing spondylitis monocyte-derived macrophages express increased level of A2A adenosine receptor and decreased level of ectonucleoside triphosphate diphosphohydrolase-1 (CD39), A1 and A2B adenosine receptors. *Clin Rheumatol.* 2018;37(6):1589-1595.
51. Walscheid K, Neekamp L, Heiligenhaus A, et al. Peripheral blood monocytes reveal an activated phenotype in pediatric uveitis. *Clin Immunol.* 2018;190:84-88.
52. de Lourdes M-G, García-Rocha R, Morales-Ramírez O, et al. Mesenchymal stromal cells derived from cervical cancer produce high amounts of adenosine to suppress cytotoxic T lymphocyte functions. *J Transl Med.* 2016;14(1):302.

53. Jiang T, Xu X, Qiao M, et al. Comprehensive evaluation of NT5E/CD73 expression and its prognostic significance in distinct types of cancers. *BMC Cancer*. 2018;18(1):267.
54. Cai X-Y, Ni X-C, Yi Y, et al. Overexpression of CD39 in hepatocellular carcinoma is an independent indicator of poor outcome after radical resection. *Medicine*. 2016;95(40):e4989.
55. Cai XY, Wang XF, Li J, et al. High expression of CD39 in gastric cancer reduces patient outcome following radical resection. *Oncol Lett*. 2016;12(5):4080-4086.
56. Antonioli L, Fornai M, Blandizzi C, Pacher P, Hasko G. Adenosine signaling and the immune system: when a lot could be too much. *Immunol Lett*. 2019;205:9-15.
57. Stagg J, Divisekera U, McLaughlin N, et al. Anti-CD73 antibody therapy inhibits breast tumor growth and metastasis. *Proc Natl Acad Sci U S A*. 2010;107(4):1547-1552.
58. Figueiró F, Mendes FB, Corbelini PF, et al. A monastrol-derived compound, LaSOM 63, inhibits ecto-5' nucleotidase/CD73 activity and induces apoptotic cell death of glioma cell lines. *Anticancer Res*. 2014;34(4):1837-1842.
59. Häusler SF, Del Barrio IM, Diessner J, et al. Anti-CD39 and anti-CD73 antibodies A1 and 7G2 improve targeted therapy in ovarian cancer by blocking adenosine-dependent immune evasion. *Am J Transl Res*. 2014;6(2):129-139.
60. Young A, Ngiow SF, Barkauskas DS, et al. Co-inhibition of CD73 and A2AR adenosine signaling improves anti-tumor immune responses. *Cancer Cell*. 2016;30(3):391-403.
61. Allard D, Chrobak P, Allard B, Messaoudi N, Stagg J. Targeting the CD73-adenosine axis in immuno-oncology. *Immunol Lett*. 2019;205:31-39.
62. Lowenstein JM. Ammonia production in muscle and other tissues: the purine nucleotide cycle. *Physiol Rev*. 1972;52(2):382-414.
63. Dunkley CR, Manery JF, Dryden EE. The conversion of ATP to IMP by muscle surface enzymes. *J Cell Physiol*. 1966;68(3):241-247.
64. Manery JF, Riordan JR, Dryden EE. Characteristics of nucleotide-converting enzymes at muscle surfaces with special reference to ion sensitivity. *Can J Physiol Pharmacol*. 1968;46(3):537-547.
65. Pipoly GM, Nathans GR, Chang D, Deuel TF. Regulation of the interaction of purified human erythrocyte AMP deaminase and the human erythrocyte membrane. *J Clin Investig*. 1979;63(5):1066-1076.
66. Rao SN, Hara L, Askari A. Alkali cation-activated AMP deaminase of erythrocytes: some properties of the membrane-bound enzyme. *Biochem Biophys Acta*. 1968;151(3):651-654.
67. Atkinson DE. Regulation of enzyme activity. *Annu Rev Biochem*. 1966;35(1):85-124.
68. Chapman AG, Atkinson DE. Stabilization of adenylate energy charge by the adenylate deaminase reaction. *J Biol Chem*. 1973;248(23):8309-8312.
69. Johnson TA, Jinnah HA, Kamatani N. Shortage of cellular ATP as a cause of diseases and strategies to enhance ATP. *Front Pharmacol*. 2019;10:98.
70. Sabina RL, Swain JL, Olanow CW, et al. Myoadenylate deaminase deficiency. Functional and metabolic abnormalities associated with disruption of the purine nucleotide cycle. *J Clin Invest*. 1984;73(3):720-730.
71. Binkley PF, Auseon A, Cooke G. A polymorphism of the gene encoding AMPD1: clinical impact and proposed mechanisms in congestive heart failure. *Congest Heart Fail*. 2004;10(6):274-279; quiz 279-280.
72. Borkowski T, Slominska EM, Orlewska C, et al. Protection of mouse heart against hypoxic damage by AMP deaminase inhibition. *Nucleosides Nucleotides Nucleic Acids*. 2010;29(4-6):449-452.
73. Stewart SA, Dykxhoorn DM, Palliser D, et al. Lentivirus-delivered stable gene silencing by RNAi in primary cells. *RNA*. 2003;9(4):493-501.
74. Sarbassov DD, Guertin DA, Ali SM, Sabatini DM. Phosphorylation and regulation of Akt/PKB by the rictor-mTOR complex. *Science*. 2005;307(5712):1098-1101.
75. Rappsilber J, Ishihama Y, Mann M. Stop and go extraction tips for matrix-assisted laser desorption/ionization, nanoelectrospray, and LC/MS sample pretreatment in proteomics. *Anal Chem*. 2003;75(3):663-670.
76. Hughes CS, Moggridge S, Müller T, Sorensen PH, Morin GB, Krijgsveld J. Single-pot, solid-phase-enhanced sample preparation for proteomics experiments. *Nat Protoc*. 2019;14(1):68-85.
77. Perez-Riverol Y, Csordas A, Bai J, et al. The PRIDE database and related tools and resources in 2019: improving support for quantification data. *Nucleic Acids Res*. 2019;47(D1):D442-D450.
78. Cossarizza A, Chang HD, Radbruch A, et al. Guidelines for the use of flow cytometry and cell sorting in immunological studies. *Eur J Immunol*. 2017;47(10):1584-1797.
79. Ziegler-Heitbrock L, Ancuta P, Crowe S, et al. Nomenclature of monocytes and dendritic cells in blood. *Blood*. 2010;116(16):e74-e80.
80. Wu CH, Apweiler R, Bairoch A, et al. The Universal Protein Resource (UniProt): an expanding universe of protein information. *Nucleic Acids Res*. 2006;34(90001):D187-D191.
81. Sonnhammer EL, von Heijne G, Krogh A. A hidden Markov model for predicting transmembrane helices in protein sequences. *Proc Int Conf Intell Syst Mol Biol*. 1998;6:175-182.
82. Jones DT. Protein secondary structure prediction based on position-specific scoring matrices. *J Mol Biol*. 1999;292(2):195-202.
83. Gautier R, Douguet D, Antonny B, Drin G. HELIQUEST: a web server to screen sequences with specific alpha-helical properties. *Bioinformatics*. 2008;24(18):2101-2102.
84. Keller RC. Identification and in silico analysis of helical lipid binding regions in proteins belonging to the amphitropic protein family. *J Biosci*. 2014;39(5):771-783.
85. Sabina RL, Mahnke-Zizelman DK. Towards an understanding of the functional significance of N-terminal domain divergence in human AMP deaminase isoforms. *Pharmacol Ther*. 2000;87(2-3):279-283.
86. Thul PJ, Akesson L, Wiking M, et al. A subcellular map of the human proteome. *Science*. 2017;356(6340):eaal3321.
87. Uhlen M, Bandrowski A, Carr S, et al. A proposal for validation of antibodies. *Nat Methods*. 2016;13(10):823-827.
88. Eltzschig HK, Faigle M, Knapp S, et al. Endothelial catabolism of extracellular adenosine during hypoxia: the role of surface adenosine deaminase and CD26. *Blood*. 2006;108(5):1602-1610.
89. Stahn C, Buttgerit F. Genomic and nongenomic effects of glucocorticoids. *Nat Clin Pract Rheumatol*. 2008;4(10):525-533.
90. Strehl C, Ehlers L, Gaber T, Buttgerit F. Glucocorticoids—all-rounders tackling the versatile players of the immune system. *Front Immunol*. 2019;10:1744.
91. Baumann G, Rappaport G, Lemarchand-Béraud T, Felber JP. Free cortisol index: a rapid and simple estimation of free cortisol in human plasma. *J Clin Endocrinol Metab*. 1975;40(3):462-469.

92. Ballard PL. Delivery and transport of glucocorticoids to target cells. *Monogr Endocrinol.* 1979;12:25-48.
93. Peterson RE, Pierce CE, Wyngaarden JB, Bunim JJ, Brodie BB. The physiological disposition and metabolic fate of cortisone in man. *J Clin Investig.* 1957;36(9):1301-1312.
94. Webel ML, Ritts RE Jr, Taswell HF, Danadio JV Jr, Woods JE. Cellular immunity after intravenous administration of methylprednisolone. *J Lab Clin Med.* 1974;83(3):383-392.
95. Montesinos MC, Takedachi M, Thompson LF, Wilder TF, Fernandez P, Cronstein BN. The antiinflammatory mechanism of methotrexate depends on extracellular conversion of adenine nucleotides to adenosine by ecto-5'-nucleotidase: findings in a study of ecto-5'-nucleotidase gene-deficient mice. *Arthritis Rheum.* 2007;56(5):1440-1445.
96. Bossennec M, Rodriguez C, Hubert M, et al. Methotrexate restores CD73 expression on Th1.17 in rheumatoid arthritis and psoriatic arthritis patients and may contribute to its anti-inflammatory effect through adp production. *J Clin Med.* 2019;8(11):1859.
97. Figueiro F, de Oliveira CP, Bergamin LS, et al. Methotrexate up-regulates ecto-5'-nucleotidase/CD73 and reduces the frequency of T lymphocytes in the glioblastoma microenvironment. *Purinergic Signal.* 2016;12(2):303-312.
98. Kabisch S, Weigand T, Plischke H, Menninger H. Bioverfügbarkeit von Methotrexat (MTX) in unterschiedlichen Applikationsarten. *Aktuelle Rheumatol.* 2004;29(4):197-200.
99. Filippini A, Taffs RE, Sitkovsky MV. Extracellular ATP in T-lymphocyte activation: possible role in effector functions. *Proc Natl Acad Sci U S A.* 1990;87(21):8267-8271.
100. Burnstock G, Boeynaems JM. Purinergic signalling and immune cells. *Purinergic Signal.* 2014;10(4):529-564.
101. Linden J, Koch-Nolte F, Dahl G. Purine release, metabolism, and signaling in the inflammatory response. *Annu Rev Immunol.* 2019;37:325-347.
102. Gorini S, Gatta L, Pontecorvo L, Vitiello L, la Sala A. Regulation of innate immunity by extracellular nucleotides. *Am J Blood Res.* 2013;3(1):14-28.
103. Zetterström T, Vernet L, Ungerstedt U, Tossman U, Jonzon B, Fredholm BB. Purine levels in the intact rat brain. Studies with an implanted perfused hollow fibre. *Neurosci Lett.* 1982;29(2):111-115.
104. Hagberg H, Andersson P, Lacarewicz J, Jacobson I, Butcher S, Sandberg M. Extracellular adenosine, inosine, hypoxanthine, and xanthine in relation to tissue nucleotides and purines in rat striatum during transient ischemia. *J Neurochem.* 1987;49(1):227-231.
105. Kékesi V, Zima E, Barát E, et al. Pericardial concentrations of adenosine, inosine and hypoxanthine in an experimental canine model of spastic ischaemia. *Clin Sci.* 2002;103(Suppl 48):198s-201s.
106. Blay J, White TD, Hoskin DW. The extracellular fluid of solid carcinomas contains immunosuppressive concentrations of adenosine. *Can Res.* 1997;57(13):2602-2605.
107. Traut TW. Physiological concentrations of purines and pyrimidines. *Mol Cell Biochem.* 1994;140(1):1-22.
108. Linden J. Molecular approach to adenosine receptors: receptor-mediated mechanisms of tissue protection. *Annu Rev Pharmacol Toxicol.* 2001;41:775-787.
109. Marton A, Pacher P, Murthy KG, Németh ZH, Haskó G, Szabó C. Anti-inflammatory effects of inosine in human monocytes, neutrophils and epithelial cells in vitro. *Int J Mol Med.* 2001;8(6):617-621.
110. Welihinda AA, Kaur M, Greene K, Zhai Y, Amento EP. The adenosine metabolite inosine is a functional agonist of the adenosine A2A receptor with a unique signaling bias. *Cell Signal.* 2016;28(6):552-560.
111. Chen J, Chaurio RA, Maueröder C, et al. Inosine released from dying or dead cells stimulates cell proliferation via adenosine receptors. *Front Immunol.* 2017;8:504.
112. Smith TM, Kirley TL. Cloning, sequencing, and expression of a human brain ecto-apyrase related to both the ecto-ATPases and CD39 ecto-apyrases1. *Biochem Biophys Acta.* 1998;1386(1):65-78.
113. Klemens MR, Sherman WR, Holmberg NJ, Ruedi JM, Low MG, Thompson LF. Characterization of soluble vs membrane-bound human placental 5'-nucleotidase. *Biochem Biophys Res Comm.* 1990;172(3):1371-1377.
114. Weil-Malherbe H. The subcellular distribution of rat brain adenylate deaminase and its association with neurostenin. *J Neurochem.* 1975;24(4):801-803.
115. Cuenda A, Henao F, Nogues M, Gutiérrez-Merino C. Quantification and removal of glycogen phosphorylase and other enzymes associated with sarcoplasmic reticulum membrane preparations. *Biochem Biophys Acta.* 1994;1194(1):35-43.
116. Sims B, Mahnke-Zizelman DK, Profit AA, Prestwich GD, Sabina RL, Theibert AB. Regulation of AMP deaminase by phosphoinositides. *J Biol Chem.* 1999;274(36):25701-25707.
117. Burn P. Amphitropic proteins: a new class of membrane proteins. *Trends Biochem Sci.* 1988;13(3):79-83.
118. Johnson JE, Cornell RB. Amphitropic proteins: regulation by reversible membrane interactions (review). *Mol Membr Biol.* 1999;16(3):217-235.
119. Halskau Ø, Muga A, Martínez A. Linking new paradigms in protein chemistry to reversible membrane-protein interactions. *Curr Protein Pept Sci.* 2009;10(4):339-359.
120. Sun X, Cárdenas A, Wu Y, Enyoji K, Robson SC. Vascular stasis, intestinal hemorrhage, and heightened vascular permeability complicate acute portal hypertension in cd39-null mice. *Am J Physiol Gastrointest Liver Physiol.* 2009;297(2):G306-G311.
121. Finn JD, Snoek S, van Ittersum J, et al. A8.12 AAV mediated expression of CD39 and CD73 is effective in reducing inflammation in the air pouch synovial inflammation model. *Ann Rheum Dis.* 2015;74(Suppl 1):A86.
122. Endo W, Arito M, Sato T, et al. Effects of sulfasalazine and tofacitinib on the protein profile of articular chondrocytes. *Mod Rheumatol.* 2014;24(5):844-850.
123. Luo Y, Zeng B, Zeng L, et al. Gut microbiota regulates mouse behaviors through glucocorticoid receptor pathway genes in the hippocampus. *Transl Psychiatry.* 2018;8(1):187.
124. Rouillard AD, Gunderson GW, Fernandez NF, et al. The harmonizome: a collection of processed datasets gathered to serve and mine knowledge about genes and proteins. *Database.* 2016;2016:baw100.
125. Lu Y, Cheng L, Li F, et al. The abnormal function of CD39(+) regulatory T cells could be corrected by high-dose dexamethasone in patients with primary immune thrombocytopenia. *Ann Hematol.* 2019;98(8):1845-1854.
126. Bavaresco L, Bernardi A, Braganhol E, Wink MR, Battastini AM. Dexamethasone inhibits proliferation and stimulates ecto-5'-nucleotidase/CD73 activity in C6 rat glioma cell line. *J Neurooncol.* 2007;84(1):1-8.

127. Sales-Campos H, de Souza PR, Basso PJ, et al. Amelioration of experimental colitis after short-term therapy with glucocorticoid and its relationship to the induction of different regulatory markers. *Immunology*. 2017;150(1):115-126.
128. Muls NG, Dang HA, Sindic CJ, van Pesch V. Regulation of Treg-associated CD39 in multiple sclerosis and effects of corticotherapy during relapse. *Mult Scler*. 2015;21(12):1533-1545.
129. Chan ES, Cronstein BN. Methotrexate—how does it really work? *Nature reviews. Rheumatology*. 2010;6(3):175-178.
130. Bedoui Y, Guillot X, Sélambarom J, et al. Methotrexate an old drug with new tricks. *Int J Mol Sci*. 2019;20(20):5023.
131. Wessels JA, Kooloos WM, De Jonge R, et al. Relationship between genetic variants in the adenosine pathway and outcome of methotrexate treatment in patients with recent-onset rheumatoid arthritis. *Arthritis Rheum*. 2006;54(9):2830-2839.
132. Peres RS, Liew FY, Talbot J, et al. Low expression of CD39 on regulatory T cells as a biomarker for resistance to methotrexate therapy in rheumatoid arthritis. *Proc Natl Acad Sci U S A*. 2015;112(8):2509-2514.
133. Taylor PC, Balsa Criado A, Mongey AB, Avouac J, Marotte H, Mueller RB. How to get the most from methotrexate (MTX) treatment for your rheumatoid arthritis patient?—MTX in the treat-to-target strategy. *J Clin Med*. 2019;8(4):515.
134. Herrath J, Chemin K, Albrecht I, Catrina AI, Malmström V. Surface expression of CD39 identifies an enriched Treg-cell subset in the rheumatic joint, which does not suppress IL-17A secretion. *Eur J Immunol*. 2014;44(10):2979-2989.
135. Akizu N, Cantagrel V, Schroth J, et al. AMPD2 regulates GTP synthesis and is mutated in a potentially treatable neurodegenerative brainstem disorder. *Cell*. 2013;154(3):505-517.
136. Ogasawara N, Goto H, Yamada Y, et al. Deficiency of AMP deaminase in erythrocytes. *Hum Genet*. 1987;75(1):15-18.
137. Dornand J, Clofent G, Bonnafous JC, Favero J, Mani JC. Purine metabolizing enzymes of lymphocyte cell populations: correlation between AMP-deaminase activity and dATP accumulation in murine lymphocytes. *Proc Soc Exp Biol Med*. 1985;179(4):448-455.
138. Guo G, Wang H, Shi X, et al. NovelmiRNA-25 inhibits AMPD2 in peripheral blood mononuclear cells of patients with systemic lupus erythematosus and represents a promising novel biomarker. *J Transl Med*. 2018;16(1):370.
139. Welihinda AA, Kaur M, Raveendran KS, Amento EP. Enhancement of inosine-mediated A(2A)R signaling through positive allosteric modulation. *Cell Signal*. 2018;42:227-235.
140. da Rocha LF, da Silva MD, de Almeida CD, Santos AR. Anti-inflammatory effects of purine nucleosides, adenosine and inosine, in a mouse model of pleurisy: evidence for the role of adenosine A2 receptors. *Purinergic Signal*. 2012;8(4):693-704.
141. Guinzberg R, Cortés D, Díaz-Cruz A, Riveros-Rosas H, Villalobos-Molina R, Piña E. Inosine released after hypoxia activates hepatic glucose liberation through A3 adenosine receptors. *Am J Physiol Endocrinol Metab*. 2006;290(5):E940-E951.
142. Shinohara Y, Tsukimoto M. Guanine and inosine nucleotides/nucleosides suppress murine T cell activation. *Biochem Biophys Res Comm*. 2018;498(4):764-768.
143. Haskó G, Kuhel DG, Németh ZH, et al. Inosine inhibits inflammatory cytokine production by a posttranscriptional mechanism and protects against endotoxin-induced shock. *J Immunol*. 2000;164(2):1013-1019.
144. Qiu FH, Wada K, Stahl GL, Serhan CN. IMP and AMP deaminase in reperfusion injury down-regulates neutrophil recruitment. *Proc Natl Acad Sci U S A*. 2000;97(8):4267-4272.
145. Möser GH, Schrader J, Deussen A. Turnover of adenosine in plasma of human and dog blood. *Am J Physiol*. 1989;256(4 Pt 1):C799-C806.
146. Viegas TX, Omura GA, Stoltz RR, Kisicki J. Pharmacokinetics and pharmacodynamics of peldesine (BCX-34), a purine nucleoside phosphorylase inhibitor, following single and multiple oral doses in healthy volunteers. *J Clin Pharmacol*. 2000;40(4):410-420.

SUPPORTING INFORMATION

Additional Supporting Information may be found online in the Supporting Information section.

How to cite this article: Ehlers L, Kuppe A, Damerau A, et al. Surface AMP deaminase 2 as a novel regulator modifying extracellular adenine nucleotide metabolism. *The FASEB Journal*. 2021;35:e21684. <https://doi.org/10.1096/fj.202002658RR>

APPENDIX

Monocytic expression of CD73 is dependent on cell culture conditions

Besides our main findings, we observed a strong increase in monocytic CD73 expression during cell culture. Interestingly, this effect was only observed in cultures containing human serum while CD73 expression remained low in monocytes cultured in medium supplemented with FCS (Appendix Figure A1). As a marked expression of CD73 has been described as a characteristic feature of M2 macrophages, we hypothesised that the presence of human serum promoted monocyte adhesion and thereby differentiation towards a macrophage phenotype.¹⁻³ As a side note, CD73 was also considerably upregulated in THP-1 cells incubated with PMA. While this activation was likewise associated with cell adhesion even in the absence of human serum, the cells remained in suspension upon stimulation with LPS and did not show an upregulation of CD73 under these conditions (Appendix Figure A2). The abundance of CD73 in macrophages as a tissue-resident cell type is consistent with the fact that adenosine as the product of this ectonucleotidase has a very short half-life in comparison with other purine metabolites.^{4,5} Its action is therefore confined to its production site, which is in accordance with the low expression of CD73 in circulating monocytes.

REFERENCES

1. Monguio-Tortajada M, Roura S, Galvez-Monton C, Franquesa M, Bayes-Genis A, Borrás FE. Mesenchymal stem cells induce expression of CD73 in human monocytes in vitro and in a swine model of myocardial infarction in vivo. *Front Immunol*. 2017;8:1577.

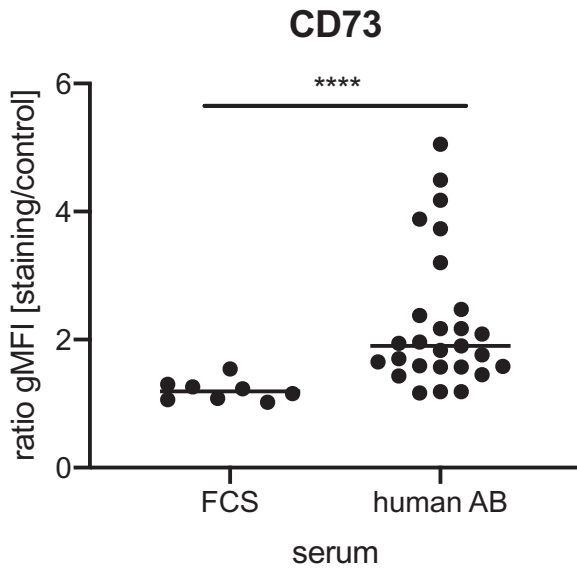


FIGURE A1 PBMCs were co-cultured in RPMI supplemented with either FCS or human AB serum for 24 hours. Monocytic CD73 surface expression was determined by flow cytometry. Monocytes were gated according to Supplementary Figure S1E for analysis. Lines on scatter dot plot represent median. **** $P < .0001$, Mann Whitney test.

- Ohradanova-Repic A, Machacek C, Charvet C, et al. Extracellular purine metabolism is the switchboard of immunosuppressive macrophages and a novel target to treat diseases with macrophage imbalances. *Front Immunol.* 2018;9:852.
- Zanin RF, Braganhol E, Bergamin LS, et al. Differential macrophage activation alters the expression profile of NTPDase and ecto-5'-nucleotidase. *PLoS One.* 2012;7(2):e31205.

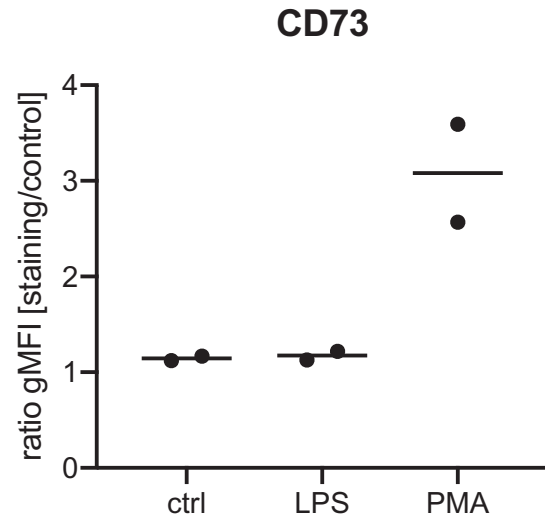
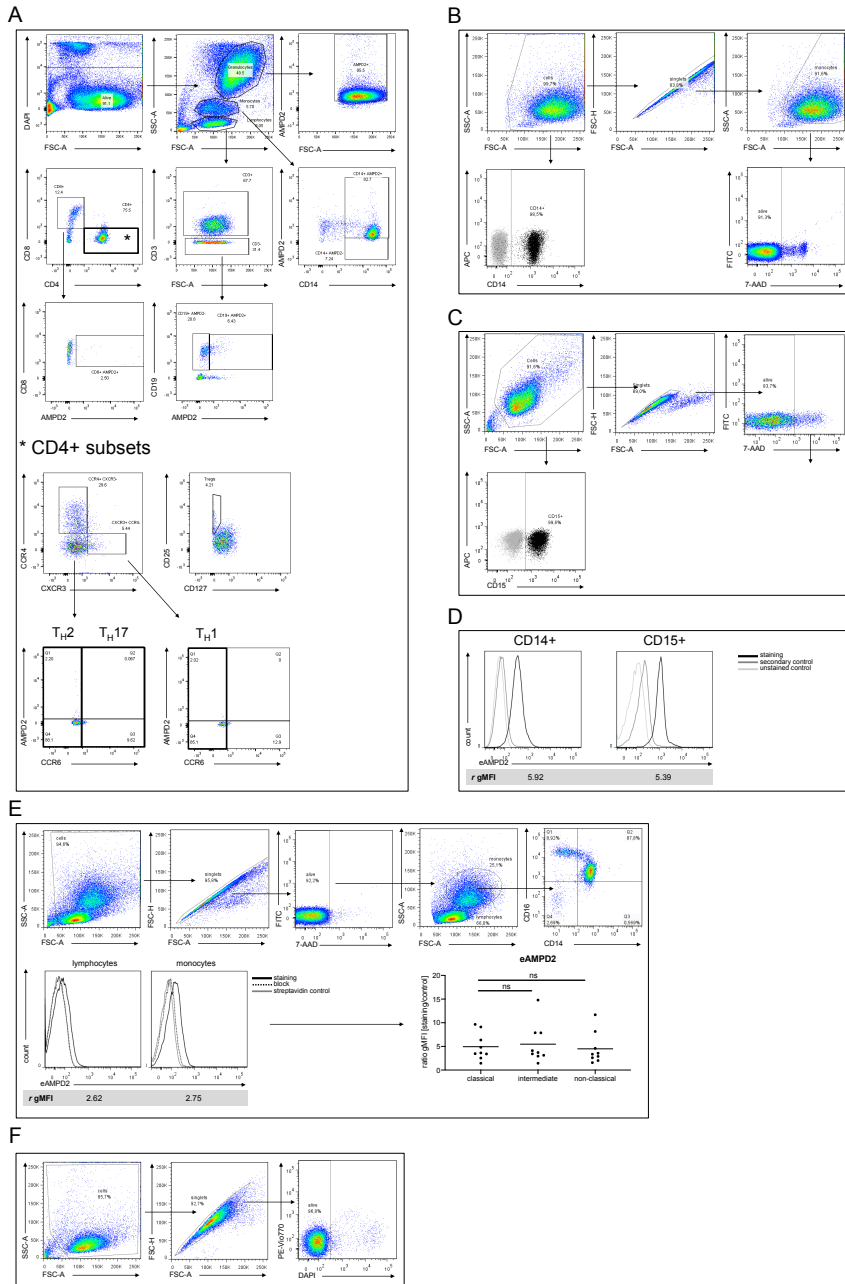


FIGURE A2 Flow cytometric analysis of CD73 surface expression on THP-1 cells stimulated with 1 $\mu\text{g}/\text{mL}$ LPS or 10 ng/mL PMA for 24 hours. Cells were gated according to Supplementary Figure S1F for analysis.

- Möser GH, Schrader J, Deussen A. Turnover of adenosine in plasma of human and dog blood. *Am J Physiol.* 1989 Apr;256(4 Pt 1):C799-C806.
- Viegas TX, Omura GA, Stoltz RR, Kisicki J. Pharmacokinetics and pharmacodynamics of peldesine (BCX-34), a purine nucleoside phosphorylase inhibitor, following single and multiple oral doses in healthy volunteers. *J Clin Pharmacol.* 2000 Apr;40(4):410-420.

Supplement

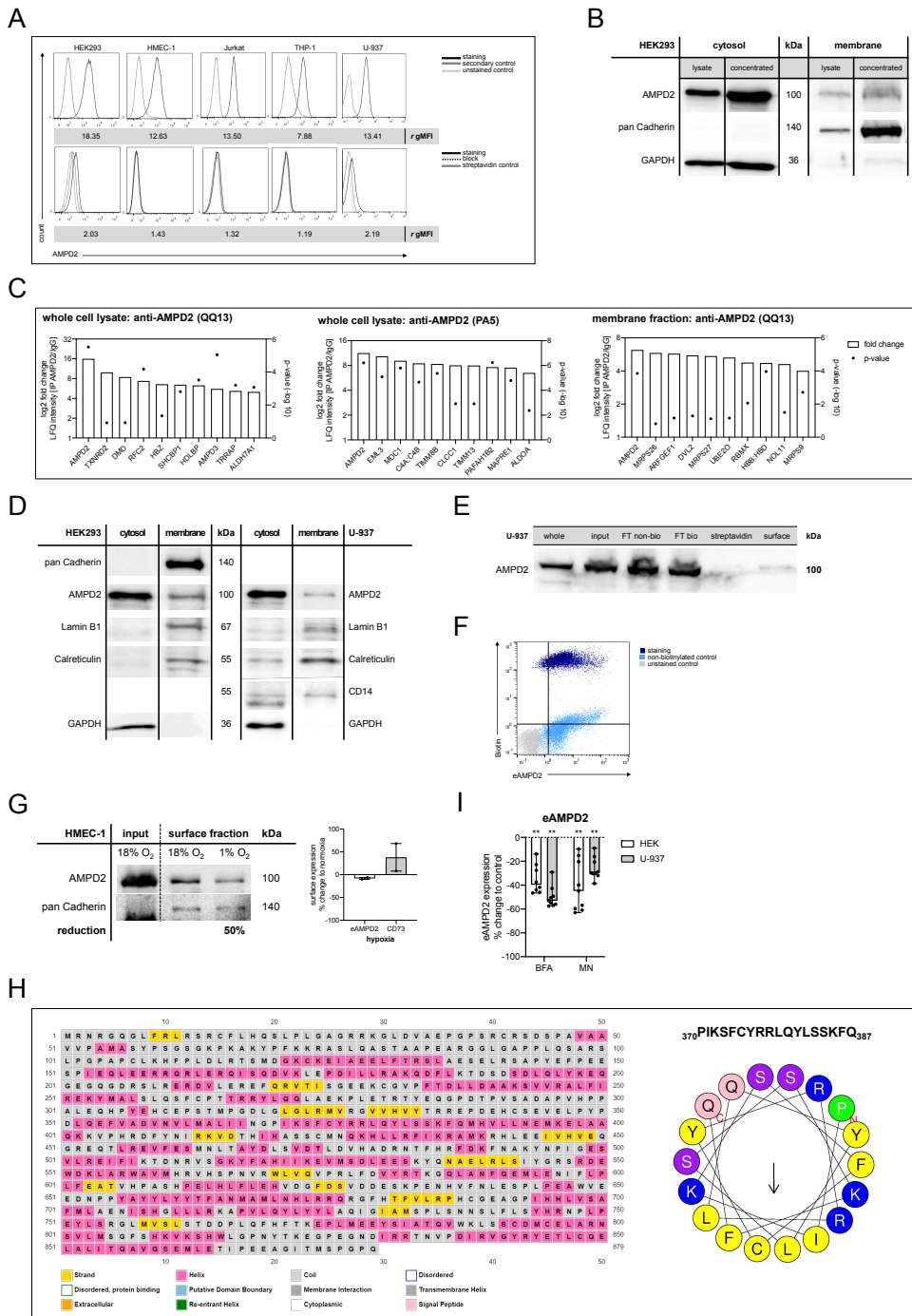
Supplementary Figure S1



Supplementary Figure S1: (A) Gating strategy. Human leukocytes were isolated by red blood cell lysis. DAPI was used to exclude dead cells. A forward-scatter and side-scatter plot served to identify the different leukocyte subsets. CD4+ T cell subsets were subdivided into Type 1 helper (T_H1) cells, Type 2 helper (T_H2) cells and IL-17-producing lymphoid T helper (T_H17) cells. T_H1 cells were identified by the expression of CXCR3 in the absence of CCR4 and CCR6. T_H2 cells were defined as CCR4+CXCR3-CCR6-, while T_H17 cells co-expressed CCR4 and CCR6 in the absence of CXCR3. CD4+CD25+CD127^{low} cells were defined as Tregs.¹ Cytotoxic T cells and B cells were identified by the expression of CD8 and CD19, respectively. (B,C) Gating strategy. CD14+ monocytes (B) and CD15+ neutrophil granulocytes (C) were sorted by magnetic cell separation. Purity of > 97% was revealed by surface staining of CD14 and CD15, respectively. Cells were gated using a forward-scatter and side-scatter plot. Doublets were excluded according to the forward-scatter area and height pattern and 7-AAD was used to exclude dead cells. (D) AMPD2 surface expression on CD14+ monocytes and CD15+ neutrophil granulocytes sorted by

magnetic cell separation. The cells were gated according to Supplementary Figures S1B and S1C. *r*gMFI represents the ratio of geometric mean fluorescence intensity of staining to secondary antibody control. (E) PBMCs were gated using a forward-scatter and side-scatter plot. Doublets were excluded according to the forward-scatter area and height pattern and 7-AAD was used to exclude dead cells. *r*gMFI represents the ratio of geometric mean fluorescence intensity of staining to streptavidin control. The staining was successfully blocked by adding 25-fold excess unconjugated antibody. Classical (CD14+ CD16-), intermediate (CD14+ CD16+) and non-classical (CD14- CD16+) monocytes were analyzed individually. The lines on scatter dot plot indicate median. Wilcoxon matched-pairs signed rank test. (F) Gating strategy. Cell lines were gated using a forward-scatter and side-scatter plot. Doublets were excluded according to the forward-scatter area and height pattern and DAPI was used to exclude dead cells.

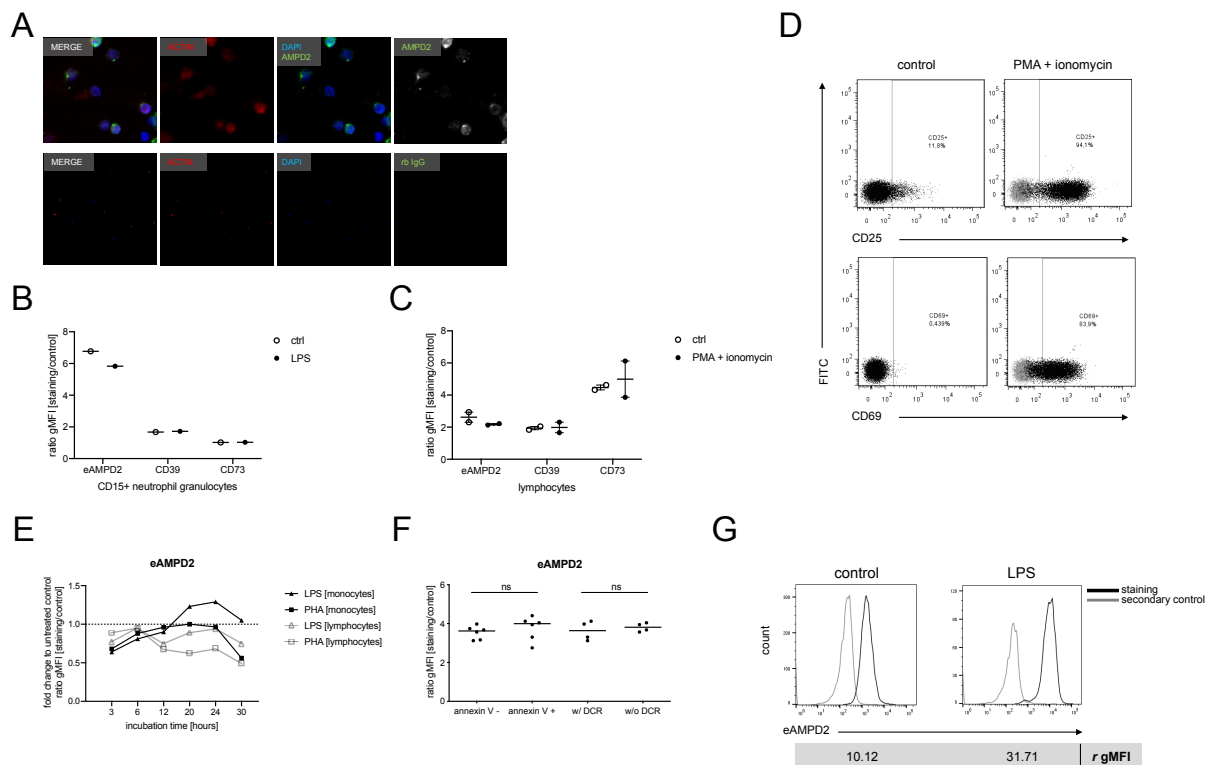
Supplementary Figure S2



Supplementary Figure S2: (A) Flow cytometric analysis of intracellular (upper row) and surface (lower row) AMPD2 expression in HEK293, HMEC-1, Jurkat, THP-1 and U-937 cell lines. *r* gMFI represents the ratio of geometric mean fluorescence intensity of staining to secondary antibody control and staining to streptavidin control for intracellular and surface stainings, respectively. The surface staining was successfully blocked by adding 25-fold excess unconjugated antibody. (B) Western blot analysis of HEK293 cytosolic and membrane fractions. The samples on the right were concentrated with the help of centrifugal filters to increase to amount of protein analyzed by SDS-PAGE. AMPD2 was detected by the mouse monoclonal anti-AMPD2 antibody clone QQ13. Purity of cytosolic and membrane fractions was verified by analyzing pan Cadherin and GAPDH. Uncropped images are provided in Supplementary Figure S7. (C) Top 10 proteins enriched by IP from HEK293 whole cell lysates and membrane fractions using anti-AMPD2 antibodies QQ13 and PA5, respectively, identified by mass spectrometric analyses. Enrichment is depicted as fold change of LFQ intensity compared to isotype control and was evaluated statistically using two-sample Student's t test. (D) Characterization of HEK293 and U-937 cytosolic and membrane fractions by western blot. Uncropped images are provided in Supplementary Figure S7. (E) Western blot analysis of U-937 cells after surface biotinylation. Intact U-937 cells were biotinylated at 4°C and subsequently lysed and subjected to streptavidin-based enrichment of biotinylated proteins. Whole cell lysates (whole) were generated by adding Laemmli sample buffer. Biotinylated cell lysates (input) and flow-through (FT) samples of protein not captured by the NeutrAvidin beads were analyzed in parallel. "streptavidin" represents a non-biotinylated control sample that was subjected to streptavidin-based pull-down, while the "surface" sample was prepared by pull-down following surface biotinylation. (F) eAMPD2 expression and surface biotinylation of U-937 cells analyzed by flow cytometry. U-937 cells were fixed after surface biotinylation and stained an anti-AMPD2-antibody (PA5) and streptavidin. Non-biotinylated cells were measured in parallel. The gating strategy is depicted in Supplementary Figure S1F. (G) AMPD2 surface expression in HMEC-1 cells is reduced by hypoxia. Western blot analysis of HMEC-1 whole cell lysate and surface protein enriched by surface biotinylation followed by streptavidin-based pull-down. Cells were cultured under normoxic (18% O₂) or hypoxic (1% O₂) conditions for 24 hours. AMPD2 protein expression was semiquantified relative to pan Cadherin by image analysis and reduction by hypoxia is depicted in relation to normoxic control. Uncropped images are provided in Supplementary Figure S7. The bar graphs show surface expression of eAMPD2 and CD73 under hypoxic conditions analyzed by flow cytometry (n=2). Doublets and dead cells were excluded for analysis as shown in Supplementary Figure S1F. The data are depicted as change in *r* gMFI (geometric mean fluorescence intensity of staining to streptavidin control) in relation to samples cultured under normoxic conditions. (H) The secondary protein structure of AMPD2 was analyzed by the PSIPRED server to identify helical areas (highlighted in pink).² The graph on the right depicts the lipid-binding helix predicted by the HeliQuest webserver represented as a helical wheel with the hydrophobic face at the bottom.³ (I) Golgi inhibition by incubation with 1 µg/mL brefeldin A and 0.5 µg/mL monensin, respectively, for 24 hours reduced AMPD2 surface expression in HEK293 and U-937 cells analyzed by flow cytometry (n=8-9). Doublets and dead cells were excluded for analysis as shown in Supplementary Figure S1F. The data are depicted as change in *r* gMFI (geometric mean fluorescence intensity of staining to secondary antibody control) in relation to untreated control samples. Bar graphs depict median and range. **p<0.01, compared to untreated control; Wilcoxon matched-pairs signed rank test.

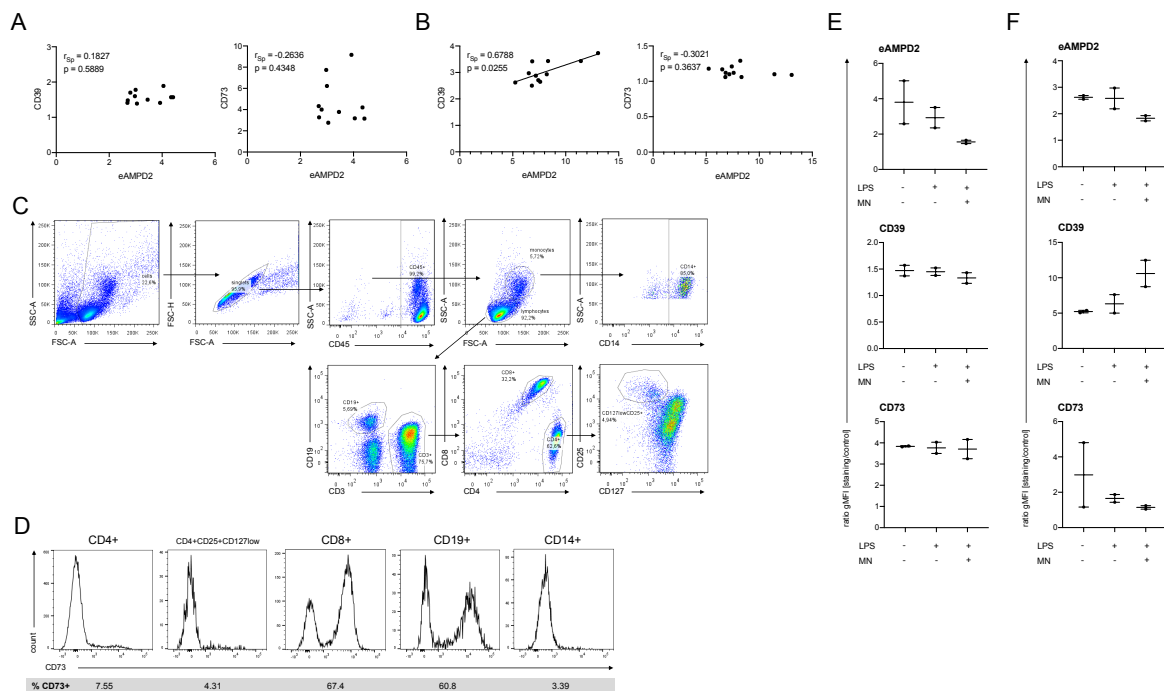
BFA, brefeldin A; MN, monensin

Supplementary Figure S3



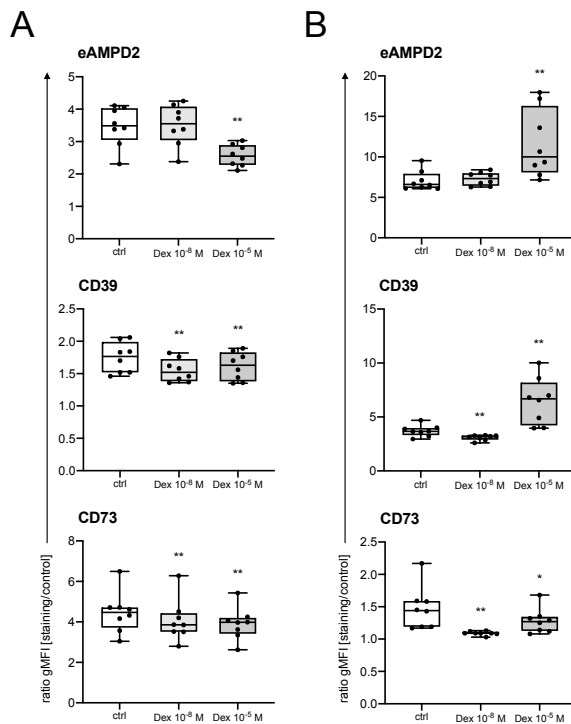
Supplementary Figure S3: (A) Localization of AMPD2 on the cell surface of PBMCs identified by immunofluorescence microscopy. Cells were stained for AMPD2 (green), actin (red) and DAPI (blue). Polyclonal rabbit IgG served as isotype control for the AMPD2 staining antibody. (B) AMPD2 surface expression on CD15+ neutrophil granulocytes sorted by magnetic cell separation. Cells were incubated for 24 hours with 1 $\mu\text{g}/\text{mL}$ LPS and expression of eAMPD2, CD39 and CD73 was measured by flow cytometry ($n=1$). The gating strategy from Supplementary Figure S1C was applied. *r gMFI* represents the ratio of geometric mean fluorescence intensity of staining to secondary antibody control. (C) AMPD2 surface expression on lymphocytes following stimulation. PBMCs were treated with 10 ng/mL PMA + 1 $\mu\text{g}/\text{mL}$ ionomycin for 24 hours and expression of eAMPD2, CD39 and CD73 was measured by flow cytometry ($n=2$). Lymphocytes were gated according to Supplementary Figure S1E for analysis. *r gMFI* represents the ratio of geometric mean fluorescence intensity of staining to secondary antibody control. (D) Proof of lymphocyte activation. Expression of CD25 and CD69 was measured by flow cytometry after 24-hour stimulation with 10 ng/mL PMA + 1 $\mu\text{g}/\text{mL}$ ionomycin compared to untreated control. Cells were incubated in PBMC co-culture and lymphocytes were gated according to Supplementary Figure S1E for analysis. (E) Kinetics of AMPD2 surface expression in human PBMC co-culture after incubation with 1 $\mu\text{g}/\text{mL}$ LPS or 5 $\mu\text{g}/\text{mL}$ PHA determined by flow cytometric analysis. The gating strategy from Supplementary Figure S1E was applied. Data are expressed as mean ($n=2$) ratio to untreated control. (F) The effect of apoptosis on eAMPD2 staining on human monocytes from PBMC co-culture treated with LPS. Apoptotic cells were identified with the help of annexin V. The gating strategy is depicted in Supplementary Figure S1E. In the right-hand approach apoptotic cells were removed by dead cell removal (DCR) after incubation. Apoptosis does not significantly influence AMPD2 surface expression. (G) AMPD2 surface staining on primary human monocytes analyzed by flow cytometry. PBMCs were incubated for 24 hours with or without 1 $\mu\text{g}/\text{mL}$ LPS. Monocytes were gated according to Supplementary Figure S1E for analysis. *r gMFI* represents the ratio of geometric mean fluorescence intensity of staining to secondary antibody control. Box plots show median and range. The lines on scatter dot plot indicate median. Wilcoxon matched-pairs signed rank test.

Supplementary Figure S4



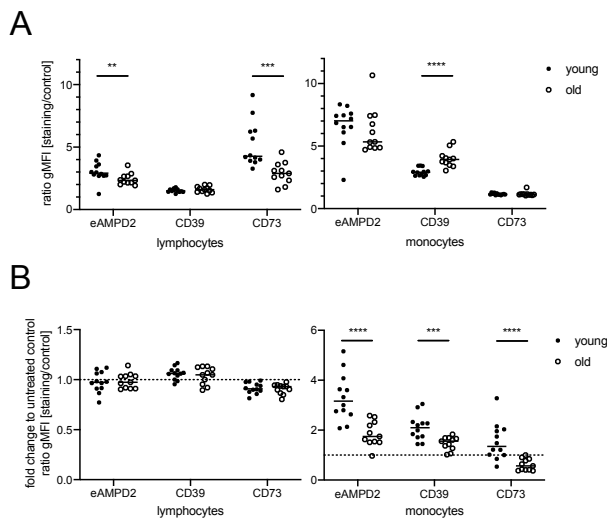
Supplementary Figure S4: Flow cytometric analysis of eAMPD2, CD39 and CD73 expression on primary human immune cell populations at baseline. Correlation between eAMPD2 and ectonucleotidase expression in (A) lymphocytes and (B) monocytes from healthy donors after PBMC isolation. eAMPD2, CD39 and CD73 expression was determined by flow cytometry. The gating strategy from Supplementary Figure S1E was applied. Expression is depicted as ratio of geometric mean fluorescence intensity of staining to secondary antibody control. eAMPD2 correlates with CD39 surface expression in monocytes. Spearman's Rank-Order Correlation. (C) PBMCs were gated using a forward-scatter and side-scatter plot. Doublets were excluded according to the forward-scatter area and height pattern and leukocytes were identified by the expression of CD45. Lymphocytes and monocytes were gated according to their distinctive appearance in a forward-scatter and side-scatter plot. Lymphocytes were subdivided depending on the surface expression of CD4 and CD8. CD4+CD25+CD127low cells were defined as regulatory T cells. CD19+ B cells and CD14+ monocytes were evaluated separately. (D) CD73 surface expression on immune cells subdivided according to Supplementary Figure S4C. (E,F) AMPD2 surface expression on human PBMCs is reduced by Golgi transport inhibition. Cells were treated with 1 $\mu\text{g}/\text{mL}$ LPS with or without 0.5 $\mu\text{g}/\text{mL}$ monensin (MN) ($n=2$) for 21-24 hours and surface expression of AMPD2, CD39 and CD73 was measured by flow cytometry. Lymphocytes (E) and monocytes (F) were incubated in co-culture and gated according to Supplementary Figure S1E for analysis. r gMFI represents the ratio of geometric mean fluorescence intensity of staining to secondary antibody control. All boxplots show median and minimum or maximum values, respectively.

Supplementary Figure S5



Supplementary Figure S5: AMPD2 surface expression on human PBMCs following immunomodulation. Cells were treated with 10^{-8} M and 10^{-5} M dexamethasone, respectively (n=8). Surface expression of eAMPD2, CD39 and CD73 was measured by flow cytometry. (A) Lymphocytes and (B) monocytes were incubated in co-culture and gated according to Supplementary Figure S1E for analysis. All boxplots show median, interquartile range, and minimum or maximum values, respectively. * $p < 0.05$, ** $p < 0.01$; Wilcoxon matched-pairs signed rank test.

Supplementary Figure S6



Supplementary Figure S6: eAMPD2, CD39 and CD73 expression depending on donor age. PBMCs were isolated from heparinized blood samples of young (≤ 40 years) and old (≥ 50 years) healthy donors. (A) eAMPD2, CD39 and CD73 expression was analyzed by flow cytometry directly after isolation (n=11-12). PBMCs were gated according to Supplementary Figure S1E for analysis. (B) Flow cytometric analysis of eAMPD2, CD39 and CD73 expression after incubation with 1 $\mu\text{g}/\text{mL}$ LPS for 21-24 hours in co-culture (n=11-12). PBMCs were gated according to Supplementary Figure S1E for analysis. Modification by LPS stimulation is

depicted in relation to untreated control samples.

Lines on scatter dot plot represent median. ** $p < 0.01$, *** $p < 0.001$, **** $p < 0.0001$, Mann Whitney test.

Supplementary Figure S7



Supplementary Figure S7: Uncropped western blot images corresponding to (A) Figure 2B, (B) Figure 2C, (C) Supplementary Figure S2E, (D) Figure 2E, (E) Figure 3C, (F) Figure 4F, (G) Supplementary Figure S2B, (H) Supplementary Figure S2D, and (I) Supplementary Figure S2G. (J) Protein standard used for all western blots.

Supplementary Table S1: Mass spectrometric analyses of top 10 proteins immunoprecipitated from HEK293 samples using anti-AMPD2 antibodies

Gene name	Peptides	Unique peptides	Student's t test Difference LFQ intensity	Student's t-test p-value (-log10) LFQ intensity	Median intensity	Intensity rank
total: IP QQ13						
AMPD2	47	1	16,303	5,516	9029000000	1
SHCBP1	3	3	7,703	2,805	338410000	60
RFC2	21	21	7,267	4,166	373610000	54
TXNRD2	11	10	6,774	0,925	3809600000	7
DMD	8	7	6,560	0,931	1460400000	15
HDLBP	81	81	5,936	3,519	18038000	319
HBZ	1	1	5,792	1,342	306520000	66
TRRAP	15	15	5,686	3,199	84882000	163
AMPD3	5	4	5,491	5,041	67224000	191
ALDH7A1	43	43	5,258	3,076	38252000	232
total: IP PA5						
AMPD2	47	1	11,237	6,215	4961800000	5
EML3	24	24	9,992	5,077	1539000000	21
MDC1	35	35	9,269	5,789	790850000	43
CLCC1	22	22	9,144	2,917	1159600000	27
C4A;C4B	7	6	8,266	4,654	452350000	84
TIMM8B	9	9	8,226	5,364	294480000	114
TIMM13	8	8	8,044	2,908	584640000	62
MAPRE1	34	31	7,755	4,784	315370000	106
PAFAH1B2	15	15	7,539	6,233	611770000	59
ALDOA	60	53	7,346	2,374	227920000	136
membrane: IP QQ13						
AMPD2	47	1	5,815	3,849	311700000	34
HBB;HBD	3	2	4,658	3,967	30926000	185
UBE2O	33	33	4,557	1,156	32560000	181
NOL11	22	22	4,392	1,494	18015000	257
MRPS27	27	27	4,349	1,114	81540000	89
ARFGEF1	4	4	4,204	1,158	35380000	164
RBMX	40	15	4,179	2,062	43027000	147
MRPS9	29	29	4,114	2,713	54771000	124
MRPS26	23	23	4,086	0,811	23443000	221
DVL2	8	6	4,041	1,285	45793000	142

IP from HEK293 whole cell lysates (total) and membrane fractions (membrane) was performed using anti-AMPD2 antibodies QQ13 and PA5, respectively. Differential protein abundance compared to isotype control was calculated using two-sample Student's t test.

Supplementary Table S2: Mass spectrometric analysis of surface-enriched protein from HMEC-1 cells

Protein name	Gene name	Peptides	Unique peptides	Intensity	iBAQ	Plasma membrane†	LFQ: surface enrichment vs. non-biotinylated control p-value (-log10)	t test Difference (log2)
Cell surface glycoprotein MUC18	MCAM	33	33	23992000000	666430000	+	4,0	10,0
CD166 antigen	ALCAM	35	35	57127000000	1680200000	+	6,1	9,3
Poliovirus receptor	PVR	9	9	9538200000	681300000	+	4,5	9,2
Dystroglycan	DAG1	20	20	8242400000	179180000	+	4,2	8,9
Beta-2-microglobulin	B2M	5	2	17015000000	2126800000	+	3,1	8,8
Receptor-type tyrosine-protein phosphatase F	PTPRF	54	51	4795000000	43198000	+	4,0	8,7
Myelin protein zero-like protein 1	MPZL1	10	6	5678400000	516220000	+	5,7	8,4
Vinculin	VCL	72	72	64726000000	752630000	+	3,7	8,4
Non-specific lipid-transfer protein	SCP2	28	28	19103000000	596960000	+	5,6	8,4
AMPD2								
Peptides	23							
Unique peptides	23							
Sequence coverage [%]	25,4							
Unique sequence coverage [%]	25,4							
Molecular weight [kDa]	100,69							
Q-value	0							
Score	30,278							
Intensity	978860000							
iBAQ	20827000							
MS/MS count	64							
LFQ: surface enrichment vs. non-biotinylated control								
t test Difference (log2)	3,6998							
p-value (-log10)	2,0048							
LFQ: surface enrichment vs. input								
t test Difference (log2)	3,1967							
p-value (-log10)	4,2404							

Top abundant proteins and enrichment of AMPD2 by surface biotinylation. Surface-enriched samples were obtained by surface biotinylation of HMEC-1 cells followed by streptavidin-based pull-down. Differential protein

abundance compared to non-biotinylated samples undergoing streptavidin-based pull-down (non-biotinylated control) and biotinylated whole cell lysate (input) was determined using two-sample Student's t test.

† Plasma membrane annotation according to the Gene Ontology project.^{4, 5}

Supplementary Table S3: Search for lipid-binding helices according to the HeliQuest decision tree

Sequence	μH	z	D	Sequence	μH	z	D	Sequence	μH	z	D	Sequence	μH	z	D
115SMDGKCKEIAEELFTRSL135	0.319	-1	0.028864	241AKSVVRFALFIREKYMALSL259	0.113	3	1.096672	322RTKGQLANFQEMLENIFL593	0.419	0	0.395536	859LYLYTFANMAMLNHLRR078	0.116	2	0.769504
116MDGKCKEIAEELFTRSLA136	0.302	-1	0.044912	242KSVVRFALFIREKYMALSL259	0.172	3	1.152368	323TKGQLANFQEMLENIFL593	0.396	-1	0.043824	860IHLVSAFMAENISHGL711	0.242	-1	0.101552
120DGKCKEIAEELFTRSLAE137	0.249	-2	0.424944	243SVVRFALFIREKYMALSLQ260	0.148	2	0.799712	324KQQLANFQEMLENIFL593	0.476	-1	0.119344	861HHLVSAFMAENISHGL712	0.24	-1	0.10344
121GKCKEIAEELFTRSLAES138	0.284	-1	0.061904	244VVRALFIREKYMALSLQ261	0.148	2	0.799712	325GQLANFQEMLENIFL593	0.468	-2	0.218208	862HHLVSAFMAENISHGL713	0.155	-1	0.18368
122PIEQLEERRQRRLERQIS169	0.455	0	0.42952	245VRFALFIREKYMALSLQ262	0.173	2	0.823312	326QLANFQEMLENIFL593	0.503	-3	0.515168	863VSAFMAENISHGL714	0.174	0	0.164256
123PIEQLEERRQRRLERQIS169	0.464	0	0.438016	246RALFIREKYMALSLQ263	0.181	2	0.830864	327LANFQEMLENIFL593	0.511	-3	0.507616	864VSAFMAENISHGL715	0.056	1	0.382864
124IEQLLEERRQRRLERQIS170	0.415	-1	0.067176	247ALFIREKYMALSLQ264	0.097	1	0.421568	328ANFQEMLENIFL593	0.441	-3	0.573696	865SAFMAENISHGL716	0.025	1	0.3536
124EQLEERRQRRLERQIS171	0.391	-1	0.039104	248VLMALINGPIKSFYRRL176	0.099	3	1.083456	329NFQEMLENIFL593	0.409	-3	0.603904	866AFMAENISHGL717	0.018	1	0.346992
125QLEERRQRRLERQIS172	0.407	1	0.714208	249LMALINGPIKSFYRRL176	0.077	3	1.062688	330FQEMLENIFL593	0.382	-3	0.629392	867FMAENISHGL718	0.056	1	0.382864
126LEERRQRRLERQIS173	0.378	1	0.688832	250MALINGPIKSFYRRLQ180	0.161	3	1.141984	331FQEMLENIFL593	0.332	-3	0.676592	868MLAENISHGL719	0.029	1	0.384752
127EERRQRRLERQIS174	0.248	0	0.234112	251ALINGPIKSFYRRLQ181	0.153	3	1.134432	332EMLENIFL593	0.345	-3	0.66432	869LAENISHGL720	0.129	2	0.781776
128EERRQRRLERQIS175	0.243	1	0.559392	252LINGPIKSFYRRLQ182	0.219	3	1.196736	333EMLENIFL593	0.314	-2	0.363584	870AENISHGL721	0.116	1	0.439504
129RRLERQIS176	0.25	1	0.566	253INGPIKSFYRRLQ183	0.287	3	1.260928	334ENIFL593	0.332	-2	0.346592	871ENISHGL722	0.19	1	0.50936
130RRLERQIS177	0.327	0	0.308688	254INGPIKSFYRRLQ184	0.346	3	1.316624	335ENIFL593	0.279	-2	0.396624	872ENISHGL723	0.177	2	0.827088
131RRLERQIS178	0.436	-1	0.081584	255NGPIKSFYRRLQ185	0.232	4	1.539008	336ENIFL593	0.279	-2	0.396624	873SHGL724	0.091	2	0.745904
132RRLERQIS179	0.366	-1	0.015504	256GPIKSFYRRLQ186	0.338	4	1.639072	337FLFL593	0.152	-2	0.516512	874SHGL725	0.09	2	0.74496
133RRLERQIS180	0.366	-1	0.015504	257PIKSFYRRLQ187	0.346	4	1.646624	338FLFL593	0.148	-2	0.520288	875SCDMCELARNSVMSGFS08	0.032	-1	0.299792
134RRLERQIS181	0.306	-1	0.041136	258IKSFYRRLQ188	0.329	4	1.630576	339FLFL593	0.143	-2	0.525008	876DMCELARNSVMSGFS09	0.036	-1	0.296016
135RRLERQIS182	0.296	1	0.609424	259KSFYRRLQ189	0.248	4	1.954112	340FLFL593	0.143	-2	0.525008	877DMCELARNSVMSGFS10	0.118	0	0.111392
136RRLERQIS183	0.255	0	0.24072	260FCYRRLQ190	0.319	3	1.221136	341FLFL593	0.09	-2	0.57504	878MCELARNSVMSGFS11	0.158	1	0.479152
137RRLERQIS184	0.264	-1	0.080784	261CYRRLQ191	0.246	3	1.222224	342FLFL593	0.116	-3	0.880496	879CELARNSVMSGFS12	0.126	2	0.778944
138RRLERQIS185	0.264	-1	0.080784	262CYRRLQ192	0.249	3	1.225056	343FLFL593	0.07	-3	0.92392	880ELARNSVMSGFS13	0.211	2	0.859184
139RRLERQIS186	0.282	-1	0.063792	263YRRLQ193	0.156	3	1.137264	344PEAWVEEDNPPYAYLYY602	0.2	-4	-1.1312	881LARNSVMSGFS14	0.231	3	1.208064
140RRLERQIS187	0.142	-2	0.525952	264YRRLQ194	0.119	2	0.772336	345EAWVEEDNPPYAYLYY603	0.183	-4	-1.147248	882ARNSVMSGFS15	0.254	3	1.229776
141RRLERQIS188	0.196	-1	0.144976	265YRRLQ195	0.011	1	0.340384	346AWVEEDNPPYAYLYY604	0.091	-3	0.904096	883RYRYTELCOELALIT080	0.166	-1	0.172396
142RRLERQIS189	0.197	-1	0.144032	266YRRLQ196	0.012	1	0.341328	347AWVEEDNPPYAYLYY605	0.091	-3	0.904096	884RYRYTELCOELALIT081	0.219	0	0.206736
143RRLERQIS190	0.072	0	0.067968	267YRRLQ197	0.139	0	0.131216	348VEEDNPPYAYLYY606	0.127	-3	0.870112	885RYRYTELCOELALIT082	0.291	0	0.274704
144RRLERQIS191	0.102	-1	0.233712	268YRRLQ198	0.185	0	0.17464	349EEDNPPYAYLYY607	0.128	-3	0.869168	886RYRYTELCOELALIT083	0.262	-1	0.082672
145RRLERQIS192	0.107	-1	0.228992	269YRRLQ199	0.165	0	0.15576	350EEDNPPYAYLYY608	0.164	-2	0.505184	887RYRYTELCOELALIT084	0.262	-1	0.082672
146RRLERQIS193	0.426	1	0.732144	270YRRLQ200	0.239	0	0.225616	351DNPYAYLYY609	0.107	-1	0.228992	888RYRYTELCOELALIT085	0.263	-1	0.081728
147RRLERQIS194	0.295	0	0.27848	271YRRLQ201	0.522	-2	0.167232	352NPPYAYLYY610	0.054	0	0.050976	889RYRYTELCOELALIT086	0.317	-1	0.430752
148RRLERQIS195	0.332	1	0.643408	272YRRLQ202	0.494	-1	0.136336	353PPYAYLYY611	0.054	0	0.050976	890RYRYTELCOELALIT087	0.325	-3	0.8832
149RRLERQIS196	0.275	2	0.9196	273YRRLQ203	0.392	-2	0.289952	354PPYAYLYY612	0.085	0	0.08024	891RYRYTELCOELALIT088	0.338	-3	0.670928
150RRLERQIS197	0.251	2	0.896944	274YRRLQ204	0.411	-2	0.272016	355PPYAYLYY613	0.095	0	0.08968	892RYRYTELCOELALIT089	0.262	-2	0.412672
151RRLERQIS198	0.249	2	0.895056	275YRRLQ205	0.436	0	0.411584	356PPYAYLYY614	0.068	1	0.394192	893RYRYTELCOELALIT090	0.304	-3	0.703024
152RRLERQIS199	0.126	3	1.108944	276YRRLQ206	0.455	0	0.42952	357PPYAYLYY615	0.133	2	0.785552				

Helical domains present in AMPD2 protein sequence as identified by the PSIPRED server (shown in Supplementary Figure 2H) were submitted to the HeliQuest webserver.^{2, 3} D was calculated as follows: $D = 0.944(<\mu H>) + 0.33(z)$. Lipid-binding helix were defined by $D > 1.34$ (highlighted in green), possible lipid-binding helices were defined by $0.68 < D < 1.34$ (highlighted in yellow). μH , hydrophobic moment; z, net charge; D, discrimination factor

Supplementary Table S4: Mass spectrometric analyses of top 10 proteins immunoprecipitated from CD14+ monocyte samples by anti-AMPD2 antibody (QQ13)

Gene name	Peptides	Unique peptides	Student's t test Difference LFQ intensity	Student's t test p-value (-log 10) LFQ intensity	Intensity
RAB5C	8	6	7,833	3,858	3500500000
PRKAA1	2	2	7,738	2,826	2328900000
LPCAT2	2	2	6,740	4,248	1221300000
GNAI2	13	7	5,932	3,962	1741800000
AMPD2	8	8	4,239	2,869	195980000
SPTBN	2	2	3,969	1,921	131030000
GNPAT	1	1	3,954	2,940	219120000
TRPV2	5	5	3,876	2,898	215710000
IDH2	11	11	3,646	3,273	1720800000
CLIP1	1	1	2,899	0,368	10001000000

CD14+ monocytes were isolated by MACS. IP from membrane fractions was performed using anti-AMPD2 antibody QQ13. Differential protein abundance compared to isotype control was calculated using two-sample Student's t test.

Supplementary Table S5: Characteristics of donors divided into age-related groups

	young	old
donors, n	12	11
age [years], median (IQR)	27 (26-31.75)	61 (55-78)
age [years], range	25-40	50-86
female, n (%)	9 (82)	7 (64)

IQR, interquartile range

References

1. Cossarizza A, Chang HD, Radbruch A, et al. Guidelines for the use of flow cytometry and cell sorting in immunological studies. *European journal of immunology*. Oct 2017;47(10):1584-1797.
2. Jones DT. Protein secondary structure prediction based on position-specific scoring matrices. *J Mol Biol*. Sep 17 1999;292(2):195-202.
3. Gautier R, Douguet D, Antony B, Drin G. HELIQUEST: a web server to screen sequences with specific alpha-helical properties. *Bioinformatics*. Sep 15 2008;24(18):2101-2.
4. Ashburner M, Ball CA, Blake JA, et al. Gene ontology: tool for the unification of biology. The Gene Ontology Consortium. *Nat Genet*. May 2000;25(1):25-9.
5. The Gene Ontology resource: enriching a GOld mine. *Nucleic acids research*. Jan 8 2021;49(D1):D325-d334.

Lebenslauf

Mein Lebenslauf wird aus datenschutzrechtlichen Gründen in der elektronischen Version meiner Arbeit nicht veröffentlicht.

Mein Lebenslauf wird aus datenschutzrechtlichen Gründen in der elektronischen Version meiner Arbeit nicht veröffentlicht.

Mein Lebenslauf wird aus datenschutzrechtlichen Gründen in der elektronischen Version meiner Arbeit nicht veröffentlicht.

Publikationsliste

Artikel

Ehlers L, Meyts I. What a difference ADA2 makes: Insights into the pathophysiology of ADA2 deficiency from single-cell RNA sequencing of monocytes. *Journal of leukocyte biology* 2021 doi: 10.1002/jlb.5ce0421-186r [published Online First: 20210616]

Ehlers L, Kuppe A, Damerau A, Wilantri S, Kirchner M, Mertins P, Strehl C, Buttgerit F, Gaber T. Surface AMP deaminase 2 as a novel regulator modifying extracellular adenine nucleotide metabolism. *The FASEB Journal* 2021;35(7):e21684. doi: <https://doi.org/10.1096/fj.202002658RR>

Strehl C, **Ehlers L**, Gaber T, Buttgerit F. Glucocorticoids-All-Rounders Tackling the Versatile Players of the Immune System. *Front Immunol* 2019;10:1744. doi: 10.3389/fimmu.2019.01744

Ehlers L, Askling J, Bijlsma HW, Cid MC, Cutolo M, Dasgupta B, Dejaco C, Dixon WG, Feltelius N, Finckh A, Gilbert K, Mackie SL, Mahr A, Matteson EL, Neill L, Salvarani C, Schmidt WA, Strangfeld A, van Vollenhoven RF, Buttgerit F. 2018 EULAR recommendations for a core data set to support observational research and clinical care in giant cell arteritis. *Annals of the rheumatic diseases* 2019;78(9):1160-66. doi: 10.1136/annrheumdis-2018-214755

Buchkapitel

Ehlers L, Strehl C, Westhovens R. Glucocorticoids in Rheumatic Diseases. In: Bijlsma JWJ, Hachulla E, eds. *EULAR Textbook on Rheumatic Diseases*. 3rd. ed. London: BMJ Publishing Group Ltd., 2018.

Vorträge

DGfI Young Immunologists Virtual Seminar, 08.10.2020

Ehlers L, Strehl C, Kirchner M, Buttgerit F, Gaber T. An antibody gone astray

Posterpräsentationen

ACR Convergence 2020, 05.-09.11.2020 (virtuell)

Ehlers L, Kuppe A, Kirchner M, Damerau A, Strehl C, Buttgerit F, Gaber T. AMP Deaminase 2 Is Expressed on the Surface of Human Immune Cells as a Novel Regulator of Extracellular Adenosine Metabolism (Abstract n° 0066)

Deutscher Rheumatologiekongress 2020, 09.-12.09.2020 (virtuell)

Ehlers L, Wiebe E, Freier D, Hermann S, Zhang YQ, Buttgerit F, Stone JH. Prospective Use of the Glucocorticoid Toxicity Index (GTI) in a Cohort of Vasculitis Patients (Abstract n° 206, Poster n° VK.19)

EULAR 2020 E-Congress: Annual European Congress of Rheumatology, 03.-06.06.2020 (virtuell)

Ehlers L, Kuppe A, Damerau A, Kirchner M, Strehl C, Buttgerit F, Gaber T. Surface AMP Deaminase 2 as a Novel Regulator Modifying the Extracellular ATP-Adenosine Balance that is Differentially Expressed in Patients with Rheumatoid Arthritis (Abstract n° 2813, Poster n° FRI0004)

40th European Workshop for Rheumatology Research (EWRR 2020), 13.02.-16.02.2020, Leuven, Belgium

Ehlers L, Kuppe A, Damerau A, Kirchner M, Strehl C, Buttgerit F, Gaber T. Surface AMP Deaminase 2 as a Novel Regulator Modifying the Extracellular ATP-Adenosine Balance that is Differentially Expressed in Patients with Rheumatoid Arthritis (Abstract n° 109, Poster n° 117)

2019 ACR/ARP Annual Meeting, 08.-13.11.2019, Atlanta, Georgia, USA

Ehlers L, Kuppe A, Strehl C, Kirchner M, Buttgerit F, Gaber T. AMP Deaminase 2 Surface Expression Counteracting CD73-Driven Generation of Anti-Inflammatory Extracellular Adenosine (Abstract n° 699189, Poster n° 0004)

2018 ACR/ARP Annual Meeting, 19.-24.10.2018 in Chicago, Illinois, USA

Ehlers L, Askling J, Bijlsma JW, Cid MC, Cutolo M, Dasgupta B, Dejaco C, Dixon WG, Feltelius N, Finckh A, Gilbert K, Mackie S, Mahr A, Matteson EL, Neill L, Salvarani C, Schmidt WA, Strangfeld A, van Vollenhoven R, Buttgerit F. EULAR Task Force Recommendations for a Minimum Core Set of Parameters to be Collected in Giant Cell Arteritis Registries and Databases (Abstract ID 75099, Poster n° 2783)

Ehlers L, Kuppe A, Damerau A, Chen Y, Strehl C, Kirchner M, Buttgerit F, Gaber T. Surface Adenosine Monophosphate Deaminase 2 As a Novel Regulator Modifying Ectonucleotidase-Driven Generation of Anti-Inflammatory Extracellular Adenosine (Abstract ID 73203, Poster n° 1000)

DGRh-Kongress 2018, 19.-22.09.2018 in Mannheim, Deutschland

Ehlers L, Kuppe A, Damerau A, Chen Y, Strehl C, Kirchner M, Buttgerit F, Gaber T. Membrane-associated AMPD2, a novel regulator in shifting the balance between extracellular ATP and adenosine? (Abstract n° 18-225, Poster n° ER.15)

Damerau A, Lang A, **Ehlers L**, Pfeiffenberger M, Gaber, T, Buttgerit F. Simulating the pathogenesis of arthritis in vitro by developing a humanbased multicomponent 3D joint model (Abstract n° 18-205, Poster n° ER.10)

Gaber T, Pienczykowski J, Damerau A, Pfeiffenberger M, **Ehlers L**, Buttgerit F, Hoff P. Tofacitinib promotes fundamental processes of bone healing including mesenchymal stromal cell recruitment and osteogenesis under hypoxia (Abstract n° 18-287, Poster n° OS-RO.04)

EULAR Annual European Congress of Rheumatology, 13.-16.06.2018 in Amsterdam, Niederlande

Ehlers L, Askling J, Bijlsma JW, Cid MC, Cutolo M, Dasgupta B, Dejaco C, Dixon WG, Feltelius N, Finckh A, Gilbert K, Mackie S, Mahr A, Matteson EL, Neill L, Salvarani C, Schmidt WA, Strangfeld A, van Vollenhoven R, Buttgerit F. EULAR 2018 core set of data to be collected in giant cell arteritis registries and databases Viewpoints from a EULAR task force (Abstract n° 18-2428, Poster n° SAT0535)

Ehlers L, Kuppe A, Damerau A, Chen Y, Buttgerit F, Gaber T. Membrane-associated AMPD2, a novel regulator in shifting the balance between extracellular ATP and adenosine? (Abstract n° EULAR18-6608, Poster n° SAT0038)

Danksagung

An dieser Stelle möchte ich mich herzlich bei den Menschen bedanken, die mir diese Promotion ermöglicht und mich auf dem Weg unterstützt haben.

Zunächst gilt mein Dank meinem Doktorvater Professor Dr. Frank Buttgereit für die Möglichkeit, an diesem und weiteren spannenden Projekten zu arbeiten, und für ein Zuhause in der Rheumatologie.

Ich danke ganz besonders meinem Betreuer Dr. Timo Gaber für Rat und Ideen und seine unermüdliche Energie als Motivationsspender. Dr. Cindy Strehl danke ich für die Einarbeitung im Labor, ihre Unterstützung und die Freiheit, auch unerwarteten Wegen zu folgen.

Manuela Jakstadt und Gabriele May danke ich als gute Seelen der Arbeitsgruppe und für ihre Unterstützung bei der Patientenrekrutierung. Weiterhin gilt ein großer Dank allen Co-Autor*innen der Publikation, die mir bei der Vollendung des Projekts geholfen haben. Ganz besonders möchte ich mich bei Alexandra Damerau und Siska Wilantri für alle gemeinsamen Laborstunden und Gespräche bedanken. Auch danke ich den vielen wunderbaren Menschen im DRFZ für ihre Hilfsbereitschaft und die tolle Zeit im Labor sowie allen Patient*innen und Spender*innen für ihre Blutspenden.

Zuletzt gilt mein größter Dank meiner Familie und meinen Freunden. Ganz besonders danke ich Laura Kreckler mit meinem Sonnenschein Evi, Lara Kuschmann, Marlene Kuschmann, Bettina Moravcsik und Lennard Ostendorf fürs Zuhören und Mutmachen, für ihr Interesse und ihre wunderbare Freundschaft. Ich danke meinem wundervollen Bruder Felix dafür, dass er immer an mich glaubt, und meinen Eltern für ihre uneingeschränkte Unterstützung bei allem, was ich tue.